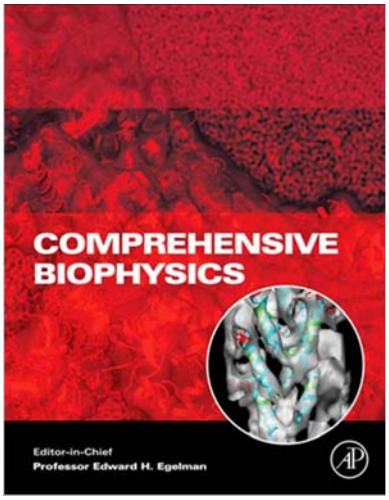

From M. Preller and D.J. Manstein, Myosin Motors: Structural Aspects and Functionality. In: Edward H. Egelman, editor: Comprehensive Biophysics, Vol 4, Molecular Motors and Motility, Yale E. Goldman, E. Michael Ostap.
Oxford: Academic Press, 2012. pp. 118-150.
ISBN: 978-0-12-374920-8

4.8 Myosin Motors: Structural Aspects and Functionality

M Preller and DJ Manstein, Institute for Biophysical Chemistry, Hannover, Germany

Abbreviations

ADP	adenosine diphosphate
ATP	adenosine triphosphate
ATPase	adenosine triphosphatase
BDM	butanedione monoxime
BTS	benzyl-*p*-toluene sulfonamide
CaM	calmodulin
CDD	conserved domain database
CM	cardiomyopathy
cryoEM	cryoelectron microscopy
ELC	essential light chain
EM	electron microscopy
ENM	elastic network model
FERM	4.1-ezrin-radixin-moesin
GTD	globular tail domain
GTPase	guanosine triphosphatase
MDFF	molecular dynamics flexible fitting
MHC	myosin heavy chain
NM-2a	nonmuscle myosin 2a
PBP	Pentabromopseudilin (2,3,4-tribromo-5-(3,5-dibromo-2-hydroxyphenyl)-1H-pyrrole)
PFAM	Protein families database
PH	pleckstrin homology
QM	quantum mechanical
RLC	regulatory light chain
SAH	single α-helix
SAXS	small-angle X-ray scattering
SMART	Simple Modular Architecture Research Tool
TFP	trifluoperazine
USH1B	Usher syndrome 1B

 doi:10.1016/B978-0-12-374920-8.00410-0

4.8.1 Introduction

4.8.1.1 Overview of the Myosin Family

Myosins are motor proteins which catalyze the conversion of chemical energy into directed movement and force. Adenosine triphosphate (ATP) serves as the energy source, and the filament-forming protein actin provides the tracks on which the myosin motors run. The resulting motile activity generated by the actomyosin complex drives muscle contraction and a wide range of cellular transportation processes. Thirty to 40% of the total body mass in humans is made up by skeletal muscle. Actin and myosin, as the major components of skeletal muscle, are thus among the most abundant proteins in nature. This abundance allowed Kühne[1] to purify a complex of actin and myosin in 1859, at a time when protein purification techniques were in their infancy. Kühne[1] named the complex 'myosin', but Straub and Szent-Györgyi[2] recognized in 1942 that Kühne's myosin contained actin as second component. During the next 40 years, the term 'myosin' was used almost exclusively to describe the group of similar, but nonidentical adenosine triphosphatases (ATPases) found in striated and smooth muscle cells.[3] We now recognize that there are hundreds of myosin isoforms from many eukaryotic organisms with diverse functionality.

Based on a phylogenetic analysis of the highly conserved head domain, the myosin superfamily of molecular motors was subdivided into 18 classes[4] (see Figure 1 in Ref. 5 for a phylogenetic tree). Additional classes were identified in parasitic protists.[5] Several myosins were designated as 'orphans', neither included in one of the existing classes nor accepted as founders of a new class. The filament-forming myosins of skeletal muscle, cardiac muscle, smooth muscle, and nonmuscle cells are generally referred to as 'conventional myosins' or class-2 myosins. All other myosins are termed 'unconventional myosins'. The designation 'class-2 myosin' originally referred to the two-headed structure of conventional myosins which resulted from the historical accident that the first unconventional myosins discovered were members of the single-headed class-1 family. However, it soon became clear that several members of other myosin classes form double-headed structures.

Skeletal muscle myoblast cells produce 13 myosin isoforms, whereas most other types of cells in our body produce about 20 different myosin isoforms from at least six different classes.[6] The human genome encodes a total of 38 myosin heavy-chain genes (**Table 1**).[7] These myosin isoforms represent 12 different classes which are specialized for particular tasks. Myosin diversity is enhanced by the existence of multiple splice isoforms, their association with various specific light chains (**Table 2**), and post-translational modifications such as the methylation of lysine residues and phosphorylation of hydroxyl-amino acids.[8] The cellular functions and roles of the various myosin isoforms are diverse, with each form playing a unique role in generating or stabilizing actin-based movements.[9] In addition to the active role played during muscle contraction, myosin motor activity contributes to cleavage furrow constriction during cytokinesis, endocytosis, organelle and vesicle transport, and the mechanical gating of ion channels. In accordance with their participation in a wide range of cellular functions, myosins have been implicated in a wide range of disease processes.

4.8.1.1.1 Conventional myosins

Myosin-2 is formed from six polypeptide chains – a pair of heavy chains (myosin heavy chain [MHC]) and two pairs of distinct light chains (**Figure 1**). The architecture of this hexamer is highly asymmetric and can be subdivided in three regions based on the appearance of the molecule in electron micrographs:

1. A globular head region, that is the common element found in all members of the myosin family. The head region is also referred to as the 'motor domain' because it contains the actin and nucleotide binding sites and is sufficient to move actin filaments *in vitro*.[10]
2. A neck domain, that is formed by the light-chain binding region, and is thought to act as a lever arm that amplifies the movement which is generated in the motor domain.[11]
3. An extended tail region, that is required for filament assembly.[12]

The motor domain is highly conserved within the myosin superfamily, that presumably maintains the productive coupling of interactions with actin filaments and the turnover of ATP, the energy source of the motors. Nonetheless, variations in the motor domain greatly affect motor properties such as velocity and force production, but also play critical roles in defining the subcellular localization and cargo binding properties of myosins.

The neck region of myosin-2 consists of a helical extension, that contains two IQ motifs conforming to the consensus sequence [I,L,V]QxxxRGxxx[R,K]. Typical IQ motifs consist of 25 amino acids forming an uninterrupted α-helix which is distinctly amphiphilic, and providing the binding site for calmodulin or a calmodulin-like light chain.[13] The light chains stabilize the helix, forming a rigid 'lever arm'. In addition, the light chains can play a regulatory role. Phosphorylation of light chains and calcium-dependent changes play a regulatory role for some myosins.[14]

The two-chain α-helical coiled-coil tails which self-assemble to form bipolar filaments are characteristic features of myosin-2. However, for other types of myosins the tail corresponds to the region which displays the greatest level of diversity with regard to its length, domain composition, and organization. Tail region-mediated interactions such as cargo binding or filament formation play an important role in linking myosin motor activity to specific cellular functions and processes (**Figure 2**).

In mammals, there are 14 genes encoding myosin-2 heavy chains. In humans, six skeletal muscle heavy-chain genes ('embryonic' MYH3, 'fast 2a' MYH2, 'fast 2x' MYH1, 'fast 2b' MYH4, 'neonatal' MYH8, and 'extraocular' MYH13) are clustered in a region of chromosome 17. The genes encoding α(*MYH6*) and β-cardiac (*MYH7*) MHCs are clustered on chromosome 14. Other genes encode smooth muscle (*MYH11*), three nonmuscle NM2a (*MYH9*), NM2b (*MYH10*), NM2c (*MYH14*), and a superfast sarcomeric MHC (*MYH16*). MHC diversity is increased by alternative splicing. The most

Table 1 Human myosin heavy-chain genes

Myosin class	*Gene name*	*Protein name*	*Chr.*
Myosin-1	*MYO1A*	Myosin-1A, 'brush border myosin-1'	12:q13.3
	MYO1B	Myosin-1B	2:q32.3
	MYO1C	Myosin-1C	17:p13.3
	MYO1D	Myosin-1D	17:q11.2
	MYO1E	Myosin-1E	15:q22.2
	MYO1F	Myosin-1F	19:p13.2
	MYO1G	Myosin-1G	7:p13
	MYO1H	Myosin-1H	12:q24.11
Myosin-2	*MYH1*	Myosin-2 (heavy chain 1), skeletal muscle, adult 2X/D	17:p13.1
	MYH2	Myosin-2 (heavy chain 2) skeletal muscle, adult 2A	17:p13.1
	MYH3	Myosin-2 (heavy chain 3) skeletal muscle, embryonic	17:p13.1
	MYH4	Myosin-2 (heavy chain 4) skeletal muscle 2B	17:p13.1
	MYH6	Myosin-2 (heavy chain 6), cardiac muscle, alpha	14:q11.2
	MYH7	Myosin-2 (heavy chain 7) cardiac muscle, beta	14:q11.2
	MYH7B	Myosin-2 (heavy chain 7B) extraocular muscles, slow tonic (messenger RNA but not the protein is not present in the myocardium)	20:q11.22
	MYH8	Myosin-2 (heavy chain 8) skeletal muscle, perinatal	17:p13.1
	MYH9	Myosin-2 (heavy chain 9) nonmuscle 2A	22:q12.3
	MYH10	Myosin-2 (heavy chain 10) nonmuscle 2B	17:p13.1
	MYH11	Myosin-2 (heavy chain 11) smooth muscle	16:p13.11
	MYH13	Myosin-2 (heavy chain 13) superfast,- extraocular muscle	17:p13.1
	MYH14	Myosin-2 (heavy chain 14) non-muscle 2C	19:q13.33
	MYH15	Myosin-2 (heavy chain 15) extraocular muscles	3:q13.13
Myosin-3	*MYO3A*	Myosin-3A, NinaC-like	10:p12.1
	MYO3B	Myosin-3B	2:q31.1
Myosin-5	*MYO5A*	Myosin-5A (heavy chain 12) 'Griscelli syndrome'	15:q21.2
	MYO5B	Myosin-5B	18:q21.1
	MYO5C	Myosin-5C	15:q21.2
Myosin-6	*MYO6*	Myosin-6 'Snell's Waltzer'	6:q14.1
Myosin-7	*MYO7A*	Myosin-7A 'Usher 1b'	11:q13.5
	MYO7B	Myosin-7B	2:q14.3
Myosin-9	*MYO9A*	Myosin-9A	15:q23
	MYO9B	Myosin-9B	19:p13.11
Myosin-10	*MYO10*	Myosin-10	5:p15.1
Myosin-15	*MYO15A*	Myosin-15A	17:p11.2
Myosin-16	*MYO16*	Myosin-16	13:q33.3
Myosin-18	*MYO18A*	Myosin-18A PDZ myosin	17:q11.2
	MYO18B	Myosin-18B PDZ myosin	22:q12.1
Myosin-19	*MYO19*	Myosin-19 (orphan)	17:q12

Table 2 Human myosin light-chain genes

Gene name	*Protein name*	*Chr.*
MYL1	Myosin light chain 1, alkali; skeletal, fast	2:q34
MYL10	Myosin light chain 10, regulatory	7:q22.1
MYL12A	Myosin light chain 12A, regulatory, non-sarcomeric	18:p11.31
MYL12B	Myosin light chain 12B, regulatory	18:p11.31
MYL2	Myosin, light chain 2, regulatory, cardiac, slow	12:q24.11
MYL3	Myosin light chain 3, alkali; ventricular, skeletal, slow	3:p21.31
MYL4	Myosin light chain 4, alkali; atrial, embryonic	17:q21.32
MYL5	Myosin light chain 5, regulatory	4:p16.3
MYL6	Myosin light chain 6, alkali; smooth muscle and nonmuscle	12:q13.2
MYL6B	Myosin light chain 6B, alkali; smooth muscle and nonmuscle	12:q13.2
MYL7	Myosin light chain 7, regulatory	7:p13
MYL9	Myosin light chain 9, regulatory	20:q11.23
MYLPF	Myosin light chain, phosphorylatable, fast skeletal muscle	16:p11.2

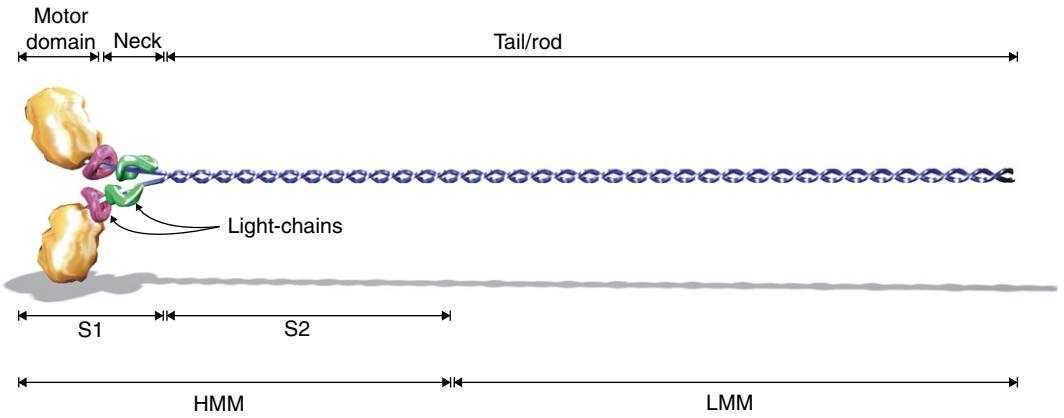

Figure 1 Schematic representation of the myosin-2 heavy-chain dimer. The proteolytically generated fragment containing the motor domain and the neck region is referred to as 'subfragment-1' or 'S1'; the insoluble α-helical coiled-coil dimeric tail is sometimes referred to as 'the rod'. The rod is mainly built by α-helical coiled-coil structures produced by a periodic repeat of hydrophobic residues in the first (a) and fourth (d) position of a septet of amino acids with the general form *abcdefg*. A second alternative proteolytic cleavage site in the myosin-2 molecule, about 45 kDa farther downstream in the myosin tail, produces the soluble, two-headed heavy meromyosin (HMM) fragment and the insoluble light meromyosin (LMM). The distal, dimeric tail part of the HMM fragment is termed 'subfragment-2' or 'S2'. Both, S1 and HMM retain the motor properties of their parent myosin.[178] The lengths of the proteolytic fragments are indicated by arrows.

prominent role of myosin-2 motors is their active contribution to muscle contraction.

Mammalian muscle fibers contain four major MHC isoforms and three major myosin light-chain (MLC) isoforms. These can interact with the 'slow' MLC1s and the two 'fast' MLC1f and MLC3f. The differential distribution of the 'slow' β(*MYH7*) and three 'fast' MHC isoforms 2a (*MYH2*), 2x (*MYH1*), and 2b (*MYH4*) defines four major fiber types containing a single MHC isoform and a number of intermediate hybrid fiber populations containing both slow- and fast heavy chain isoforms or combinations of the latter. Expression of the genes encoding the MHCs in developing and adult muscle is regulated by neural, hormonal, and mechanical factors. Further details about muscles and the role of myosins in muscle tissue are covered later in this volume.

Class-2 conventional myosins accomplish a wide range of cellular functions, in addition to muscle contraction. Members of the conventional myosins are involved in the formation of lamellipodia and the associated migration of fibroblasts and other cells.[15] Furthermore, they play a role in exocytosis and endocytosis, as reported, for example, for the internalization of the chemokine receptor CSCR4 by nonmuscle myosin 2a (NM-2a).[16] The same myosin isoform also participates in the hearing process, although its molecular role is not known. Diseases like May-Hegglin anomaly, Fechtner, Sebastian, Epstein and Alport-like syndromes are related to mutations in the human gene which encodes NM-2a.[17] The R705H mutation in the SH1 helix of NM-2a has been linked to nonsyndromic deafness DFNA17.[18] One nonsense mutation and three point mutations in the MYH14 gene encoding NM-2c, that is produced in cochlea cells, are associated with nonsyndromic autosomal dominant hearing impairment DFNA4.[19] In invertebrates it was shown, that nonmuscle myosins are involved in cell development and cell differentiation.[20] Knockout studies revealed a critical function of NM-2b in heart development.[21] Recent studies reported the critical roles of NM-2a and NM-2b for the spreading and migration of breast cancer cells, with NM-2b having a preferential role in the mechanics of lamellar protrusion.[22] NM-2c is present in high amounts in other cancer cell lines.[23] Moreover, it has been suggested that NM-2a may be involved in intracellular transport of herpes simplex virus after infection.[24]

4.8.1.1.2 Unconventional myosins

Unconventional myosins vary greatly in size and function. They share the globular motor domain with conventional myosins, that in most instances is positioned at or near the N terminus. The kinetic and functional properties of members of class-1, 3, 5, 6, 7, 9, 11, and 14 motor domains are tuned to specific functions, but share the same mechanistic principles with conventional myosin motors. However, it is by no means clear that all unconventional myosins can produce force and movement in a cyclic interaction with ATP and F-actin. The neck region displays diversity in regard to length and sequence. The number of clearly identifiable copies of the IQ motif in the neck regions of unconventional myosins varies between zero and seven. C-terminally positioned domains, such as the highly charged single α-helix (SAH) domain can extend the functional length of the myosin lever. Structural diversity is greatest in the tail region, that mediates specificity in regard to cargo binding. Tail regions consist, in some cases, of very short and unstructured membrane or protein binding regions, whereas the tails of other unconventional myosins are formed by large multidomain structures containing various combinations of protein-protein interaction modules, membrane binding domains, signaling modules, and structural motifs which may simply act as spacers, or they may mediate heavy-chain dimer formation.

4.8.1.1.2.1 Myosin-1

Members of the class-1 myosins are small, single-headed motors which are found in most organisms – from yeast to humans. They are often associated with membranes and were

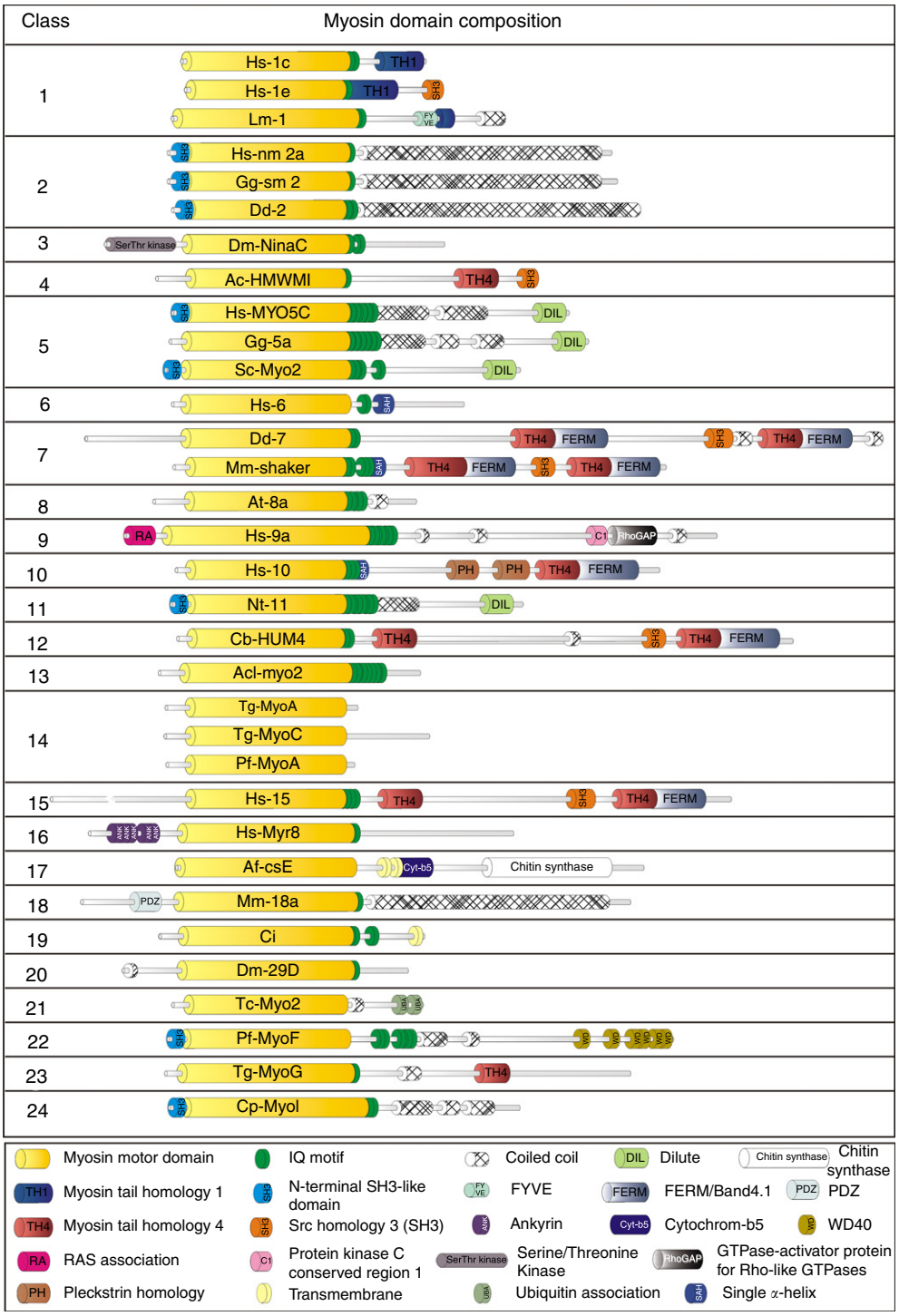

Figure 2 Schematic illustration of the different myosin classes and their domain composition. Predictions of the protein domains are mainly based on Simple Modular Architecture Research Tool (SMART) (http://smart.embl-heidelberg.de/), Protein families database (PFAM) (http://pfam.sanger.ac.uk/), and conserved domain database (CDD) (http://www.ncbi.nlm.nih.gov/ Structure/cdd/cdd.shtml). Ac, *Acanthamoeba castellanii;* Acl, *Acetabularia cliftonii;* Af, *Aspergillus fumigates;* At, *Arabidopsis thaliana;* Cb, *Caenorhabditis briggsae;* Ci, *Ciona intestinalis;* Cp, *Cryptosporidium parvum;* Dd, *Dictyostelium discoideum;* Dm, *Drosophila melanogaster;* Gg, *Gallus gallus;* Hs, *Homo sapiens;* Lm, *Leishmania major;* Mm, *Mus musculus;* Nt, *Nicotiana tabacum;* Pf, *Plasmodium falciparum;* Sc, *Saccharomyces cerevisiae;* Tc, *Trypanosoma cruzi;* Tg, *Toxoplasma gondii.*

shown to be involved in the organization of the cytoskeleton, phagocytosis, pinocytosis, the mechanical gating of ion channels, and transcription. Consistent with their diverse functions is the wide range of kinetic properties displayed by members of this class. Actin-activated ATPase activities range from 0.032 s^{-1} to 17.6 s^{-1}, and similar changes are observed for the speed of movement.[25] Class-1 myosins can be subdivided into long-tailed and short-tailed isoforms. In general, the long-tailed myosin-1 isoforms possess a higher ATPase activity. Short-tailed mammalian class-1 myosins include Myo1a, Myo1b, Myo1c, Myo1d, Myo1g, and Myo1h. Myo1a is produced in the polarized epithelial cells of sensory organs, glands, and the intestine. In intestinal microvilli, it connects the core bundle of actin filaments to the microvillar membrane. Six point mutations and one nonsense mutation in the gene encoding Myo1a were identified to be linked to sensorineural deafness DFNA48.[26] Myo1b is found enriched at cell membranes, cell surface projections, and the cleavage furrow of cells in the heart, brain, lung, liver, and intestine. Myo1c is found in the cortical regions of many different cell types. Special roles include the cycling of GLUT4 transporters from intracellular compartments to the cell membrane of adipocytes and the insertion and/or removal of epithelial Na^+ channels in the plasma membrane of kidney collecting duct cells. In addition, Myo1c is a component of the adaptation-motor complex in auditory hair cells.[27]

A nuclear isoform of Myo1c (nMyo1c) interacts with RNA polymerase II and appears to play a role in transcription together with actin.[28] The transcription start site for nMyo1c is in an exon which is located upstream to the start site for cytoplasmic Myo1c, leading to the production of nMyo1c with a unique N-terminal peptide.[28b,29] Further functions attributed to nMyo1c include chromatin remodeling and the movement of chromosomal regions in the nuclei of mammalian cells.[28a,30]

Myo1d plays a role in membrane trafficking and is widely produced. The highest levels are observed in neuronal cells. The long-tailed myosins, Myo1e and Myo1f, are predominantly found at the cell periphery. Myo1e is found in phagocytic cups and at sites of cell-cell contact in a wide range of cells. Myo1f is mainly produced in the lung and cells of the immune system. Accordingly, Myo1f depletion leads to an impaired immune system.

4.8.1.1.2.2 Myosin-3

Members of the class-3 myosins are single-headed motors involved in vision and phototransduction. They are characterized by a unique N-terminal serine/threonine kinase domain. Class-3 myosins can be categorized on the basis of the pattern of IQ motifs within the molecule. Invertebrate class-3 myosins typically have two IQ motifs in the neck domain, frequently separated by 34 to 48 amino acids. Vertebrate class-3 myosins contain two to four neck IQ motifs and, with the exception of mice, have additional IQ motifs in their tail domain. Myosin-3 is produced predominantly in sensory cells in both invertebrates and vertebrates, where it localizes to complex actin filament-rich structures – rhabdomeres of invertebrate photoreceptors, calycal processes of vertebrate retinal photoreceptors, and stereocilia of inner ear hair cells. Null mutations cause abnormal phototransduction and photoreceptor degeneration in flies, and progressive hearing loss in humans.[31] Systematic mutational studies of the NinaC gene, that encodes the *Drosophila melanogaster* (*Dm*) myosin-3 isoform, suggest that the kinase and myosin domains have distinct roles. The kinase subunit participates directly in phototransduction by regulating rhabdomeric activity, whereas myosin motor function is required to transport the kinase domain to rhabdomeres, to regulate calmodulin localization in rhabdomeres, and to maintain the structure of rhabdomeres.[32] Phosphorylation appears to be important for the regulation of this myosin and its signaling interactions with other proteins. So far, there is no established link between mutations in human myosin-3 genes and blindness, but mutations in myosin-3a genes were linked to progressive nonsyndromic hearing loss DFNB30.

4.8.1.1.2.3 Myosin-5

Myosin-5 is a double-headed myosin which dimerizes via a coiled-coil domain. The heavy chain is composed of an N-terminal motor domain, a neck region containing six IQ motifs, a central 'stalk' domain responsible for dimerization, and a globular tail domain (GTD), that mediates cargo transport. In evolutionary terms, myosin-5 is thought to be as old or older than myosin-2. The double-headed class-5 myosins are produced in a wide range of organisms including yeast, protists, insects, and vertebrates. Moreover, they share many structural and enzymatic properties with class-11 myosins from plants. Myosin-5 moves organelles, vesicles, and nonvesicular cargos such as smooth endoplasmic reticulum, melanosomes, and messenger RNA. The processive nature of myosin-5-based motility supports transport over a distance of several micrometers. Outward actin-based movement toward the plasma membrane is frequently dependent on the motor activity of myosin-5 and its ability to move processively along actin filaments, taking tens to hundreds of steps before dissociation. Myosin-5 has evolved five molecular properties to enable its function as an organelle motor: (1) the GTD for regulated cargo binding, (2) two-headed dimer formation mediated by the coiled-coil stalk domain, (3) a biochemical cycle time which is dominated by states with a high affinity for actin, (4) a strain-dependent kinetic gating mechanism between the two heads, and (5) a long neck which allows the two heads to bind 36 nm apart when stepping along the actin filament. Myosin-5 is a high duty-ratio motor, where 'duty ratio' is defined as the fraction of time a myosin spends strongly bound to actin during its kinetic cycle. At duty ratios greater than 0.5, double-headed myosins can take more than one step without diffusing away from the actin filament. However, at a typical duty ratio observed for myosin-5, one can expect no more than eight processive steps per diffusional encounter with actin.[33,34] Processivity is greatly increased by mechanical gating between the heads. Load-dependent dynamics keep the biochemical cycles of the two heads out of synchrony, and increase the processive run length by reducing the probability that both heads detach from actin simultaneously. Relative to the rates of the single-headed construct, the rate of adenosine diphosphate (ADP) release on the trailing head was determined to be about 2.5-fold accelerated, but up to 250-fold slowed on the leading head by the two heads exerting strain on each other.[35] A distance of 36 nm

equals the pseudo-repeat of the helical actin filament[36], that allows myosin-5 to walk straight along the longitudinal axis of the actin filament instead of spiraling around the filament.[37] Motor and cargo can thus stay on the surface of dense cytoskeleton networks.

The development of Griscelli's syndrome type 1 – a rare autosomal recessive disorder characterized by albinism, immunodeficiency and, sometimes, neurological symptoms – is associated with mutations in the myosin-5a gene.[38] Griscelli's syndrome types 2 and 3 are caused by mutations in Rab27a and melanophilin, that form part of the myosin-5 cargo binding complex.

4.8.1.1.2.4 Myosin-6

Myosin-6 encoding genes are found in many multicellular organisms, where they are expressed ubiquitously. Members of the class-6 myosins are the only motors which move toward the pointed, or minus, end of actin filaments. Class-6 myosins display the basic myosin domain organization. They are formed from an N-terminal motor domain, a single IQ neck domain, a central tail region which is formed in part by an SAH helix, and a C-terminal cargo-binding domain. Unique inserts are found in the motor domain, the neck region, and the tail. A 22 amino acid insert (insert-1) near the ATP-binding pocket may control nucleotide on and off rates. A 53-amino acid calmodulin-binding insert (insert-2) in the neck redirects orientation of the lever arm to allow retrograde movement. The insert-2 domain, that associates with a calmodulin (CaM), is followed by an IQ motif which binds Ca^{2+}-depleted calmodulin (apo-CaM), a proximal tail domain which forms a three-helix bundle as seen crystallographically,[39] an α-helical[40] medial tail domain, a distal tail domain, and a cargo-binding domain.[40]

A large and a small insert in the tail domain generate alternatively spliced isoforms of myosin-6 with distinct intracellular locations and functions. Because it lacks a region which can mediate heavy-chain dimer formation, myosin-6 is thought to be a monomeric motor but may dimerize when the C-terminal cargo-binding domain is bound to lipid membranes.[41] Class-6 myosins play a role in the maintenance of the Golgi complex, participate in endocytosis, and are required for cell migration.[42] Myosin-6 interacts with a number of different binding partners at two specific sites in its C-terminal targeting region.[42c,43] This region contains no obvious structural motifs. It is composed of two proteolytically defined domains which are connected by a trypsin-sensitive linker. Each domain contains either a single RRL or WWY site for interaction with binding partners such as the 96-kDa protein disabled-2 (Dab2/DOC-2), the 67-kDa protein optineurin (FIP-2/nemo-related protein), the member of the postsynaptic density-95 like MAGUK (membrane associated guanylate kinase) protein family (SAP97), and GIPC (homologous to GLUT1 C-terminal-binding protein, SEMCAP-1 and synectin). In addition, each C-terminal domain contains a high-affinity binding site ($K_d = 0.3\ \mu M$) which mediates the association with PtdIns(4,5)P_2 (PIP_2)-containing vesicles. PIP_2-lipid binding induces a large structural change, including a 31% increase in helicity, which appears to regulate the recruitment of myosin-6 to clathrin-coated vesicles at the plasma membrane. Association with lipid vesicles appears to facilitate myosin-6 dimerization.[42c]

Myosin-6 depletion is not lethal, despite the finding that it is the only minus end-directed myosin motor protein so far identified, and it appears to play crucial roles in a large variety of cellular processes. Mutations in the myo6 gene in humans have been linked to hypertrophic cardiomyopathy.[44] It was shown, that class-6 myosins play a decisive role in the migration, and hence metastasis, of certain cancer cells, such as prostate cancer cells.[45] In *Drosophila*, myosin-6 was shown to play a role in gametogenesis, both in male[46] and female[47] individuals, and in spindle orientation during embryogenesis.[48] Mice with mutated myosin-6 genes develop Snell's Waltzer deafness, and the C442Y mutation in the motor domain of human myosin-6 causes the nonsyndromic hearing loss DFNA22.[49] It is assumed that myosin-6 can stabilize stereocilia in inner ear hair cells by anchoring the stereocilia to the cuticular plate.

4.8.1.1.2.5 Myosin-7

Class-7 myosins are among the most widely expressed myosins in the animal kingdom and display broad tissue expression. In the inner ear, *MYO7A* expression is restricted to the sensory cells of the vestibular and cochlear organs (hair cells). Two isoforms, myosin-7a and myosin-7b, have distinct kinetic and functional properties, and are expressed in vertebrates and some invertebrates. Myosin-7 is a single-headed motor protein. The myosin-7 heavy chain is composed of the N-terminal motor domain, the neck region with four to five IQ motifs, and a complex tail region which contains an SAH domain (absent in vertebrate myosin-7b and *Caenorhabditis elegans* myosin-7), an ~460-amino acid segment formed by a myosin tail homology 4 (MyTH4) domain and a band 4.1-ezrin-radixin-moesin (FERM) domain, an SH3 domain, and a second, C-terminal MyTH4-FERM tandem domain. Myosin-7a activity was shown to be regulated by an interaction between the tip of the tail and the motor domain.[50] Moreover, it was shown that the SAH domain can act as an extension of the lever arm.[51] It has been suggested that myosin-7 acts by exerting local tension, especially at the plasma membrane, and moving cargos. Recently, myosin-7a was found to associate with lysosomes and may be involved in lysosome trafficking.[52]

Abnormal phenotypes associated with myosin-7b mutations have not been described. In contrast, deleterious effects of myosin-7a dysfunction were reported for a wide range of organisms. Class-7a myosins appear to play an important role in the proper functioning of the auditory system by interconnecting adjacent stereocilia and adherens junctions. In mice, mutations in the gene encoding myosin-7a were linked to nonsyndromic deafness DFNA11 and DFNB2.[53] Mutated mice develop the *shaker-1* phenotype and typically display neuroepithelial defects manifested by hearing loss and vestibular dysfunction, but no retinal pathology.

Usher syndrome is a relatively rare genetic disorder which is a leading cause of deaf-blindness. Patients with Usher syndrome I are usually born deaf, patients with Usher syndrome II are generally hard-of-hearing rather than deaf, and patients with Usher syndrome III experience a progressive loss of hearing. All patients with Usher syndrome experience gradual vision loss associated with retinitis pigmentosa – a

degeneration of the retinal cells. More than 80 mutations in human *MYO7A*, the gene encoding myosin-7a, are related to Usher syndrome 1B (USH1B), and more than 100 different *MYO7A* mutations distributed throughout the gene have been identified. In addition to mutations in *MYO7A*, discreet forms of Usher syndrome have been associated with mutations in the genes encoding harmonin (USH1C), cadherin-23 (USH1D), protocadherin-15 (USH1F), SANS (USH1G), usherin (USH2A), VLGR1b (USH2C), whirlin (USH2D), and clarin-1 (USH3A). USH1B causes congenital deafness, vestibular dysfunction, and prepubertal onset retinitis pigmentosa leading to blindness.[54] Some mutations in *MYO7A* result in USH3-like phenotypes, leading to a progressive loss of hearing and a lower incidence of vestibular dysfunction. Rare dominantly or recessively inherited forms of isolated deafness have also been associated with mutations in *MYO7A*.

4.8.1.1.2.6 Myosin-9

Members of class-9 myosin are found exclusively in metazoans. Vertebrates contain two myosin-9 genes, *MYO9A* and *MYO9B*. Mammalian myosin-9b, the only class-9 myosin studied so far, has unique motor properties.[55] Myosin-9 contains an N-terminal extension with sequence similarity to Ras-association domains. This N-terminal domain is followed by the conserved myosin head domain, carrying a loop 2 insertion of ~145 amino acids. The neck region of vertebrate myosin-9a consist of six unevenly spaced IQ motifs and, in the case of myosin-9b, of four evenly spaced IQ motifs. The tail regions contain domains C1 (C6H2, that binds two zinc ions) and a guanosine triphosphatase (GTPase)-activator protein domain for Rho-like GTPases (RhoGAP). Although invertebrate class-9 myosins have two C1 domains in their tail regions, the vertebrate members harbor only a single C1 domain positioned N-terminally to the RhoGAP domain. Myosin-9b acts as a single-headed processive motor, moving with a very slow but constant velocity of 20 to 40 nm s^{-1}.[56] The cellular role of class-9 myosins remains uncertain, but the RhoGAP domain might be involved in regulating actin organization and dynamics.[57] As motorized signaling molecules containing the RhoGAP domain in their tail, mammalian class-9 myosins may act by moving into actin-rich areas of the cell periphery, locally converting RhoA, RhoB, and RhoC in the inactive GDP form and thereby affecting processes such as cell adhesion, formation of lamellipodial extensions, and cell polarity.

4.8.1.1.2.7 Myosin-10

Class-10 myosins are specific to chordates and related organisms. Their neck region is formed by three IQ motifs and an SAH domain extension (see Section 4.8.2.3). Three PEST sequences separate the SAH helix from three pleckstrin homology (PH) domains. The PH domains in the tail allow myosin-10 to interact with membranes and phosphatidylinositol-3,4,5-trisphosphate. The C-terminal segment of the tail is formed by a MyTH4-FERM tandem domain. It has been shown that the myosin-10 MyTH4 domain mediates binding to microtubules, whereas the FERM domain mediates interactions with certain β-integrins and netrin receptors, and deleted in colorectal cancer (or DCC)/neogenin.[58] In addition to the main role of myosin-10 in the formation of filopodia, it was shown recently that myosin-10 is required for the proper assembly of meiotic spindles in *Xenopus laevis* oocytes.[59] It mediates F-actin-microtubule interactions in mitotic spindles, promoted by its ATP-dependent motor domain binding to F-actin and its binding to microtubules via a MyTH4/FERM domain in its tail.[60] Myosin-10 is essential for proper spindle anchoring, normal spindle length, spindle pole integrity, and progression through metaphase in oocytes.

4.8.1.1.2.8 Myosin-15

Two genes, *MYO15a* and *MYO15b,* encoding myosin-15 family members have been found in humans. However, *MYO15b* has been identified as an unprocessed pseudogene.[61] Myosin-15a messenger RNA and protein are present in a narrowly defined subset of neurosensory cells in the inner ear, and in neuroendocrine cells of the gut and pancreas.[62] Myosin-15a is produced by cells in the inner ear, and in neuroendocrine cells of the gut and pancreas. It is found at the tips of hair-cell stereocilia in the inner ear, mechanosensitive rodlike protrusions on the apical surface of cochlear and vestibular sensory cells. *In vitro* motility experiments suggest that myosin-15a functions as a plus end-directed motor and can deliver proteins to the tips of actin-based cellular protrusions.[63]

Myosin-15a is a single-headed myosin. Its heavy chain is composed of the N-terminal motor domain, the neck region with two IQ motifs, and a complex tail region which contains a MyTH4 domain, a region with weak FERM similarity, an SH3 domain, a MyTH4-FERM domain module, and a predicted class-1 PDZ-ligand at the C terminus.[64] The conserved motor domain is followed by a neck region which is composed of two consensus IQ motifs and potentially a third degenerate IQ motif. Whether the light chain of myosin-15a is CaM or a unique light chain remains to be determined.

Both human and mouse *Myo15a* are encoded by 66 exons. Thirty predicted myosin-15a isoforms ranging in molecular weight from 92 to 395 kDa have been identified. Exon 2 is alternatively spliced and encodes an approximate 1200-amino acid N-terminal extension of human and mouse myosin-15a.[65] The two most abundant isoforms of myosin-15a are identical in sequence except that isoform 2 lacks the 1187-amino acid amino-terminal domain preceding the motor.[64a] The long N-terminal extension does not contain any well-defined domains or motifs. Part of it may be intrinsically unstructured. Several proline-tyrosine (PY and YP) and tyrosine-glycine (YG) repeats are found in the two-thirds of the N-terminal extension which are closer to the N terminus. It has been speculated that the N-terminal extension forms elastic connections between the cytoskeleton and the plasma membrane, and can serve as an effective gating spring in the context of stereocilia.[66]

Mutations in myosin-15a are related to nonsyndromic deafness DFNB3 and the corresponding murine model *shaker-2*.[65a] Most of these mutations were found in the myosin tail (MyTH4/FERM domain), except for two mutations which were discovered in the motor domain at the N terminus (Q1229X) and the active site (G1358S).[67]

4.8.1.1.2.9 Myosin-16

Class-16 myosins are found solely in higher vertebrates. Myosin-16 exists in two isoforms; the long isoform (human,

1858 amino acids) corresponds to myosin-16b/myr8b. Shorter isoforms are splice variants which have a truncated tail domain and correspond to myosin-16 A/myr8a.[68] Class-16 myosins have an N-terminal extension of about 400 amino acids containing eight ankyrin repeats which possibly interact with protein phosphatase 1. The myosin motor domain is followed by a neck domain containing a single IQ. The tail domain of myosin-16b (amino acids 1177–1858) is extended and reveals several stretches of polyproline residues. Myosin-16b is the predominantly expressed isoform in developing neural tissue.[69] During interphase, myosin-16b localizes to the nucleoplasm of neurons, whereas myosin-16 A does not localize to the nucleus. Although the ankyrin repeat region may contribute to the nuclear localization of myosin-16b, its distal tail domain is necessary and sufficient to target the protein to the nucleus.[69]

4.8.1.1.2.10 Myosin-18

Class-18 myosins are produced by a wide range of vertebrates and many metazoan species, including arthropods and echinoderms. They are composed of a unique N-terminal domain, a motor domain with an unusual sequence around the ATPase site, a single IQ motif, a segmented coiled-coil region for dimerization, and a C-terminal globular tail. Class-18 myosins can be grouped into two subclasses, myosin-18 A and myosin-18B. Additional diversity is generated by variable splicing. The N-terminal 405 amino acids of the longest human myosin-18 A isoform (2054 amino acids) contain a KE motif and a PDZ domain. Following the single IQ motif, a long coiled-coil region in the tail domain mediates heavy-chain dimerization.[70] Human myosin-18 Aα is produced ubiquitously, whereas myosin-18 Aβ is produced specifically in hematopoietic cells.[71]

Myosin-18 Aα containing the PDZ domain seems to colocalize with the ER-Golgi complex, whereas myosin-18 Aβ lacking the PDZ domain localizes diffusely in the cytoplasm.[71] Recently, it was shown that myosin-18 A is a novel binding partner of the PAK2/betaPIX/GIT1 complex.[72] This suggests that myosin-18 A may play an important role in regulating epithelial cell migration via affecting multiple cell machineries. In addition, it was shown that GOLPH3 binds to myosin-18 A and connects the Golgi to F-actin. It has been speculated that this interaction enable myosin-18 A to provide the tensile force required for efficient tubule and vesicle formation.[73]

Much less information is available on myosin-18B. This myosin is encoded by a candidate tumor suppressor gene involved in human lung, ovarian, and colorectal carcinogenesis.[74] It was shown that myosin-18B interacts with the proteasomal subunit Sug1 via its C-terminal domain and is degraded by the ubiquitin-proteasome pathway.[75] In human striated muscle myogenic cells, myosin-18B is found predominantly in the cytoplasm and moves to the nucleus of myocytes upon differentiation of these cells.[76] In cardiomyocytes and the sarcomeres of adult muscle, this myosin is produced not only in nuclei, but also in a cytoplasmic striated pattern alternating with α-actinin. Furthermore, myosin-18B was shown to interact with HOMER2, a Homer/Ves1 family protein, forming a complex which is able to suppress anchorage-independent growth in tumor suppression.[77]

4.8.1.1.2.11 Plant myosins

There are three classes of plant myosins – the double-headed class-8 and class-11 myosins, and the single-headed class-13 myosins. Little is known about their functions. Myosin-8 contains a motor domain, a neck domain comprising three to four tandem IQ motifs, an α-helical coiled-coil domain, and a globular cargo binding domain. The protein appears to support the transport of small molecules, virus particles, and specific macromolecules through plasmodesmata, channels connecting plant cells. Myosin-11 shares a high degree of structural similarity with myosin-5, but the length of its neck region is more variable, with the number of IQ motifs varying between four and six. Myosin-11 appears to be abundantly produced in plant cells and is thought to be the motor supporting cytoplasmic streaming and organelle transport. *Chara corallina* myosin-11 exhibits motility rates of 100 $\mu m\ s^{-1}$, and is the fastest actin-based motor protein described.[78] It has been reported that myosin-11 moves processively in *in vitro* motility assays.[79] Myosin-13 has only been found in the green alga *Acetabularia cliftonii*, that belongs to the order Dasycladale.[5]

4.8.1.1.2.12 Parasite myosins

Apicomplexa parasites, such as *Toxoplasma* or the malaria parasite *Plasmodium*, use sophisticated, ingenious invasion strategies to infect their host cells. Parasites belonging to the apicomplexa which infect animals or humans[80] include *Toxoplasma* and *Plasmodium*, and the genera *Eimeria*, *Isospora*, *Cyclospora*, *Babesia*, *Cryptosporidium*, *Theileria*, and *Sarcocystis*. Most protozoa use flagella or cilia for active movement. In contrast, apicomplexa move and actively penetrate host cells based on an actomyosin-dependent mode of motion, that is generally referred to as 'gliding motility'.[81] Class-14 myosins are generally small and display sequence similarity only ~30% with the motor domains of conventional myosins. They lack a conventional neck region, as indicated by the absence of proper IQ motifs.[82] The parasitic cytoskeletal actomyosin motor, composed of unusually short actin filaments and the short myosin A, is a key component in the motility and invasion of the parasites.[81c] In addition to their role in the motility and invasion, the class-14 myosin C was found to be involved in cell division and replication of *Toxoplasma gondii*.[83] A recent reassessment of myosin phylogeny and classification, incorporating a number of novel sequences uncovered by several genome sequencing initiatives, has expanded the known repertoire of myosin heavy chains from apicomplexans and other protists. It established six new myosin classes, three of which are restricted to alveolates (class-22, –23, –24), and includes 12 sequences from the ciliate *Tetrahymena thermophila* in class-14.[5]

4.8.1.2 Recombinant Production and Molecular Genetic Manipulation of Myosin

Myosins are among the most abundant proteins with regard to biomass and can be easily enriched from a wide range of sources. Nevertheless, progress on functional and structural characterization was delayed by difficulties in obtaining homogeneous preparations of individual isoforms and their soluble fragments until the advent of recombinant DNA

technology. Kinetic characterization of myosin requires the generation of soluble fragments. Recent progress in our understanding of actomyosin-dependent chemomechanical transduction has, to a large extent, been facilitated by the Genome Project-related identification of the entire complement of myosin encoding gene sequences for humans and many other species, and the generation of molecular genetic tools for the production of recombinant myosin motor domains. The use of RNA interference as research tool, and the tagging of recombinant myosin and myosin mutant constructs with fluorescent proteins, have opened the way for the molecular genetic dissection of myosin function in a wide range of organisms.

4.8.1.3 Domain Topology and Structure of the Myosin Head

Figure 3 shows the structure of the myosin head fragment as a ribbon diagram and a schematic topology map indicating the subdomains and their secondary structural elements. The core of the myosin motor domain is formed by a central, seven-stranded β sheet which is surrounded by α-helices. A SH3-like β-barrel domain is positioned close to the N terminus. The function of this small domain is unknown; however, it is absent in class-1 myosins and thus appears not to be essential for motor activity. A large structural domain, that accounts for six of the seven strands of the central β sheet, is formed by residues 81 to 454 and 594 to 629. Unless otherwise stated, sequence numbering refers to the *Dictyostelium discoideum* myosin-2 heavy chain throughout this chapter. This domain is usually referred to as the upper 50-kDa domain (U50). A large cleft divides the upper 50-kDa domain from the lower 50-kDa domain (L50), a well-defined structural domain formed by residues 465 to 590. The actin binding region and nucleotide binding site of myosin are on opposite sides of the seven-stranded β sheet and phosphate moiety of the nucleotide at the rear of the nucleotide binding pocket. The P-loop, Switch-1, and switch-2 are located in the upper 50-kDa domain close to the apex of the large cleft. All three nucleotide binding motifs contact the phosphate moiety of the nucleotide at the rear of the nucleotide binding pocket and act as β-phosphate sensors. Structures obtained in the absence and presence of ATP analogues indicate that the switch motifs move toward each other when ATP is bound, and move away from each other in its absence. Switching between ATP and ADP states is associated with specific intramolecular movements, analogous to the nucleotide-dependent conformational transitions in G-proteins.[84] Conformational changes during the transition between different nucleotide states appear mostly to correspond to rigid-body rotations of secondary and tertiary structural elements. The motor domain can thus be regarded as consisting of communicating functional units, with substantial movement occurring in only a few residues. Residues 411 to 441 form a long helix which runs from the actin binding region at the tip of the large cleft to the fifth strand of the central β sheet. A broken helix is formed by residues 669 to 689. The broken helix is frequently referred to as the 'SH1-' and 'SH2-helix region', named for reactive cysteine residues. The SH1/SH2 region is tightly linked to the converter domain, that functions as a socket for the C-terminal light-chain binding domain. The relay helix, a long helix which emerges from the Switch-2 region, is in contact with the SH1 helix. As its name implies, the relay helix functions in communicating conformational information between the actin binding site, nucleotide binding site, and the mechanical amplifier elements in the neck region.

There are approximately 70 myosin motor domain structures deposited in the protein database (www.rcsb.org) derived from X-ray crystallography (Table 3), with most derived from *Dd* myosin-2. Other structures were derived from scallop (*Pm* and *Ai*), squid (*Lp*), chicken (*Gg*), or pig (*Ss*). Crystals were obtained under various conditions, with and without bound nucleotide or in complex with a series of nucleotide analogues. There are no structures of human myosins yet, and there are no high-resolution structures of full-length myosins or myosins in complex with actin filaments (F-actin). Despite their highly conserved features, only the motor domains of members of four myosin classes have been characterized structurally. In addition to the various structures of class-2 myosins, the structure of one myosin-1 motor domain (Protein Data Bank [PDB] 1LKX), four structures of chicken myosin-5a motor domains (PDB 1W7I, 1W7J, 1W8J, and 1OE9), and five structures of class-6 myosin motor domains (PDB 2VAS, 2VB6, 2V26, 2BKH, and 2BKI) have been solved. In other words, our understanding of structure-function relationships in the myosin and actomyosin systems is restricted to the motor domain, several more common interaction motifs in the tail region of unconventional myosins, and the neck regions of a small selection of myosin superfamily members. However, hybrid approaches, combining high-resolution structural information with results obtained using other biophysical and computational techniques, have produced insights into many aspects of the molecular mechanisms governing myosin function).[11,85]

4.8.1.4 A Chemomechanical Model of the Actomyosin ATPase Cycle

A model combining kinetic and mechanical states during the cyclic interaction of the myosin motor domain with ATP and F-actin was first proposed by Lymn and Taylor,[86] based on insights gained from transient kinetic studies on F-actin and soluble myosin head fragments, and from electron micrographs of cross-striated muscle. On the basis of experimentally solved high-resolution X-ray structures, electron microscopy (EM) experiments with the isolated proteins, and solution kinetics, this chemomechanical cycle was further refined by assigning chemical states, that are defined by the nucleotide bound at the active site, to experimentally observed structural states (Figure 4). Starting with a nucleotide-free myosin or 'apo-state' and the lever arm in the 'postrigor' position, the motor protein is tightly bound to the actin filament [$A \cdot M$]. Binding of ATP to myosin initiates the dissociation of the actomyosin complex as a result of the negative cooperativity between actin and ATP, converting the motor to a state which is referred to as 'postrigor' or 'prehydrolysis state'. Conformational changes in the motor domain lead to the repositioning of the lever arm and the formation of the hydrolysis competent 'postrecovery stroke state' [$M^* \cdot T$]. In this detached state,

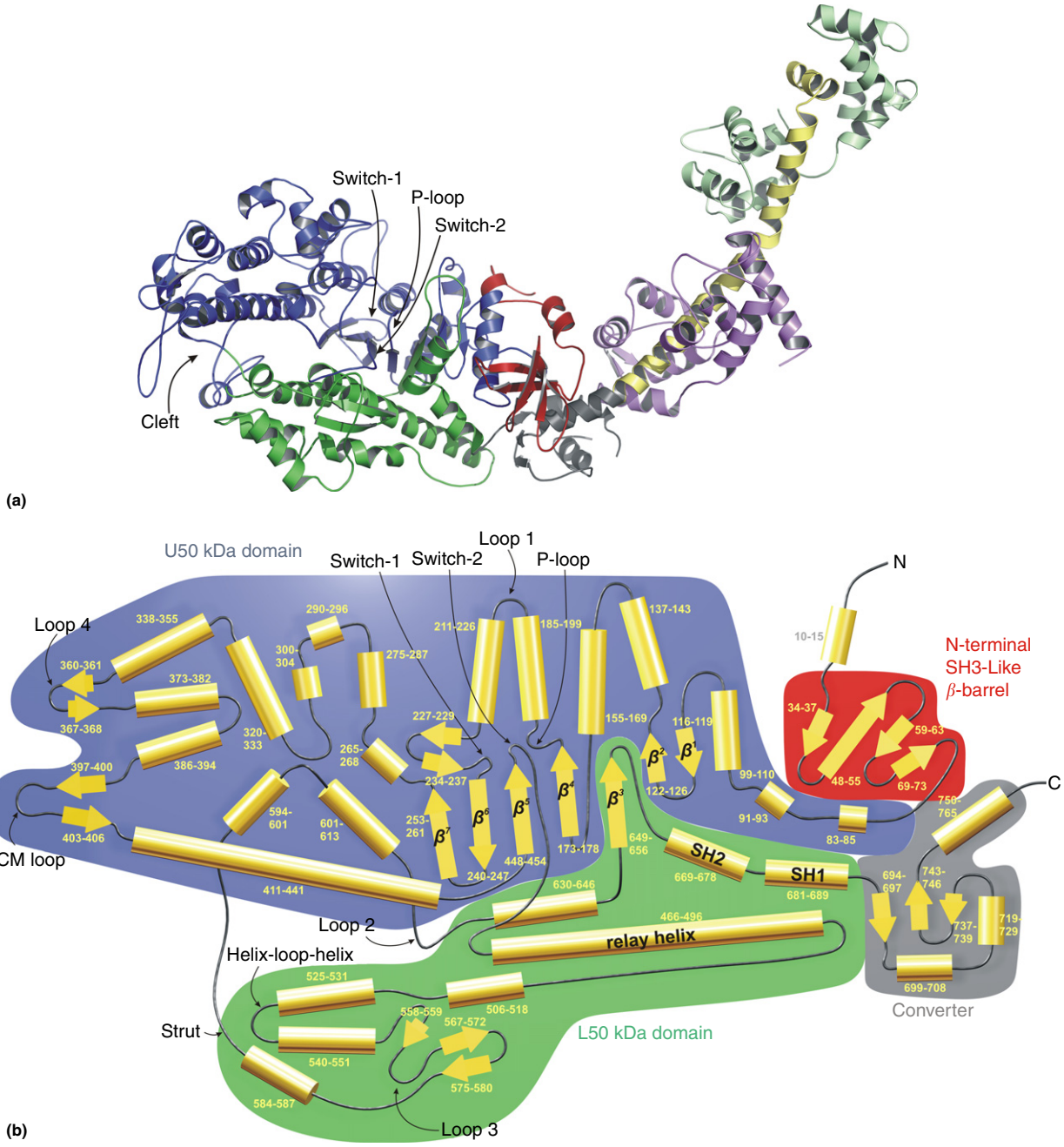

Figure 3 (a) Ribbon representation of the chicken myosin head fragment X-ray structure (PDB2MYS) color coded for the proteolytic subdomains. Red, N-terminal SH3-like domain; blue, U50-kDa domain; green, L50-kDa domain; gray, converter domain; purple, essential light chain; pale green, regulatory light chain; yellow, light-chain binding IQ motifs. (b) Topology map of the myosin-2 motor domain. Helices are shown as cylinders and β strands as arrows.

the hydrolytic cleavage of the ATP to ADP $\cdot$ P_i takes place. The equilibrium constant for the hydrolysis step is close to one for most myosins examined. Subsequently, myosin rebinding to the actin filament takes place, initially resulting in the formation of the weak affinity, metastable 'pre-power stroke state' $[A \cdot M^* \cdot D \cdot P_i]$ and progressing to the 'posthydrolysis state' with moderate actin affinity $[A \cdot M^* \cdot D + P_i]$. Isomerization steps concurrent with strong binding to actin, swinging of the lever arm, and force generation are coupled to the release of inorganic phosphate (P_i) $[A \cdot M \cdot D]$ and subsequently ADP $[A \cdot M]$. Except for the 'rigor state', most of the states described in this scheme are difficult to approach experimentally. Electron density maps of the actomyosin complex obtained by cryoelectron microscopy (cryoEM) are still of comparatively low resolution, and crystal structures of the myosin head were only obtained in the absence of actin. Nevertheless, it is possible to ascribe individual X-ray structures to certain states of the ATPase cycle.

Table 3 Available myosin X-ray structures in the Protein Data Bank (PDB) database (www.rcsb.org)

Myosin class	*Organism*	*Ligand 1 (active site)*	*Ligand 2*	*State (ATPase cycle)*	*Cleft*	*Active site*	*Lever arm position*	*Resolution (Å)*	*No. of amino acids*	*PDB ID*	*Ref.*
Motor domain											
1	*Dd*	Mg · ADP · VO_4	—	Prepower stroke	Partially closed	Closed	Up	3.0	697	1LKX	118
2	*Dd*	Mg · ADP	—	Postrigor	Open	Open	Down	2.3	776	1JWY	179
2	*Dd*	Mg · ADP	—	Postrigor	Open	Open	Down	2.3	776	1JX2	179
2	*Dd*	Mg · ADP/R238E	—	Postrigor	Open	Open	Down	2.8	1010	1G8X	116b
2	*Dd*	—	—	Postrigor	Open	Open	Down	2.1	761	1FMV	180
2	*Dd*	Mg · ATP	—	Postrigor	Open	Open	Down	2.15	761	1FMW	180
2	*Dd*	Mg · *m*-NphAE · BeF_3	—	Postrigor	Open	Open	Down	2.0	761	1D0X	181
2	*Dd*	Mg · *o*-NphAE · BeF_3	—	Postrigor	Open	Open	Down	2.0	761	1D0Y	181
2	*Dd*	Mg · *p*-NphAE · BeF_3	—	Postrigor	Open	Open	Down	2.0	761	1D0Z	187
2	*Dd*	Mg · *o, p*-NphAE · BeF_3	—	Postrigor	Open	Open	Down	2.0	761	1D1A	181
2	*Dd*	Mg · *o, p*-NPhAP · BeF_3	—	Postrigor	Open	Open	Down	2.0	761	1D1B	181
2	*Dd*	Mg · *N*-methyl-NphAE · BeF_3	—	Postrigor	Open	Open	Down	2.3	761	1D1C	181
2	*Dd*	Mg · MNT	—	Postrigor	Open	Open	Down	1.9	762	1LVK	182
2	*Dd*	Mg · ADP	—	Postrigor	Open	Open	Down	2.1	762	1MMA	183
2	*Dd*	Mg · ATPγS	—	Postrigor	Open	Open	Down	2.1	762	1MMG	183
2	*Dd*	Mg · AMP · PNP	—	Postrigor	Open	Open	Down	2.1	762	1MMN	183
2	*Dd*	Mg · ADP · BeF_3	—	Postrigor	Open	Open	Down	2.0	762	1MMD	104
2	*Dd*	Mg · PPi	—	Postrigor	Open	Open	Down	2.7	762	1MNE	184
2	*Dd*	Mg · ADP · BeF_3	—	Postrigor	Open	Open	Down	1.75	770	1W9I	185
2	*Dd*	Mg · ADP · BeF_3	—	Postrigor	Open	Open	Down	2.0	770	1W9K	185
2	*Gg*	Mg · ADP · AlF_4	—	Prepower stroke	Partially closed	Closed	Up	3.5	820	1BR1	144
2	*Gg*	Mg · ADP · AlF_4	—	Prepower stroke	Partially closed	Closed	Up	2.9	791	1BR2	144
2	*Dd*	Mg · ADP · VO_4	—	Prepower stroke	Partially closed	Closed	Up	1.9	762	1VOM	186
2	*Dd*	Mg · ADP · AlF_4	—	Prepower stroke	Partially closed	Closed	Up	2.6	762	1MND	104
2	*Dd*	Mg · ADP · VO_4	Blebbistatin	Prepower stroke	Partially closed	Closed	Up	2.0	762	1YV3	169
2	*Dd*	Mg · ADP · VO_4	BL4	Prepower stroke	Partially closed	Closed	Up	2.0	762	3BZ7	187
2	*Dd*	Mg · ADP · VO_4	BL6	Prepower stroke	Partially closed	Closed	Up	2.2	762	3BZ8	187
2	*Dd*	Mg · ADP · VO_4	BL7	Prepower stroke	Partially closed	Closed	Up	2.1	762	3BZ9	187
2	*Dd*	Mg · ADP · AlF_4	—	Prepower stroke	Partially closed	Closed	Up	2.0	770	1W9J	185
2	*Dd*	Mg · ADP · AlF_4	—	Prepower stroke	Partially closed	Closed	Up	1.95	770	1W9L	185
2	*Dd*	Mg · ADP · BeF_3	—	Postrecovery stroke	Partially closed	Closed	Up	3.6	820	1BR4	144
2	*Dd*	Mg · ADP · VO_3	—	Postrecovery stroke	Partially closed	Closed	Up	2.3	788	2JJ9	173
2	*Dd*	Mg · ADP · VO_3	PBP	Postrecovery stroke	Partially closed	Closed	Up	2.8	788	2JHR	173
2	*Dd*	—	—	Rigorlike	Closed	Closed	Down	1.9	776	2AKA/ 1Q5G	188
5	*Gg*	SO_4^{2-}	—	Rigorlike	Closed	Closed	Down	2.7	766	1W8J	189
5	*Gg*	SO_4^{2-}	—	Rigorlike	Closed	Closed	Down	2.05	795	1OE9	114
5	*Gg*	Mg · ADP · BeF_3	—	Postrigor	Open	Open	Down	2.0	795	1W7J	189
5	*Gg*	Mg · ADP	—	Rigorlike	Closed	Closed	Down	3.0	795	1W7I	189
6	*Ss*	—	—	Rigorlike	Closed	Open	Down	2.4	814	2BKH	123

(*Continued*)

Table 3 Continued

Myosin class	Organism	Ligand 1 (active site)	Ligand 2	State (ATPase cycle)	Cleft	Active site	Lever arm position	Resolution (Å)	No. of amino acids	PDB ID	Ref.
6	*Ss*	SO_4^{2-}	—	Rigorlike	Closed	Open	Down	2.9	858	2BKI	123
6	*Ss*	Mg · ADP · BeF_3	—	Postrigor	Open	Open	Down	2.4	788	2VAS	190
6	*Ss*	Mg · ADP · BeF_3	—	Postrigor	Open	Open	Down	2.3	788	2VB6	190
6	*Ss*	Mg · ADP · VO_4	—	Prepower stroke	Partially closed	Closed	Up	1.75	784	2V26	126
S1											
2	*Lp*	—	—	Rigorlike	Closed	Closed	Down	2.6	839	3I5G	191
2	*Lp*	—	—	Rigorlike	Closed	Closed	Down	3.4	839	3I5H	191
2	*Lp*	SO_4^{2-}	—	Rigorlike	Closed	Partially closed	Down	3.3	839	3I5I	191
2	*Pm*	—	—	Rigorlike	Closed	Closed	Down	3.25	838	2EC6	191
2	*Lp*	—	—	Rigorlike	Closed	Closed	Down	3.4	839	2EKV	191
2	*Lp*	SO_4^{2-}	—	Rigorlike	Closed	Partially closed	Down	3.3	839	2EKW	191
2	*Lp*	—	—	Rigorlike	Closed	Closed	Down	2.6	839	2OVK	191
2	*Pm*	—	—	Rigorlike	Closed	Open ?	Down	3.3	840	2OS8	191
2	*Gg*	SO_4^{2-}	—	Postrigor	Open	Open	Down ?	2.8	843	2MYS	192
2	*Lp*	Mg · ADP	—	Postrigor	Open	Open	Down	3.1	839	3I5F	191
2	*Pm*	Mg · ADP	—	Postrigor	Open	Open	Down	3.1	840	2OTG	191
2	*Lp*	Mg · ADP	—	Postrigor	Open	Open	Down	3.0	839	2OY6	191
2	*Ai*	Mg · ADP/SO_4^{2-}	—	Postrigor	Open	Open	Down	3.1	840	1S5G	193
2	*Ai*	SO_4^{2-}	—	Postrigor	Open	Open	Down	2.75	840	1SR6	193
2	*Ai*	$Mg^{2+} \cdot SO_4^{2-}$	—	Postrigor	Open	Open	Down	3.2	837	1KK7	194
2	*Ai*	—	—	Postrigor	Open	?	Down	4.2	830	1DFK	195
2	*Ai*	Mg · ADP · VO_4	—	Prepower stroke	Partially closed	Closed	Up	2.5	840	1QVI	196
2	*Ai*	Mg · ADP · VO_4	—	Prepower stroke	Partially closed	?	Up	4.2	831	1DFL	195
2	*Ai*	Mg · ADP	—	Internally uncoupled	Open	?	Uncoupled	2.5	835	1B7T	197
2	*Ai*	Mg · AMP · PNP	—	Internally uncoupled	Open	?	Uncoupled	3.0	835	1KQM	194
2	*Ai*	Mg · ATPγS	*p*-PDM	Internally uncoupled	Open	?	Uncoupled	3.8	835	1KWO	194
2	*Ai*	Mg · ADP	*p*-PDM	Internally uncoupled	Open	?	Uncoupled	2.8	835	1L2O	194
2	*Ai*	Mg · ADP · BeF_3	—	Internally uncoupled	Open	?	Uncoupled	2.3	837	1KK8	194

As its name implies, actin was recognized early on to serve not only as the passive track on which myosins move, but also to play an active role in catalysis. Myosin displays poor ATPase activity in the absence of actin and requires the interaction with F-actin for fast release of the products of the hydrolysis reaction – P_i and ADP.

4.8.2 Structural Features of the Myosin Motor Domain

4.8.2.1 The Actin Binding Region

The exact details of the actomyosin interface, and the modulation of the interaction between the myosin motor domain and the actin filament during nucleotide turnover are of crucial importance for force generation and chemomechanical coupling. The interaction strength undergoes a stepwise increase from the low-affinity myosin-ATP state to the ~10 000-fold stronger bound nucleotide-free state (rigor; **Figure 4**). As a result of its filamentous nature, the actomyosin system is inaccessible to high-resolution structural analysis using crystallographic approaches. Structural information of the actomyosin complex has been obtained for the myosin motor domain bound to F-actin in the strong-binding nucleotide-free and ADP conformations. These states of the actomyosin complex are structurally accessible to cryoEM and small-angle X-ray scattering (SAXS), methods which are currently capable of delivering structural information on macromolecules up to a resolution of 1 nm. Models providing atomic-level details of the complex have been obtained by hybrid approaches which combine high-resolution X-ray structures of the globular myosin head and F-actin with the SAXS and cryoEM data (>13 Å).[87] The resulting models show each myosin head to interact mainly with one actin monomer in the filament (**Figure 5(a)** and **5(b)**[85b]).

The total contact area between the actin filament and myosin corresponds to about 2000 $Å^2$. The actin binding

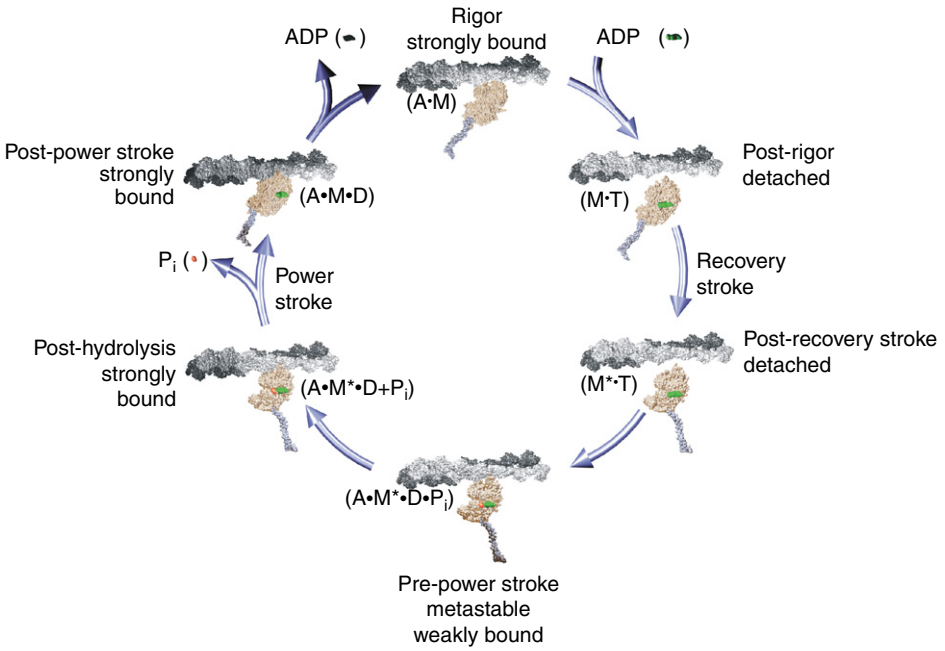

Figure 4 The actomyosin adenosine triphosphatase cycle.

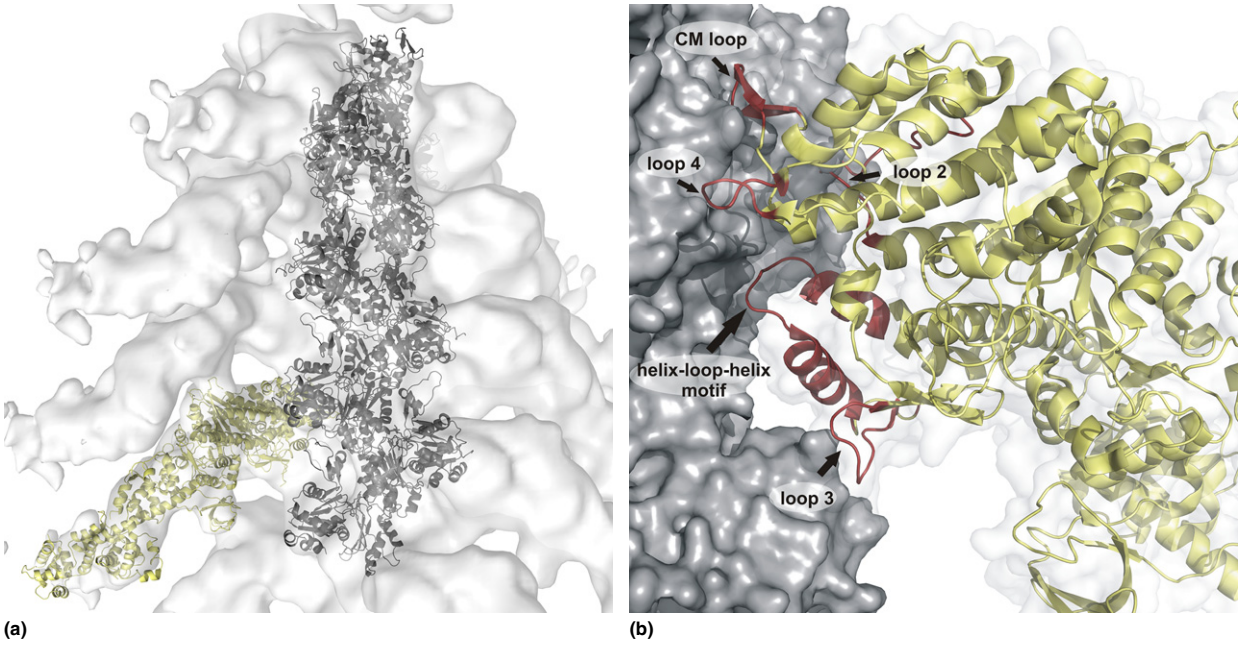

Figure 5 (a) The actomyosin complex. X-ray structures of myosin S1 (yellow) and actin (gray) are fitted into the cryoelectron microscopic map of actomyosin.[85b] (b) The actomyosin interface. The myosin motor domain is shown in cartoon representation (yellow), with F-actin as surface (gray). The actin binding region consists of a number of structural elements, including the cardiomyopathy (CM) loop, loop 2, loop 3, and loop 4, and the helix-loop-helix motif (shown in red).

region of myosin comprises topologically separate structures of the myosin motor domain. Loop 3 and the helix-loop-helix motif of the L50-kDa subdomain, the cardiomyopathy (CM) loop and loop 4 of the U50-kDa domain, and loop 2 linking L50 and U50 contribute to actin binding. Loop 2 has been shown to be involved in both weak and strong binding interactions with F-actin. Electrostatic contacts are formed in the initial weak binding of myosin to actin between positively charged lysine residues of this loop and negatively charged residues of the N-terminal region of actin.[88] A large number of mutagenic studies highlighted the role of loop 2 in the formation of the actin-myosin complex.[89] Loop 2 appears to be

highly variable in sequence between different myosins, and it was shown that the length and charge distribution of loop 2 have effects on actin affinity and the actin-activated ATPase activity of myosins.[88b,90] However, a more detailed analysis of the relative rates of observed evolutionary change reveals that the sequence of loop 2 is among the most constrained parts of the myosin molecule.[91] Key features like overall charge and charge density are similar for the loop 2 regions of most myosins; and myosins which are known to be kinetically or developmentally similar show only minor changes in this region. The most divergent loop 2 part is displayed by class-9 myosins. They contain a large 140- to 175-amino acid insertion in loop 2 and exhibit a significant affinity for actin even in the ATP-bound state.[92]

The CM loop lies at the tip of the motor domain, in close proximity to the entrance of the large cleft which separates the L50-kDa and U50-kDa subdomains. The CM loop plays an important role in the modulation of actin binding. A point mutation at position R403 in human β-cardiac myosin was the first mutation which was found to be associated with familial hypertrophic CM. Analyses of a recombinant R403Q mutant of human β-cardiac myosin, as well as the equivalent R397Q mutant of *Dd* myosin-2, show normal basal ATPase activity, a threefold reduced actin-activated ATPase activity, and a fivefold reduced motility in the *in vitro* motility assay.[93] The CM loop is the only region of the myosin motor domain which has been implicated to play a role in the physiological regulation of motor activity. In some unconventional myosin isoforms, the CM loop holds a phosphorylation site at the amino acid which is 16 residues upstream to the D in the consensus sequence DALAK (residue D403 in *Dd* myosin-2). These myosins are characterized by a threonine (T) or serine (S), where conventional myosins have an aspartate (E) or glutamate (D) residue. The site is generally referred to as the 'TEDS rule site'.[94] Phosphorylation of the threonine or serine residue at this particular position increases actin affinity in the presence of ATP, the coupling efficiency between actin and nucleotide binding sites, and the motor activity.[95] A cluster of hydrophobic residues in the CM loop was found to maintain the strong binding state. Replacement of residues 398–405 in *Dd* myosin-2 leads to the same phenotypic defects as observed following molecular genetic depletion of myosin-2.[96]

The positively charged loop 3 is primarily involved in electrostatic interactions with F-actin. Because the model fitting brings loop 3 into proximity with the neighboring actin monomer, on the long-pitch actin helix below the primary site of actomyosin interaction, it is also referred to as the 'secondary actin binding site of myosin'.[11b,88a] Crosslinking of loop 3 with F-actin was obtained with skeletal muscle myosin and with a chimeric construct of the *Dd* myosin-2 motor domain containing loop 3 of skeletal muscle myosin. Significant crosslinking between loop 3 and actin occurred with the N-terminal region of actin.[88a]

The helix-loop-helix motif is conserved in structure between different myosin classes. Hydrophobic residues are flanked by ionic and/or polar amino acids, and the motif is involved in both hydrophobic and electrostatic interactions. The motif was predicted to be the main, strong stereospecific binding site to actin.[97] Charge changes at positions 530 through 532 in this region resemble the effects of phosphorylation of the TEDS site. The presence or absence of a single negative charge at position 531 or 532 has a major effect on actin affinity, with little change being communicated to the nucleotide binding pocket. The E531Q mutation leads to a reduced actin affinity and reduced motility, whereas the Q532E mutation increases the affinity fivefold.[88c,98]

A high degree of functional conservation has been found in the way actin and different myosin isoforms interact with each other. Therefore, it was assumed that the docking process and the molecular details of the actomyosin interface in most instances are similar for myosins from different organisms and classes. Unfortunately, actomyosin models which are obtained by the current hybrid approaches are still ill-defined. New approaches or significant technical advances are required to improve the quality of the models and to allow better predictions about the features and structural details of the actomyosin interface. Here, technical advancement in the area of cryoEM will provide more accurate insights into the actomyosin interaction. Computer-assisted flexible docking of the high-resolution X-ray structures into lower resolution EM maps represents a new means to enhance the models and gain more detailed information. In addition, 'normal mode analysis'[99] and the use of spatial inverse distance weighting interpolation[100] have been used for flexible fitting of myosin head fragment X-ray structures into the envelopes of EM electron density maps of the acto-S1 complex, thereby allowing structural features of the protein to adjust to the docked environment.

The spatial interpolation approach in combination with the use of coarse-grained models was applied to the modeling of the acto-S1 complex based on an $\sim$14-Å cryoEM map. Compared with rigid-body docking of the individual domains, spatial interpolation produced a much better fit to the EM envelope and an overall root mean square deviation conformational change of 5.3 Å. The results are in good agreement with the result from constrained molecular dynamics simulations. It is thus an efficient alternative which requires only seconds of computing time. Another promising new technique is the molecular dynamics flexible fitting (MDFF) method.[85a,101] Atomic structures are flexibly fitted into the EM maps using classic molecular dynamics simulations. Forces proportional to the density gradient of the EM map are added in the molecular dynamics simulations to adapt the high-resolution X-ray structures to the EM envelope. The MDFF method avoids the use of reduced structural representations, as coarse model techniques inherently do, and enables the flexible and stereochemically correct fitting of atomic structures, while making use of all features contained in the EM maps during the simulations. A first report describing the use of the MDFF approach to fit atomic models into the interface, using a 13-Å resolution cryoEM density map as a constraint, describes more extensive contacts between actin and the myosin head.[85a] In the resulting model, the motor domain interacts clearly with two adjacent actin monomers. In particular, loop 3 and loop 4 move in toward the actin binding interface. Compared with previous models, these changes lead to a twofold increase of the contact surface between actin and myosin.[85a]

A disadvantage of the MDFF method is its high computational cost. The wider use of computer-assisted flexible fitting

methods, in combination with biochemical and biophysical validation, holds great promise for gaining new, important insights into details of the actomyosin interface and the underlying interactions.

4.8.2.2 The Mechanism of ATP Hydrolysis

Despite the importance of the hydrolysis reaction for myosin motor activity, details of the reaction mechanism still remain elusive. Partial information was revealed by the use of oxygen isotope exchange techniques in mechanistic quench flow studies. With the use of these biophysical techniques, it was shown that the hydrolysis reaction in myosin is carried out as a single-step reaction, with Walden inversion taking place at the γ-phosphate.[102] In addition, by using ^{32}P-labeled ATP as substrate for the hydrolysis reaction, it was shown that no phosphorylated myosin intermediate is formed during the reaction. Moreover, the results of subsequent ^{18}O exchange measurements indicated the formation of a pentavalent transition state of the nucleotide, rather than the formation of a metaphosphate intermediate.[103] All these investigations led to the assumption that the nucleotide hydrolysis reaction in myosin motors occurs preferentially via an associative mechanism rather than a dissociative one, although definitive proof is still missing. Recent investigation of the energy landscape around the hydrolysis transition state found a rather flat energy landscape in which the associative, dissociative, or concerted mechanisms are equally likely.[104] Nevertheless, the associative mechanism is well accepted as the predominant hydrolysis pathway in myosin. In the context of a hydrolysis mechanism with more associative character, the attacking water molecule needs to be activated by deprotonation, and the final attack is accomplished by the resulting hydroxide ion. Nucleophilic attack of the γ-phosphate by a water molecule would be energetically unfavorable. Kinetic studies demonstrated that the produced proton is released at the same time as the inorganic phosphate.[105] The key questions are: Where does the proton go and what acts as the general base? In the literature, several mechanisms for the activation have been proposed (**Schemes 1**).

1. The γ-phosphate itself acts as the base and the proton is directly transferred from the attacking water.[106]
2. S181 acts as a proton relay (the proton is transferred to the γ-phosphate).[107]
3. S236 acts as a proton relay (the proton is transferred to the γ-phosphate).[106]
4. K185 acts as a base and deprotonates the attacking water.[107]
5. K185 acts as an acid and protonates the γ-phosphate.[108]
6. The 'two-water hypothesis': The attacking water transfers the proton to a helper water molecule which is positioned by E459. In addition, E459 may act as the final base.[109]

Unfortunately, the individual steps of the hydrolysis reaction are difficult to approach experimentally. This gap is filled by the use of computer simulations which facilitate modeling enzymatic reactions at atomic resolution. Several computational approaches have been performed for the hydrolysis reaction in myosin motors and, altogether, five of the six proposed activation mechanisms have been examined. The simulations assumed an associative hydrolysis mechanism. Hybrid quantum mechanical (QM) and molecular mechanical reaction path calculations were used, because molecular mechanical reaction path calculations are not suitable for the modeling of processes involving bond breakage, and QM reaction path calculations are not practical for modeling the behavior of the entire motor domain as a result of the large size of the system.

Interestingly, the only two computational attempts where the entire myosin motor domain was included focused on the 'direct' activation pathway or pathways including proton relay mechanisms (S236 and S181),[110] although mutational studies of the corresponding serine residues did not abolish the ATP hydrolysis activity of myosin. These studies differ in the choice of initial X-ray structure, in the QM basis set, and in the treatment of electrostatic solvent effects. Within the error of the methods used, the three examined activation pathways for a direct, S236- and S181-mediated water attack were found to be equally likely, as represented by the small differences in the height of the calculated reaction barriers. The lowest barrier height was observed for the S236 proton relay pathway.[113a] However, all the calculated barriers are much higher than the experimental values. In general, the energy barrier for ATP hydrolysis in myosins is found experimentally to be reduced to approximately 14.5 kcal mol^{-1} [110b] compared with 28.9 to 29.3 kcal mol^{-1} in aqueous solution.[111] In the product state obtained by the simulations, the coordination of Mg^{2+} and S237 of Switch-1 appears to be broken. This loss of strong coordination between the Switch-1 loop and the metal ion was suggested to be coupled to the opening of Switch-1 after hydrolysis. Thus, it was proposed to constitute the key element for the initiation of the communication pathway between the active site and the actin binding region. Theoretical approaches, using only small-model systems of the nucleotide binding pocket, have provided additional support for the 'direct' pathway.[112] Calculations suggest mechanisms in which K185 acts as the acid which protonates the γ-phosphate,[108] or a mechanism supporting the two-water hypothesis with E459 acts as the final base.[113] In addition, the authors of the latter study speculated about E459 acting as a transient proton acceptor. Protonation of E459 might facilitate the opening of the salt bridge. This could, in turn, lead to the release of P_i together with the proton liberated during ATP hydrolysis. However, it is known that the protein environment exerts a large effect on the chemical reaction. Neglecting most of the protein during the calculations and confining the model system to residues in the active site thus lowers the reliability of the results dramatically. The consideration of additional activation pathways, such as dissociative or concerted mechanisms, still appears beneficial for gaining a better understanding of the progress of the enzymatic reaction. Other issues which arise from a static theoretical treatment of the hydrolysis reaction concern the neglect of thermal fluctuations of the protein and the possible occurrence of multiple transition states along the reaction path.

4.8.2.3 The Mechanism of Chemomechanical Coupling

Basic features of the mechanism of chemomechanical coupling in the actomyosin system are apparent from the model

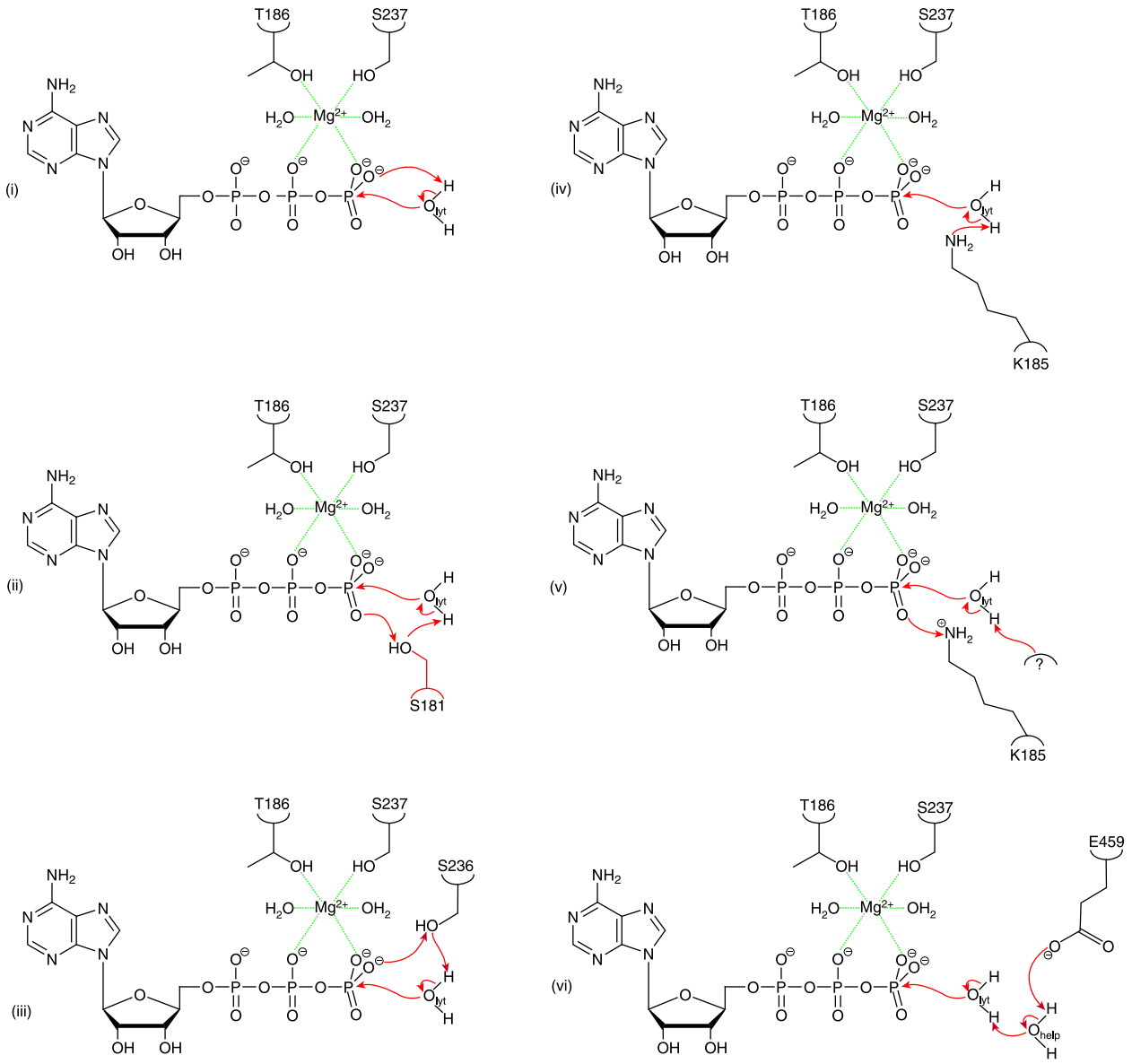

Scheme 1 Schematic diagram of six proposed associative mechanisms for the ATP hydrolysis in myosin. Electron transfer is indicated by red arrows. The six mechanisms differ in the way the lytic water (H_{lyt}) is activated and the liberated proton is transferred. (i) Direct activation; (ii) S181 acts as proton relay; (iii) S236 acts as proton relay; (iv) K185 acts as a base; (v) K185 acts as an acid; (vi) 'two-water hypothesis'.

shown in **Figure 4**. The energy liberated by the hydrolysis of Mg^{2+}-ATP is not directly converted into mechanical energy, because hydrolysis occurs while the myosin motor is detached from F-actin. Rather, ATP acts by releasing myosin from the stable rigor complex, inducing the formation of a hydrolysis competent state, followed by the stepwise return to the rigor state via a number of metastable intermediates with increasing affinity for F-actin. The process is strictly vectorial because ATP binding is irreversible. After ATP hydrolysis, progression through the various metastable states is accompanied by rebinding to F-actin and the emergence of small-scale movements in the nucleotide binding pockets, that are related to product release. These small movements are amplified within the motor domain and the adjacent neck region. The size of the power stroke is determined by the extent of this amplification, with the length of the lever arm and the size of the angular change as the major parameters. The direction of movement is determined by two factors. First, the myosin motor domain binds to the polar actin filament in a fixed orientation under formation of stereochemically well-defined interactions. Second, the directions in which the distal tip of the neck region projects away from the motor at the start and end of the power stroke is important. The velocity is determined by the stroke size and the rate-limiting step of ATP turnover. The duty cycle is defined by the ratio of time spend in strongly vs. detached or weakly attached states.

4.8.2.3.1 ATP-induced changes at the active site

High-resolution structures show large conformational changes in the active site between the nucleotide-free and the

catalytically competent structures.[84,114] In the structures thought to represent a rigorlike state with high actin affinity, the phosphate moiety sensing loops – Switch-1, Switch-2, and P-loop – are moved outward. This leads to an opening of the active site and a concomitant loss of its binding and catalytic competence. Biochemical studies indicate an ~10 000-fold lower ATP affinity in the rigor state compared with states with low actin affinity.[84] However, the reaction proceeds efficiently in the presence of physiological levels of Mg^{2+}-ATP, that are typically in the millimolar range. The P-loop senses the γ-phosphate of ATP entering the pocket and initiates the process of closing of the nucleotide binding loops. Triggered by this small initial conformational change and concomitant with the formation of a tight network of hydrogen bonds, Switch-1 and Switch-2 move toward each other. The concerted movement of the P-loop and closure of the Switch motifs position the nucleotide and create the active site primed for the enzymatic cleavage of the γ-phosphate. This sequence of events explains why ATP, but not ADP, can induce active site closure.

Figure 6(a) shows the conformation of the nucleotide in the catalytically active, closed pocket. A schematic representation of the hydrogen bond network, as observed in crystal structures of the hydrolysis-competent state of the myosin motor domain in complex with nucleotide analogues is shown in **Figure 6(b)**. More than 20 interactions are formed between the protein and the nucleotide. The Mg^{2+} ion is required for nucleotide binding to the active site. The divalent cation chelates the ATP with high affinity, stabilizes the protein-substrate complex, and is required for productive coupling of hydrolysis to motor function. A cation of similar size and overall charge, like Mn^{2+}, can be used both in crystallographic experiments as well as in kinetic studies without large changes in the rate of ATP turnover or motile activity.

The Mg^{2+} ion is coordinated by six ligands – two oxygens of the γ- and the β-phosphates of ATP, respectively; the side chains of S237 and T186; and two water molecules. Site-directed mutagenesis revealed additional contributions of the interacting residues to the hydrolysis reaction.[115] On the basis of these mutational studies, crucial roles in the ATP hydrolysis reaction were found for the residues K185 of the P-loop, R238 of Switch-1, and G457 as well as E459 of Switch-2. Mutation of these residues resulted in a loss or substantial decrease of myosin ATPase activity. Alanine scanning mutagenesis showed the involvement of N233, S237, and D454 in binding and retaining the nucleotide in the active site, because the binding of a fluorescent-labeled ATP was negatively affected in these mutants. No effects on ATPase activity or motility were observed for mutants involving residues S181, N235, S236, I455, and S456. Residues R238 and E459 form a salt bridge between Switch-1 and Switch-2. Myosin motor domains with mutations E459R or R238E, blocking salt bridge formation, show defects in nucleotide binding, reduced rates of ATP hydrolysis, and a 10-fold reduction in actin affinity. Inversion of the salt bridge in the double-mutant R238E/E459R eliminates most of the defects observed for the single mutants.[116] With the exception of a 2500-fold higher K_M value for ATP, the double mutant displayed enzymatic and functional properties very similar to those of the wild-type protein. These results show that, independent of its orientation, the salt bridge between Switch-1 and Switch-2 is required to support efficient ATP hydrolysis, normal communication between different functional regions of the myosin head, and motor function.[116]

4.8.2.3.2 Coupling between actin and nucleotide binding sites

Subsequent to the hydrolysis reaction and formation of the ADP · P_i complex, the myosin head rebinds to F-actin. Actin binding induces cleft closure and a series of subdomain movements leading to changes in the orientation of the three edge β strands: β1, β2 and β3 of the central β-sheet. Additional changes upon cleft closure are observed in the relative position of the U50 and L50 subdomains (**Figure 7**). The Switch-1 loop preceding β6, the Switch-2 loop following β5, and the P-loop following β4 move outward during the stepwise transition

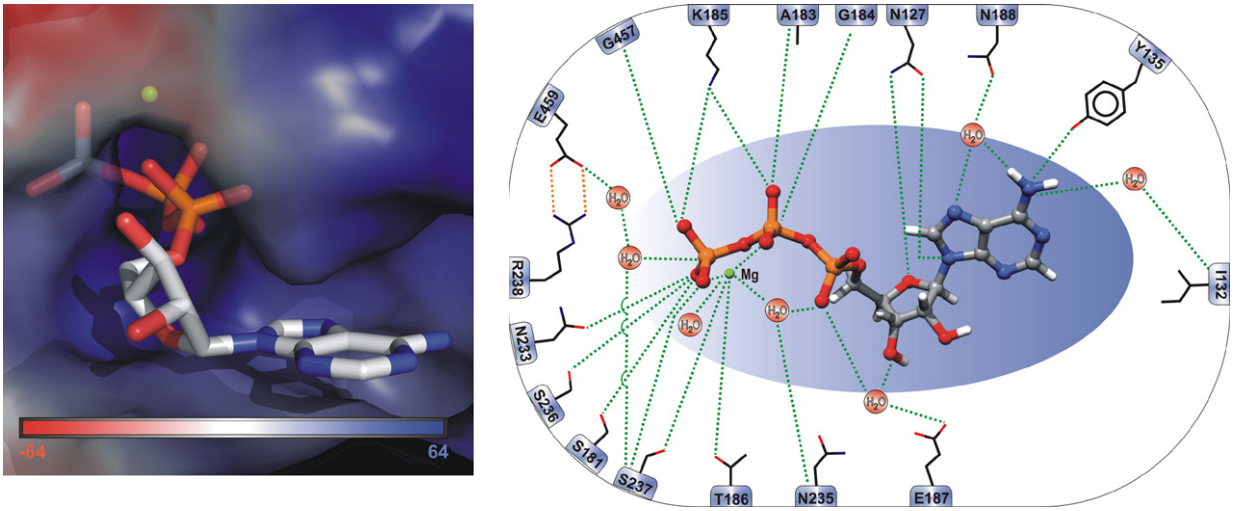

Figure 6 (a) The nucleotide binding pocket. The electrostatic potential is mapped on the surface representation of the nucleotide binding pocket. Blue, electropositive; red, electronegative. The values of the electrostatic potential are given as multiples of 25.85 mV ($k\,T\,e_c^{-1}$ at $T = 300$ K). (b) Schematic interaction diagram of ATP and myosin-2.

Figure 7 Cleft opening in myosin-5. Coupling between Switch-1 movement and the opening of the cleft (indicated by the arrows). Superposition of the rigorlike (red, Protein Data Bank [PDB] 1OE9) and postrigor state (cyan, PDB 1W7J).

from the catalytically competent structure with low actin affinity to the nucleotide-free structure displaying high actin affinity. Changes in the actin interface are thereby coupled to significant movements of nucleotide binding loops, resulting in the disruption of interactions which stabilize γ-phosphate binding and the coordination of the Mg^{2+} ion and, therefore, ADP binding. The loss of the Mg^{2+} ion coordination induced by actin binding is similar to the effect of GTPase exchange factors on the release of GDP by small G-proteins. Therefore, actin can be viewed as an ADP exchange factor for myosin.[84] This sequence of events explains the role of the central β sheet and associated loops as a transducer in the communication between the actin and nucleotide binding sites, and the reciprocal relationship between actin and nucleotide affinity.

4.8.2.3.3 Coupling to the neck region

In addition to the coupling between the nucleotide binding site and the actin binding region, a communication pathway is apparent leading to the converter and neck regions. The changes along this communication pathway are thought to be reversed but otherwise mostly similar for recovery and power strokes. Because the recovery stroke occurs while myosin is dissociated from F-actin, the recovery stroke is experimentally much more accessible and therefore better understood. The formation of the tight myosin-nucleotide complex triggers the converter domain, together with the neck region, to rotate by about 60° (recovery stroke), thus priming the lever arm for the power stroke. The recovery stroke is driven by the closing of the nucleotide binding pocket around ATP, as was shown by spectroscopic studies.[118] As described earlier, the P-loop senses the γ-phosphate upon ATP binding and initiates the process of closing of the nucleotide binding loops. High-resolution crystal structures of the myosin motor domain in the open nucleotide binding pocket state (postrigor) with the lever arm in the down position, and in structures in the closed active site state with the lever arm in the up position (pre-power stroke) were obtained with the help of nucleotide analogues.

A striking difference between the X-ray structures of the rigor and the pre-power stroke states is the presence or absence of a kink in the long relay helix (**Figure 8**). As its name implies, the relay region functions by communicating conformational information between the actin binding site, the nucleotide binding site, and the converter domain. The relay helix receives its input directly via Switch-2, to which it is directly connected, and indirectly via rearrangements in the central β sheet. The relay helix responds to the closing of Switch-2 and a change in the twist of the central β sheet by forming a kink. This change induces a rotation of the C-terminal end of the relay helix, that is transmitted to and enhanced by the SH1 helix, and results in a rotation of the converter domain by 60 to 70° in the case of myosin-2 (Animation 1). Hydrophobic contacts between the first turn of the lever arm helix and the N-terminal domain further stabilize the up conformation.[118] The extent of kink formation determines the size of the converter rotation. The structure of a class-1 myosin indicates that this type of motor can produce a 20 to 30° greater power stroke than myosin-2. *Dd* myosin-1E forms a more pronounced kink as a result of a hydrogen bond between Asn616 in the SH1 helix and Thr418 in the relay helix at the position of the kink. The Cα of Thr418 can thus move 1.5 Å farther into the core of myosin. Because the C-terminal end of the relay helix is tightly coupled to the converter domain, this kinking leads to a rotational movement of the converter domain. Highly conserved hydrophobic residues are responsible for the coupling, that occurs primarily in the area between the tip of the relay loop and the converter domain β core. Hydrophobic contacts between the first turn of the lever arm helix and the N-terminal domain further stabilize the lever arm in the up conformation. In myosin-1E, contacts are formed between Phe686, Tyr69, and Tyr71. Although these residues are completely conserved in class-1 myosins, similar hydrophobic contacts are absent in myosin-2.

Additional information about the mechanism underlying energetic coupling between changes in the nucleotide binding pocket and the position of the lever arm were obtained by combining the results of structural studies with calculations of minimum energy pathways between crystallographically defined end states, targeted molecular dynamics, and normal mode analysis.[119] The results of the individual approaches differ in details, but the combined complementary pathways give insights into a possible mechanism for the conformational transition, and reveal a number of "hot spot" residues which are involved in the 'chemomechanical coupling' of the recovery stroke. Although the minimum energy pathway approach does not provide a very detailed solution, the targeted molecular dynamics simulations identified a number of polar and hydrophobic residues which are involved in and required for the transition. According to the simulations, important polar interaction between Switch-2 and the relay helix are formed by E409, S456, Q468, N472, and N475. F458 of Switch-2 is buried in a hydrophobic pocket of surrounding residues which follow the motion of F458 during the closing of the nucleotide binding pocket. The formation of a crucial

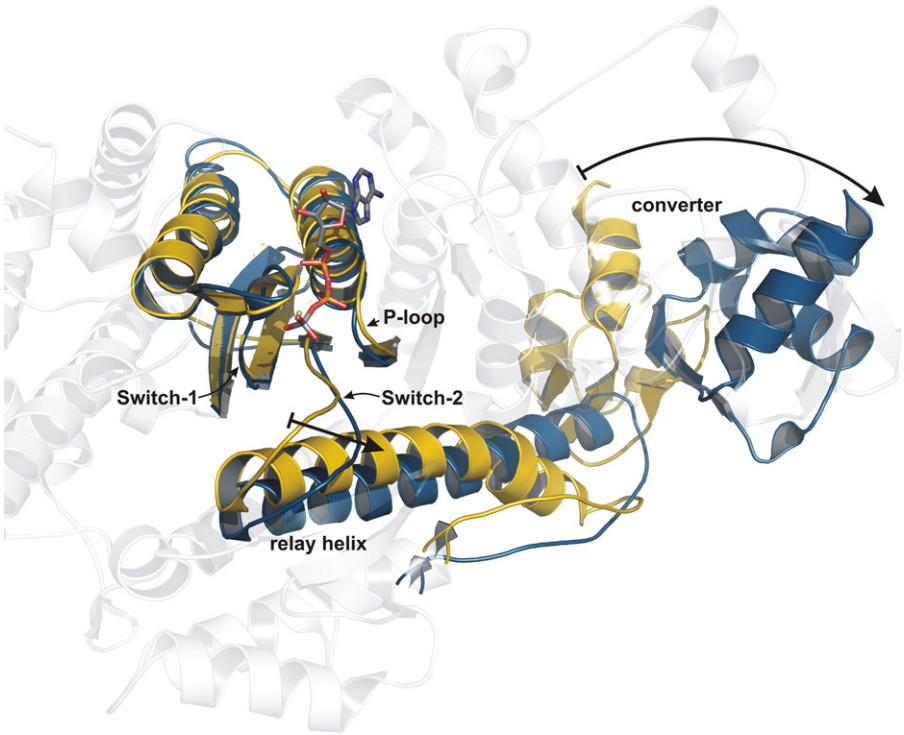

Figure 8 Power stroke and recovery stroke of myosin-2. Coupling between Switch-2 movement, the kinking/unkinking of the relay helix, and rotation of the converter during the power stroke (indicated by arrows) are shown. The postrigor (blue, Protein Data Bank [PDB] 1G8X) and pre-power stroke states (yellow, PDB 2JHR) are compared.

hydrogen bond between G457 to the γ-phosphate of the nucleotide is identified as the trigger for the kinking of the relay helix. In both theoretical approaches, the relay helix in its kinked form is stabilized by a hydrophobic core of surrounding aromatic residues (F482, F487, F503, F506, and F652). Polar residues which were identified to be important for the coupling between the relay helix and the SH1 helix are E490, E493, E497, R695, R738, and K743. The importance of many of these residues for myosin motile activity was confirmed by mutational studies.[115b,120]

4.8.2.3.4 Direction of movement

Besides its crucial role for force generation, the converter domain defines the directionality of the motor proteins. Most myosins share a high structural and sequence similarity among their converter domains, and move directionally along actin filaments toward the plus end (barbed end) of the actin filament. It was shown by molecular engineering that the direction of movement of a native plus end-directed myosin can be reversed simply by changing the direction the lever arm projects away from the motor domain by 180°.[121] This artificial backward-moving myosin was constructed from three preexisting molecular building blocks: a plus end-moving myosin-1 motor domain, a human guanylate-binding protein-1-derived four-helix bundle as the directional inverter, and two α-actinin repeats, forming an artificial lever arm. α-Actinin repeats were determined earlier to be functional replacements for the myosin lever arm (**Figure 9**).[122] Class-6 myosins are the only known myosins which naturally move toward the minus end of the actin filaments. Structural analysis revealed a unique insert (P774-W812 of myosin-6) in the converter domain which wraps around the converter and thereby redirects the attached lever arm by about 180° compared with plus end-directed myosins (**Figure 10**).[123] In addition, the distal part of the insert exhibits a previously undetected CaM binding site. Both, the insert and the associated CaM form specific interactions with the converter, whereas most interactions of the converter with the relay are maintained. *In vitro* motility experiments of chimeras of the myosin-6 motor domain and the myosin-5 lever arm, with and without the unique insert, demonstrated the insert in the myosin-6 converter to be the only determinant of directionality.[124]

Another issue related to class-6 myosins is the observed large step size (20–40 nm), despite myosin-6 possessing just a small neck region.[125] However, crystallographic analysis of the myosin-6 head fragments in the pre-power stroke state (PDB 2V26) reported an unusual conformation of the motor, facilitated by the unique insert, which enables class-6 myosins to rotate the converter together with the lever arm through a much larger angle (~180°) than observed with myosin-2 (~60°).[126] This large rotation of the lever arm during the power stroke is consistent with measurements in an optical trap[127] and fluorescence experiments measuring simultaneously the step size and angular changes of the lever arm.[128] Thus, the unique insert appears to be responsible both for the reversed directionality and the large step size of myosin-6 motors. In addition, a second unique insert (C278 to A303 in myosin-6) in the motor domain, close to Switch-1 of the nucleotide binding pocket, affects the nucleotide association

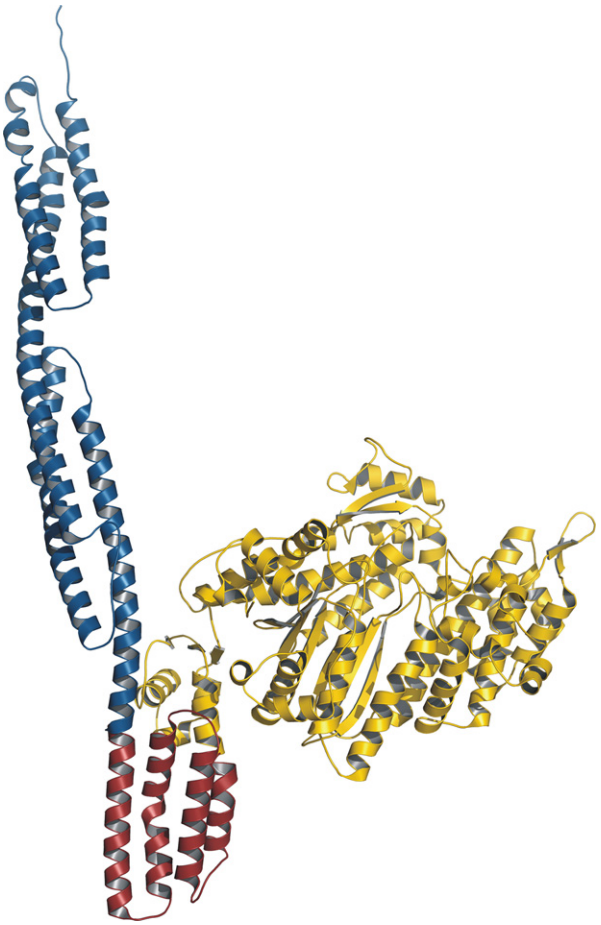

Figure 9 A model of an engineered, artificially reversed myosin. Reverse-direction movement of myosins can be achieved simply by rotating the direction of the lever arm 180°. The artificial minus end-directed motor consists of three building blocks: a myosin-1 motor domain (yellow), a directional inverter formed by a four-helix bundle segment of human guanylate-binding protein-1 (red), and an artificial lever arm formed by two α-actinin repeats (blue).

and dissociation rates and is responsible for the slow rate of nucleotide-induced dissociation of myosin-6 from the acto-myosin complex (40 times slower than myosin-5).[95e]

4.8.2.4 Unconventional Neck Extensions

In 2005, it was shown that myosin-10 has a 120-amino acid-long stable, single α-helical domain (SAH) in the neck region in addition to the IQ motifs.[129] SAH domains are found in several proteins, but were previously unseen in any myosin. In fact, this particular domain in myosin-10 was previously predicted to be a coiled-coil region. In contrast to coiled-coil α-helices, that are mainly hydrophobic, SAH domains are highly charged (rich in E, K, and R) with many stabilizing ionic interactions along the helix either between lysine and glutamate or between arginine and glutamate.[130] EM of myosin-10 showed that only the distal end of the SAH domain dimerizes, and the length of the lever arm corresponds to the length of three IQ motifs plus the 15-nm-long SAH domain.[129] In addition to myosin-10, class-6 myosins as well as myosin-7a and *Dd* MyoM contain E-, R-, and

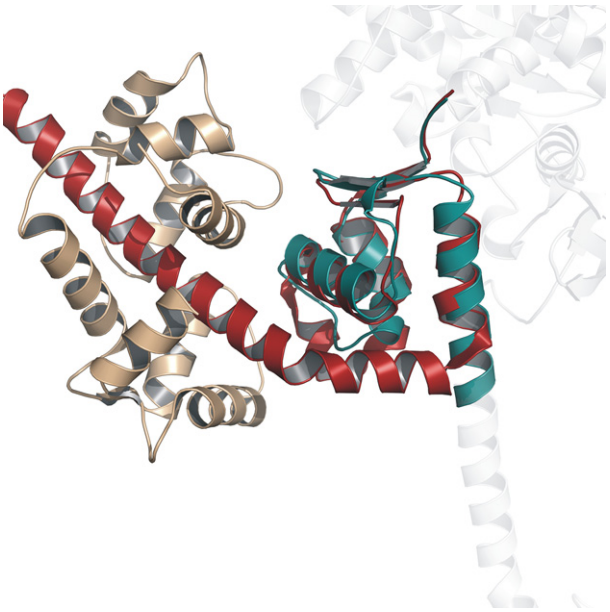

Figure 10 Comparison of the ~180° redirected myosin-6 converter domain (red, Protein Data Bank [PDB] 2BKI) and the myosin-2 converter (teal, PDB 1Q5G). A calmodulin light chain (pale brown) binds to the redirecting insert-2 of myosin-6. Myosin-2 is indicated as transparent silhouette. The myosin-2 light-chain binding region extends downward.

K-rich sequences, and are thus predicted to contain SAH domains in their neck regions. SAXS studies of a myosin-6 dimer, artificially linked by a leucine zipper, support the prediction of an SAH domain rather than a coiled-coil motif.[131] To test directly the capability of the SAH domain as an extension of the lever arm to increase the step size, EM experiments were carried out using a chimeric myosin-5 construct with only two of the six native IQ motifs as well as the putative SAH domain of *Dd* MyoM attached to the IQ region.[51] The results indicate that the SAH domain indeed functions as a part of the lever arm (**Figure 11**). The Myo5-2IQ-SAH chimera restored the length of the wild-type myosin-5 with its 6 IQ motifs, was capable of processive movement along actin filaments at physiological conditions, and yielded only a slightly reduced power stroke in an optical trap compared with the wild type. Thus, the SAH domain is part of the neck region in some myosin isoforms – mainly members of class-6, 7, and 10, as well as *Dd* MyoM. It serves presumably as an extension of the lever arm to increase the step size of these isoforms. Consequently, the results suggest the SAH domain to be at least partly responsible for the large step size in class-6 myosins. An alternative model for the extension of the myosin-6 lever arm was suggested by Mukherjea et al.[39] According to their model, the triple-helix proximal tail domain can extend from a zig-zag-zig geometry, that supports the length of a single α-helix (4 nm), to a length of 12 nm.[39]

4.8.3 Allosteric Communication

Allostery is defined as the modulation of a protein's activity by the binding of an effector or the modification of a residue at a

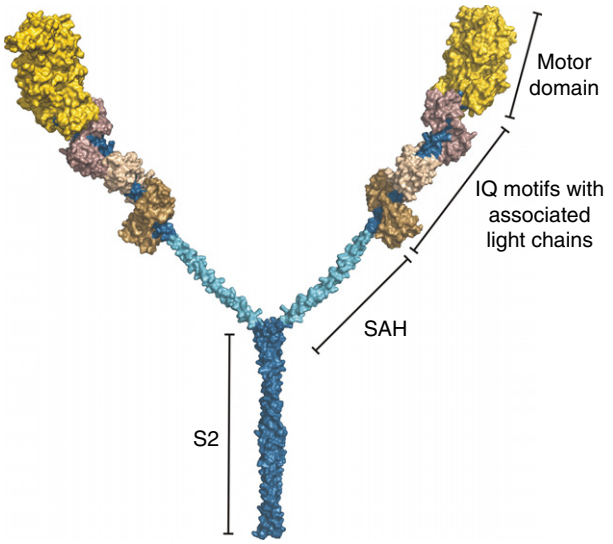

Figure 11 Model of a two-headed heavy meromyosin-like myosin-10 fragment with the single α-helix inserted between the IQ domain region and S2.

site distant from the active site. The allosteric trigger can be the binding of a small molecule ligand, the interaction with another protein, or the post-translational modification of an amino acid side chain. The concept of allostery is not the same as cooperativity, but cooperativity is rather a specific case of allosteric regulation. The term 'cooperativity' has been used extensively to describe the allosteric modulation in quaternary proteins with four binding sites, such as hemoglobin and CaM, in which the binding of a ligand to one site increases the affinity of the other sites for the same type of ligand. In that context, two models were proposed during the early 1960s – the Monod, Wyman and Changeux model, in which all subunits of a protein assembly must be in the same state to allow binding of a ligand to one subunit; and the Koshland, Nemethy and Filmer model, in which the binding of a ligand to one subunit induces all other subunits to take the same state. Nowadays, it is generally recognized that allostery occurs and can play a critical role in monomeric proteins.[132] Traditionally, the binding of an allosteric effector has been described to induce a conformational change in a remote site, thus changing the geometry or charge distribution at the active site. However, it has been recognized that a more accurate description of the structural changes underlying allosteric regulation requires that the dynamic properties of proteins are considered as well. In quite a number of cases, the binding of an allosteric modulator is not associated with discrete and well localized structural changes in a remote site, but rather has an impact on the global flexibility of the protein, leading to a population shift in the statistical ensemble of conformers.[133]

4.8.3.1 Myosin Regulation

The myosin motor itself is an intrinsic, allosterically regulated protein. Remote sites in the molecular motor communicate via pathways which connect distant sites, and trigger large conformational changes and ~10 000-fold changes in actin and nucleotide affinity during a normal mechanical cycle.[84,134] This intrinsic allostery is a specific type of allosteric modulation, because it does not include the binding of another effector molecule. In Section 4.8.2, the individual cases of intrinsic allosteric communication within the myosin head fragment are depicted. With regard to the chronological occurrence during the mechanical actomyosin ATPase cycle, these instances are as follows:

1. The coupling between the opening of the 50-kDa cleft (**Animation 2**) and the closing of the nucleotide binding site on binding of ATP
2. The coupling between the nucleotide binding pocket and the converter during the recovery stroke
3. The communication between the actin binding region (closure of the cleft) and the opening of the nucleotide binding pocket after ATP hydrolysis
4. The coupling between the nucleotide binding pocket and the converter domain leading to the power stroke

In all four cases, the opening or closing of the active site is involved in the allosteric communication, as described in detail earlier. However, details of structural changes occurring along the reaction coordinate of the actomyosin ATPase cycle can be further refined. The results of an elastic network model (ENM)-based normal mode analysis of the myosin-2 head, that specifically addressed the question of correlations between movements of the switch motifs and the opening/closing of the cleft on the one hand and the converter rotation on the other hand, are consistent with the coupling mechanisms deduced from structural analysis.[135] The ENM method describes the protein under study as a coarse-grained model with the C_α atoms connected by springs with a standard force constant. Correlation analysis of the low-frequency modes obtained from myosin-2 in the pre-power stroke state produces positive and significant correlation between the opening of Switch-1 and the closing of the 50-kDa cleft, as well as between the opening of Switch-2 and the downward rotation of the converter domain. No coupling was found between the opening of Switch-2 and the closure of the cleft. A significant correlation was also obtained between the opening of Switch-1 and the rotation of the converter domain, presumably transmitted through the closure of the cleft. Thus, the ENM analysis reflects the indirect coupling between actin binding and converter rotation, because binding of the actin filament to the myosin head has a positive allosteric effect on the rate of P_i release from the motor.

Allostery, likewise, plays an important role in the regulation of myosin motors. *In vivo*, the catalytic function and motor activity of most myosins are highly regulated. The major ways in which conventional myosins are regulated are through phosphorylation of their heavy chains or the associated regulatory light chains. Phosphorylation of the myosin-2 heavy chain by myosin heavy chain-kinases has been shown to influence filament formation of some isoforms negatively.[136] Studies on the regulation of *Dd* myosin-2 revealed that MHC phosphorylation occurs mainly at three threonines, positioned in the α-helical coiled-coil tail region (T1823, T1833, and T2029).[137] T1823 is located at the fourth (*d*) position of a heptad repeat, a key position reserved for hydrophobic residues.

Phosphorylation of T1823 is suggested to disturb the local coiled-coil structure whereas phosphorylation of T1833 or T2029, both located at the seventh position of a heptad repeat on the outside of the coiled coil, most likely interferes with electrostatic interactions between the tails of different myosin molecules. Mutational studies of the three threonines supported the importance of these residues for the filament assembly.[138] Aspartate mutants, mimicking the phosphorylated residues, led to an inhibited filament formation *in vitro* and a loss of function *in vivo*. The largest effect was found for T1833. Threonine-to-alanine mutations resulted in the formation of myosin filaments *in vivo*, but motility was inhibited. In *Dictyostelium*, dephosphorylation of the MHC is the most important mechanism which drives myosin-2 filament formation.[139]

Dd myosin-2 and class-2 myosins in general also hold a regulatory phosphorylation site, that has a direct impact on the motor activity. The introduction of a phosphate group on a single serine residue (S13) of the regulatory light chain (RLC) of *Dd* myosin-2 by myosin light-chain kinase A has been implicated in the four- to sixfold enhancement of motor activity of filamentous myosin, but has been proved to have no effect on filament assembly.[122a,140] The phosphorylation of S13 is stimulated by cyclic adenosine monophosphate, and mutation of the serine to alanine (S13A) resulted in no detectable phosphorylated RLC *in vivo* and *in vitro*, suggesting that it is the only phosphorylation site in the RLC.[141]

All class-2 myosins appear to have a motif of hydrophobic residues clustered in the region of the heavy chain where the RLC binds.[142] This conserved cluster of hydrophobic residues interrupts the α-helical coiled-coil structure of the heavy chain and causes the neck region to bend by $\sim 60^{\circ}$ to form a 'hooklike' structure (**Figure 12(a)**). The N terminus of the RLC embeds the 'hook' in a hydrophobic cavity. In general, binding of the RLC rather than CaM is restricted to class-2 myosins. The chemical removal of the RLC leads to the formation of large aggregates, in which the myosins are not able to form the highly ordered, helical filaments.

A framework for the underlying mechanism for the allosteric transmission of information from the regulatory light chain (RLC) to the more than 10-nm distant active site came from visualization of two-dimensional crystalline arrays as well as three-dimensional reconstruction of cryoEM maps (~ 20 Å) of dephosphorylated smooth muscle HMM.[143] Fitting the crystal structure of the vertebrate smooth muscle myosin motor domain, including part of the neck and the essential light chain (ELC),[144] into the EM maps revealed an asymmetric head-head interaction in which the actin binding region of one head is positioned on the converter and ELC of the neighboring head. This interaction interferes with the rearrangements of the domains needed for P_i release and activation. The corresponding state had already been observed in earlier EM experiments under conditions favoring an

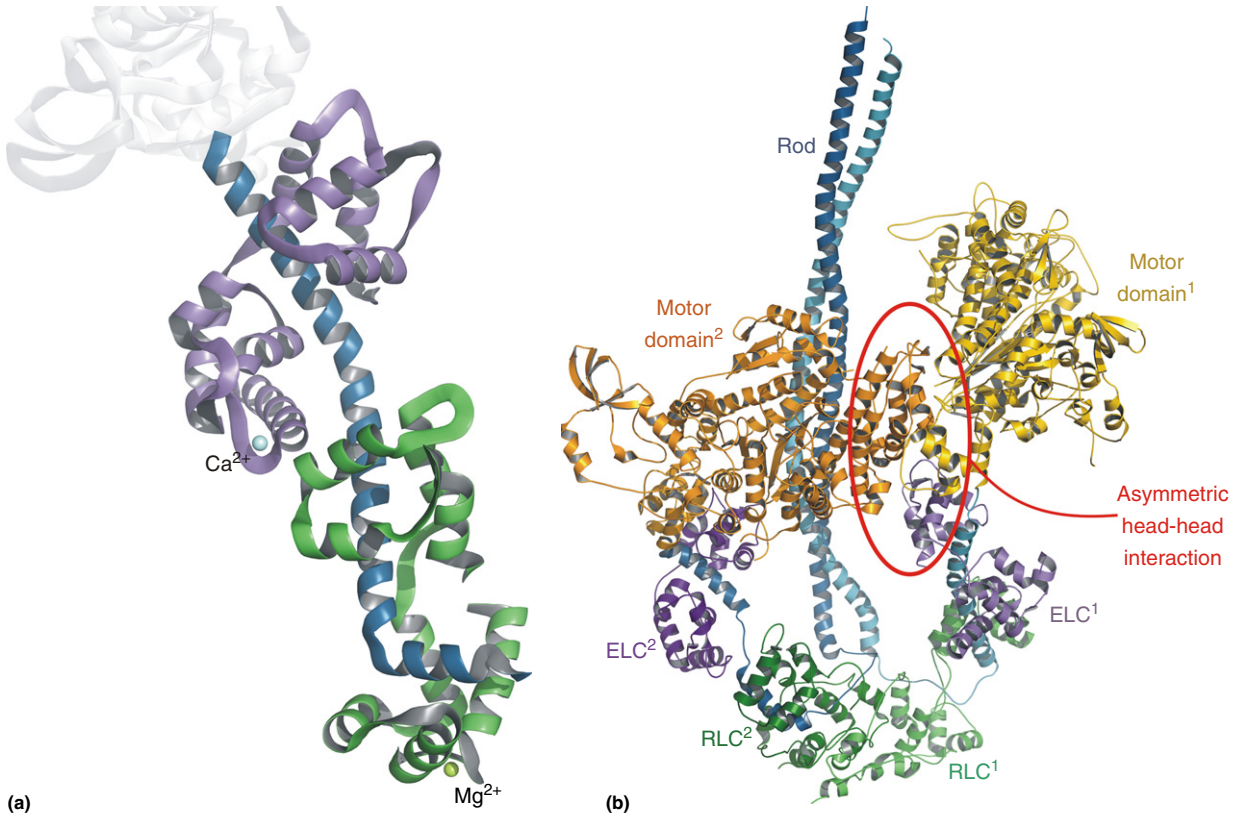

Figure 12 (a) Regulatory neck region of scallop myosin-2 (Protein Data Bank [PDB] 1WDC). The three-chain calcium binding site is formed by the essential light chain (ELC) (purple), the regulatory light chain (RLC) (green), and the myosin heavy chain (blue). The N-terminus of the RLC embeds the 'hook' of the myosin-2 heavy chain. (b) Asymmetric head-head interaction which stabilizes the 'off' state observed in *Tarantula* muscle myosin (PDB 3DTP).

inactive state, although the details of the head-head interaction had not been resolved.[145] In addition, the tails of these dimeric myosins were folded twice at about 50 nm and 100 nm away from the head-tail junction, instead of being extended α-helical tails (**Figure 12(b)**). The folded smooth muscle myosin had virtually no ATPase activity, thus constituting an 'off' state.[146] The structural results are consistent with mutational studies, showing the region K11 to R16 of the RLC to be important for stabilization of the 'off' state. Phosphorylation of the serine residue (S13 in *Dd* myosin-2) disrupts the interactions between the two myosin heads in the 'off' state. The occurrence of the asymmetric head-head interaction in the 'off' state has now been confirmed in thick filament structures of many other species, including *Tarantula*,[147] scallop,[148] *Limulus*,[149] as well as in vertebrate murine[150] and rabbit[151] cardiac muscles.

Folded intermediates have also been implicated in the regulation of myosin-5 activity. In the absence of calcium ions, myosin-5a sediments at 14S instead of 11S and adopts a compact, folded conformation.[152] However, binding of the GTD of myosin-5a to a cargo receptor is thought to be the physiological regulator of its motor activity, rather than changes in calcium ion concentration. GTD binding to cargo receptors disrupts the interaction between the motor domain and the tail, leading to the activation of both ATPase and motor activity.[153] An elegant aspect of this model is that only motors which are bound to cargo are functional.

4.8.3.2 Small-Molecule Inhibitors of Myosin Motor Activity

Several small chemical compounds have been identified that affect myosin motor activity in an allosteric manner (**Scheme 2**). 2,3-Butanedione monoxime (BDM) was one of the first noncompetitive myosin-2 inhibitors.[154] Although it binds only with a low affinity to myosin ($K_I \approx 5$ mM for skeletal muscle myosin-2), it was used widely in cell biological experiments. BDM decreases the ATPase rate and force production by inhibiting P_i release and stabilizing the weakly actin-bound Myosin · ADP · P_i state.[155] Because BDM was originally supposed to reactivate alkylphosphate-inhibited acetylcholinesterase,[156] it also has an effect on serine and threonine residue phosphorylation.[157] Unfortunately, BDM was found to affect many other proteins in addition to myosin, including potassium channels,[158] L-type calcium channels,[159] and myosin-2 light-chain kinase.[160] A targeted screening of a chemical library for new myosin inhibitors resulted in the discovery of *N*-benzyl-*p*-toluene sulfonamide (BTS), that inhibits the Ca^{2+}-stimulated ATPase of fast muscle myosin-2 S1 with an IC_{50} of ~5 μM.[161] BTS was shown to weaken the actin-myosin interaction, inhibit *in vitro* gliding motility in a reversible manner, and slow force production in muscle fibers. The observed inhibitory effect was much weaker in slow muscle skin fibers and in mammalian cardiac myosin.

Additional compounds which have been reported to inhibit the myosin Mg^{2+} · ATPase activity are the fluorescent

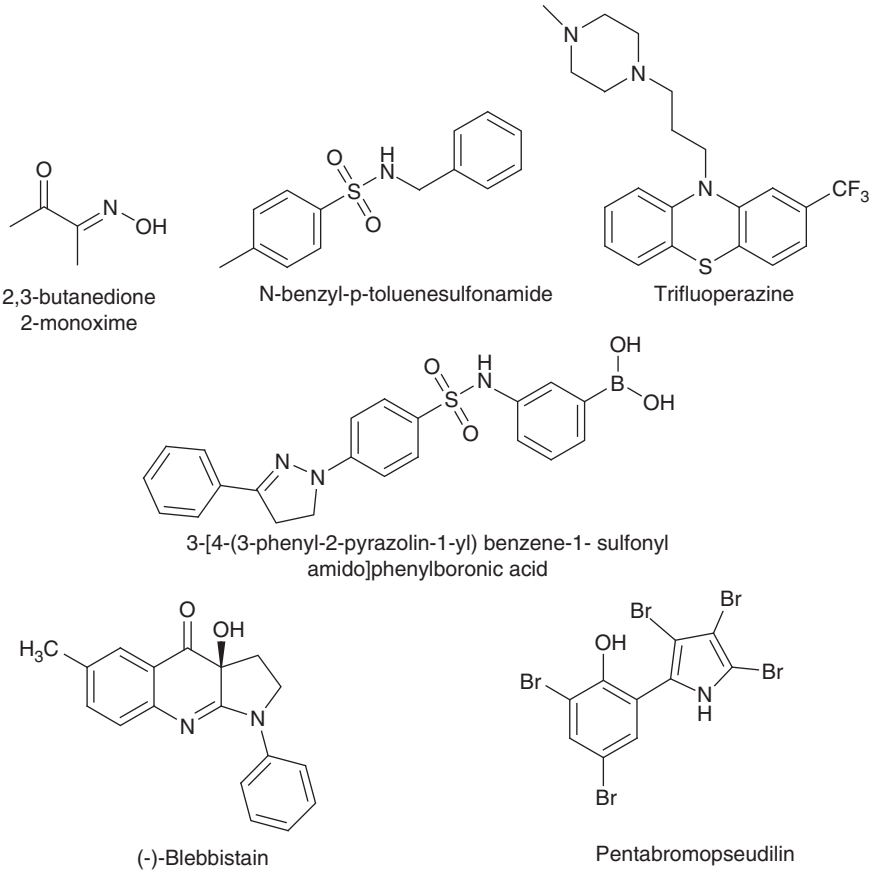

Scheme 2 Overview of known allosteric inhibitors of myosin motor function.

dye 3-[4-(3-phenyl-2-pyrazolin-1-yl) benzene-1-sulfonylamido]-phenylboronic acid (PPBA) as well as the common antipsychotic drug trifluoperazine (TFP). The former was initially assumed to inhibit the skeletal S1 motor function competitively with a $K_i \approx 0.8$ μM.[162] Later, it was surmised to form a ternary complex with the myosin motor domain and nucleotide, and operate in an allosteric manner both on skeletal muscle S1 and *Dd* myosin-2.[163] Based on manual fitting of the energy-minimized coordinates of the fluorescent compound to the X-ray structure of the *Dd* myosin-2 motor domain, PPBA was speculated to bind to a hydrophobic site distant to the active site and interact with the amino acid F472.[163a]

The second substance, TFP, has long been known as a potent CaM antagonist which was used in millimolar concentrations for the removal of regulatory light chains from smooth muscle myosins[164] and scallop striated muscle myosins.[165] Furthermore, it appeared to interact with the motor domain of myosins as a result of its potent inhibition of the ATPase activity and motility in lower concentrations (100–200 μM) than are usually required for light-chain removal (1–2 mM).[166] However, the specific binding sites of both compounds and their mechanism of action are not known so far, because of a lack of structural information. PPBA and TFP are not suitable as probes for cell biological applications or as pharmaceutical drug candidates because they have effects on multiple proteins and targets in the cell.

The only structurally well-characterized inhibitors of myosin motor activity are (−)-blebbistatin and pentabromopseudilin (**Figure 13**). Blebbistatin was discovered in 2003 and exhibits high affinity and selectivity for myosin-2.[167] Myosins from classes-1, -5, -10, but also smooth muscle myosin-2, are weakly or not affected by blebbistatin, whereas skeletal and nonmuscle myosin-2 are potently inhibited ($IC_{50} = 0.5$–2 μM).[168] The other enantiomer (+)-blebbistatin was found to have no inhibitory effect on myosin. The X-ray structure of *Dd* myosin-2 in the pre-power stroke state with bound (−)-blebbistatin (PDB 1YV3) revealed the allosteric binding site in the myosin motor domain.[169] Blebbistatin binds to a hydrophobic pocket at the apex of the large cleft, less than 4 Å away from Switch-1 and Switch-2 of the nucleotide binding pocket. The inhibitor binds mainly through hydrophobic interactions to myosin. The interacting myosin residues include L262, Y261, S465, F466, E467, I471, T474, V630, Y634, Q637, and L641. Hydrogen bonds are formed between the hydroxyl group of the compound and the main chains of G240 as well as L262. Furthermore, the carbonyl group of the methylquinolinone moiety forms a direct hydrogen bond to S456, a water-mediated hydrogen bond to S456 of Switch-2, and a water-mediated interaction to the main chain of I471. As indicated by the low root mean square deviation (0.407 Å) of the C_α atoms between the inhibitor bound and unbound structures, no major conformational changes occurred in the overall motor domain. Nevertheless, the X-ray structure revealed some local rearrangements of the side chains L262 and Y634 by 3 to 4.5 Å upon binding of blebbistatin, suggesting an induced fit docking process. Comparison of the myosin-2 blebbistatin structure with the structures of unconventional myosins gave also an explanation for the specificity of the compound. The residues S456,

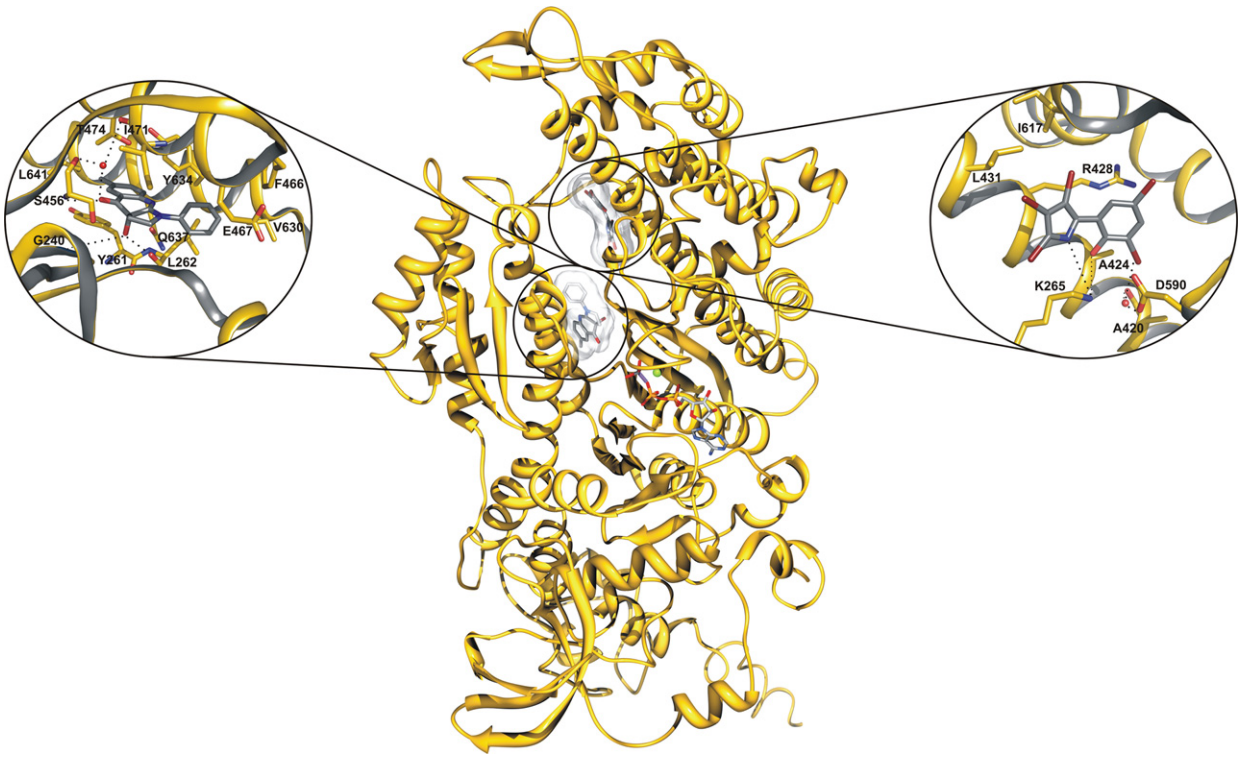

Figure 13 Ribbon diagram of the superimposed *Dd* myosin-2 X-ray structures in the pre-power stroke state. The allosteric binding sites for (−)-blebbistatin (left, Protein Data Bank [PDB] 1YV3) and pentabromopseudilin (right, PDB 2JHR) are shown.

T474, Y634, and Q637 are variable among the different myosin classes and thus dictate the affinity of the inhibitor. Especially at the position corresponding to S459, myosin-1, -5, and -10 isoforms have a large aromatic amino acid side chain which could prevent binding of blebbistatin. The mechanism of myosin-2 inhibition by blebbistatin was elucidated by comprehensive kinetic studies[170] in combination with the structural crystallographic analysis. Blebbistatin does not interfere with either actin binding of myosin or ATP-induced dissociation from actin. It traps the myosin heads in a pre-power stroke ADP · P_i state with low affinity to actin.[22] Recent studies using a combination of EM and kinetic measurements reported that myosin-2, in complex with ADP and blebbistatin, appeared to resemble the 'start of the working stroke' or posthydrolysis state.[171]

Pentabromopseudilin (2,3,4-tribromo-5-(3,5-dibromo-2-hydroxyphenyl)-1*H*-pyrrole) (PBP) was first described as is a marine antibiotic with antitumor and phytotoxic activities, and was reported to inhibit both 12- and 15-human lipoxygenase.[172] Recently, it was discovered that the compound acts as a potent inhibitor of myosin-dependent processes such as isometric tension development and unloaded shortening velocity in muscle.[173] In the case of *Dd* myosin-2, using X-ray crystallography pentabromopseudilin was shown to bind to a previously unobserved allosteric site about 7.5 Å away from the blebbistatin binding pocket and 16 Å away from the active site (PDB 2JHR). This novel binding site in the myosin motor domain is close to the actin binding region at the tip of the 50-kDa domain, open to the exterior and to the large cleft. Both hydrogen bonds and hydrophobic interactions contribute to binding of the inhibitor to the protein. Either polar groups of PBP, the hydroxyl group of the phenol ring as well as the amino group of the pyrrole ring, form crucial hydrogen bonds to K265, that in turn moves ~3.4 Å from its original position on pentabromopseudilin binding. Further residues which are involved in the coordination of the halogenated pseudilin include A420, A424, R428, L431, D590, I617, and A618. The inner face of the pentabromopseudilin binding pocket is formed by helix 13 (K265 to V268) and helix 21 (V411 to L441) from the upper 50-kDa domain. The outer face is contributed by the strut loop (N588 to Q593) and loop-2 (D614 to T629). Besides the local rearrangements, the low root mean square deviation of 0.695 Å between the pentabromopseudilin-bound and -unbound structures indicates no major conformational changes. The total contact area with pentabromopseudilin comprises 255 $Å^2$. The specificity of pentabromopseudilin differs from that observed with other myosin inhibitors. It displays the highest inhibitory effect on certain members of class-5 myosins (IC_{50} = 1.2 μM for chicken myosin-5a) over myosin-2 and -1 isoforms.

4.8.4 Summary and Conclusions

Myosins form a large family of molecular machines which are composed of a limited set of building blocks with a range and number which varies according to class and isoform. The diversity which is achieved by the expression of multiple genes encoding myosin heavy chains from different classes is potentiated in most organisms by splice isoform diversity, association with different light chains, and post-translational modifications. This variability in design in combination with distinct expression profiles for the individual myosin isoforms appears to correlate with the need to serve highly specific functions and to adapt to changes related to physical activity, metabolic status, age, or disease. The common feature of all myosins is the motor domain with a highly conserved nucleotide binding pocket, actin binding region, and mechanism for conformational amplification. Changes in the rates of ATP hydrolysis and product release, and mechanical modulation of these rates, determine the velocity, rate of force development, and whether movement is processive or non-processive. The myosin motor is an intrinsic allosterically regulated protein. Regulatory mechanisms have evolved that affect selective steps during ATP turnover and can fine-tune or switch on and off the motile activity of selected myosins. The relatively large size of the motor domain and the importance of allosteric coupling between the different functional regions of the motor provide ample opportunities for the development of small-molecule effectors which interfere in a well-defined and specific manner with the communication pathways in the motor domain. The light-chain binding region serves primarily as a lever arm which increases the size of the power stroke per ATP molecule hydrolyzed, although the lever arm confers regulatory control in some myosins. Moreover, the direction in which the lever arm projects away from the motor domain determines the direction in which a myosin moves over F-actin.[121]

The tail regions of the known myosin classes differ widely in size and domain composition. In many instances, the actual functions for the various domains and motifs found in myosin tails were defined from studies on other proteins and remain to be confirmed biochemically for myosins. Moreover, many myosin tail regions contain protein segments without any structural or functional link to known protein motifs. One of the most common protein-protein interaction domains in the tail region is a coiled-coil-forming α-helix based on the presence of multiple, minimally interrupted heptad repeats. Nearly half the known myosin classes are predicted to dimerize by tail region-mediated coiled-coil formation. In addition, protein-protein interactions can be promoted by the presence of SH3 domains, WD-40 repeats, dilute domains, MyTH4/ FERM tandem domains, ankyrin repeats, PDZ binding domains, and FYVE zinc binding domains. Direct binding to lipids is mediated by the TH1 and PH domains (see Glossary).

Myosin motor domains are ideal model systems for developing and advancing experimental techniques which facilitate the physical characterization of biomolecules. In addition to producing spectroscopic signals and chemical changes during their catalytic cycle, they produce mechanical changes which can be followed directly. Consequently, work on actomyosin has been consistently at the vanguard of biophysical methods development. Key contributions emerging first in the actin-based motor field include the development of approaches to image biomolecules in the electron microscope, ensemble enzyme kinetics, single molecule observations, single molecule mechanics, and combinations of the latter approaches.[36,86,174] High-speed atomic force microscopy at video rates was used to image myosin-5 molecules walking

along actin tracks and to visualize lever arm swinging.[175] Structural analysis of the actomyosin system using hybrid approaches has proved to be of extraordinary value. Hybrid approaches were first used by combining high-resolution structural information obtained by X-ray crystallography with X-ray fiber diagrams from oriented gels to obtain atomic models of the actin filament and vertebrate smooth muscle thin filaments.[176] Atomic models of F-actin decorated with myosin S1 were obtained by fitting atomic models of actin and the myosin cross-bridge into high-resolution cryoEM three-dimensional reconstructions.[11,85b] Recent advances make it possible to include molecular dynamics techniques in the hybrid analysis of actomyosin complexes, thus complementing atomic details with dynamic information and thereby bridging the gaps between the structurally well-defined states along the actomyosin ATPase cycle.[85a,177]

References

[1] Kühne, W. Untersuchungen über Bewegung und Veränderung der contraktilen Substanzen. *Arch. Anat. Physiol. Wiss. Med.* **1859**, *564–642*, 748–835.

[2] (a) Szent-Györgyi, A. In *Studies from the Institute of Medical Chemistry University Szeged*; Szent-Györgyi, A., Ed.; S. Karger AG: Basel, 1942; vol. 1, pp 17–26 (b) Straub, F. B. In *Studies from the Institute of Medical Chemistry University Szeged* Szent-Györgyi, A., Ed.; S. Karger AG: Basel, 1942; vol. 2, pp 3–15.

[3] Pollard, T. D.; Korn, E. D. *Acanthamoeba* myosin. I. Isolation from *Acanthamoeba castellanii* of an enzyme similar to muscle myosin. *J. Biol. Chem.* **1973**, *248*(13), 4682–4690.

[4] Hodge, T.; Cope, M. J. A myosin family tree. *J. Cell Sci.* **2000**, *113*(Pt 19), 3353–3354.

[5] Foth, B. J.; Goedecke, M. C.; Soldati, D. New insights into myosin evolution and classification. *Proc. Natl. Acad. Sci. USA* **2006**, *103*(10), 3681–3686.

[6] (a) Wells, C.; Coles, D.; Entwistle, A.; Peckham, M. Myogenic cells express multiple myosin isoforms. *J. Muscle Res. Cell Motil.* **1997**, *18*(5), 501–515. (b) Resnicow, D. I.; Deacon, J. C.; Warrick, H. M.; Spudich, J. A.; Leinwand, L. A. Functional diversity among a family of human skeletal muscle myosin motors. *Proc. Natl. Acad. Sci. USA* **2010**, *107*(3), 1053–1058.

[7] (a) McPherson, J. D.; Marra, M.; Hillier, L.; Waterston, R. H.; Chinwalla, A.; Wallis, J.; Sekhon, M.; Wylie, K.; Mardis, E. R.; Wilson, R. K.; Fulton, R.; Kucaba, T. A.; Wagner-McPherson, C.; Barbazuk, W. B.; Gregory, S. G.; Humphray, S. J.; French, L.; Evans, R. S.; Bethel, G.; Whittaker, A.; Holden, J. L.; McCann, O. T.; Dunham, A.; Soderlund, C.; Scott, C. E.; Bentley, D. R.; Schuler, G.; Chen, H. C.; Jang, W.; Green, E. D.; Idol, J. R.; Maduro, V. V.; Montgomery, K. T.; Lee, E.; Miller, A.; Emerling, S.; Kucherlapati, R.; Gibbs, R.; Scherer, S.; Gorrell, J. H.; Sodergren, E.; Clerc-Blankenburg, K.; Tabor, P.; Naylor, S.; Garcia, D.; de Jong, P. J.; Catanese, J. J.; Nowak, N.; Osoegawa, K.; Qin, S.; Rowen, L.; Madan, A.; Dors, M.; Hood, L.; Trask, B.; Friedman, C.; Massa, H.; Cheung, V. G.; Kirsch, I. R.; Reid, T.; Yonescu, R.; Weissenbach, J.; Bruls, T.; Heilig, R.; Branscomb, E.; Olsen, A.; Doggett, N.; Cheng, J. F.; Hawkins, T.; Myers, R. M.; Shang, J.; Ramirez, L.; Schmutz, J.; Velasquez, O.; Dixon, K.; Stone, N. E.; Cox, D. R.; Haussler, D.; Kent, W. J.; Furey, T.; Rogic, S.; Kennedy, S.; Jones, S.; Rosenthal, A.; Wen, G.; Schilhabel, M.; Gloeckner, G.; Nyakatura, G.; Siebert, R.; Schlegelberger, B.; Korenberg, J.; Chen, X. N.; Fujiyama, A.; Hattori, M.; Toyoda, A.; Yada, T.; Park, H. S.; Sakaki, Y.; Shimizu, N.; Asakawa, S.; Kawasaki, K.; Sasaki, T.; Shintani, A.; Shimizu, A.; Shibuya, K.; Kudoh, J.; Minoshima, S.; Ramser, J.; Seranski, P.; Hoff, C.; Poustka, A.; Reinhardt, R.; Lehrach, H. A physical map of the human genome. *Nature* **2001**, *409*(6822), 934–941. (b) Lander, E. S.; Linton, L. M.; Birren, B.; Nusbaum, C.; Zody, M. C.; Baldwin, J.; Devon, K.; Dewar, K.; Doyle, M.; FitzHugh, W.; Funke, R.; Gage, D.; Harris, K.; Heaford, A.; Howland, J.; Kann, L.; Lehoczky, J.; LeVine, R.; McEwan, P.; McKernan, K.; Meldrim, J.; Mesirov, J. P.; Miranda, C.; Morris, W.; Naylor, J.; Raymond, C.; Rosetti, M.; Santos, R.; Sheridan, A.; Sougnez, C.; Stange-Thomann, N.; Stojanovic, N.; Subramanian, A.; Wyman, D.; Rogers, J.; Sulston, J.; Ainscough, R.; Beck, S.; Bentley, D.; Burton, J.; Clee, C.; Carter, N.; Coulson, A.; Deadman, R.; Deloukas, P.; Dunham, A.; Dunham, I.; Durbin, R.; French, L.; Grafham, D.; Gregory, S.; Hubbard, T.; Humphray, S.; Hunt, A.; Jones, M.; Lloyd, C.; McMurray, A.; Matthews, L.; Mercer, S.; Milne, S.; Mullikin, J. C.; Mungall, A.; Plumb, R.; Ross, M.; Shownkeen, R.; Sims, S.; Waterston, R. H.; Wilson, R. K.; Hillier, L. W.; McPherson, J. D.; Marra, M. A.; Mardis, E. R.; Fulton, L. A.; Chinwalla, A. T.; Pepin, K. H.; Gish, W. R.; Chissoe, S. L.; Wendl, M. C.; Delehaunty, K. D.; Miner, T. L.; Delehaunty, A.; Kramer, J. B.; Cook, L. L.; Fulton, R. S.; Johnson, D. L.; Minx, P. J.; Clifton, S. W.; Hawkins, T.; Branscomb, E.; Predki, P.; Richardson, P.; Wenning, S.; Slezak, T.; Doggett, N.; Cheng, J. F.; Olsen, A.; Lucas, S.; Elkin, C.; Uberbacher, E.; Frazier, M.; Gibbs, R. A.; Muzny, D. M.; Scherer, S. E.; Bouck, J. B.; Sodergren, E. J.; Worley, K. C.; Rives, C. M.; Gorrell, J. H.; Metzker, M. L.; Naylor, S. L.; Kucherlapati, R. S.; Nelson, D. L.; Weinstock, G. M.; Sakaki, Y.; Fujiyama, A.; Hattori, M.; Yada, T.; Toyoda, A.; Itoh, T.; Kawagoe, C.; Watanabe, H.; Totoki, Y.; Taylor, T.; Weissenbach, J.; Heilig, R.; Saurin, W.; Artiguenave, F.; Brottier, P.; Bruls, T.; Pelletier, E.; Robert, C.; Wincker, P.; Smith, D. R.; Doucette-Stamm, L.; Rubenfield, M.; Weinstock, K.; Lee, H. M.; Dubois, J.; Rosenthal, A.; Platzer, M.; Nyakatura, G.; Taudien, S.; Rump, A.; Yang, H.; Yu, J.; Wang, J.; Huang, G.; Gu, J.; Hood, L.; Rowen, L.; Madan, A.; Qin, S.; Davis, R. W.; Federspiel, N. A.; Abola, A. P.; Proctor, M. J.; Myers, R. M.; Schmutz, J.; Dickson, M.; Grimwood, J.; Cox, D. R.; Olson, M. V.; Kaul, R.; Shimizu, N.; Kawasaki, K.; Minoshima, S.; Evans, G. A.; Athanasiou, M.; Schultz, R.; Roe, B. A.; Chen, F.; Pan, H.; Ramser, J.; Lehrach, H.; Reinhardt, R.; McCombie, W. R.; de la Bastide, M.; Dedhia, N.; Blocker, H.; Hornischer, K.; Nordsiek, G.; Agarwala, R.; Aravind, L.; Bailey, J. A.; Bateman, A.; Batzoglou, S.; Birney, E.; Bork, P.; Brown, D. G.; Burge, C. B.; Cerutti, L.; Chen, H. C.; Church, D.; Clamp, M.; Copley, R. R.; Doerks, T.; Eddy, S. R.; Eichler, E. E.; Furey, T. S.; Galagan, J.; Gilbert, J. G.; Harmon, C.; Hayashizaki, Y.; Haussler, D.; Hermjakob, H.; Hokamp, K.; Jang, W.; Johnson, L. S.; Jones, T. A.; Kasif, S.; Kaspryzk, A.; Kennedy, S.; Kent, W. J.; Kitts, P.; Koonin, E. V.; Korf, I.; Kulp, D.; Lancet, D.; Lowe, T. M.; McLysaght, A.; Mikkelsen, T.; Moran, J. V.; Mulder, N.; Pollara, V. J.; Ponting, C. P.; Schuler, G.; Schultz, J.; Slater, G.; Smit, A. F.; Stupka, E.; Szustakowski, J.; Thierry-Mieg, D.; Thierry-Mieg, J.; Wagner, L.; Wallis, J.; Wheeler, R.; Williams, A.; Wolf, Y. I.; Wolfe, K. H.; Yang, S. P.; Yeh, R. F.; Collins, F.; Guyer, M. S.; Peterson, J.; Felsenfeld, A.; Wetterstrand, K. A.; Patrinos, A.; Morgan, M. J.; de Jong, P.; Catanese, J. J.; Osoegawa, K.; Shizuya, H.; Choi, S.; Chen, Y. J. Initial sequencing and analysis of the human genome. *Nature* **2001**, *409*(6822), 860–921.

[8] (a) Hayashida, M.; Maita, T.; Matsuda, G. The primary structure of skeletal muscle myosin heavy chain: I. Sequence of the amino-terminal 23 kDa fragment. *J. Biochem* **1991**, *110*(1), 54–59. (b) Warrick, H. M.; Spudich, J. A. Myosin structure and function in cell motility. *Annu. Rev. Cell Biol.* **1987**, *3*, 379–421.

[9] Titus, M. A. *Myosins. Curr. Opin. Cell Biol.* **1993**, *5*(1), 77–81.

[10] Anson, M.; Geeves, M. A.; Kurzawa, S. E.; Manstein, D. J. Myosin motors with artificial lever arms. *EMBO J.* **1996**, *15*(22), 6069–6074.

[11] (a) Rayment, I.; Holden, H. M.; Whittaker, M.; Yohn, C. B.; Lorenz, M.; Holmes, K. C.; Milligan, R. A. Structure of the actin-myosin complex and its implications for muscle contraction. *Science* **1993**, *261*(5117), 58–65. (b) Schröder, R. R.; Manstein, D. J.; Jahn, W.; Holden, H.; Rayment, I.; Holmes, K. C.; Spudich, J. A. Three-dimensional atomic model of F-actin decorated with *Dictyostelium* myosin S1. *Nature* **1993**, *364*(6433), 171–174.

[12] Nachmias, V. Filament formation by purified *Physarum* myosin. *Proc. Natl. Acad. Sci. USA* **1972**, *69*(8), 2011–2014.

[13] Espreafico, E. M.; Cheney, R. E.; Matteoli, M.; Nascimento, A. A.; De Camilli, P. V.; Larson, R. E.; Mooseker, M. S. Primary structure and cellular localization of chicken brain myosin-V (p190), an unconventional myosin with calmodulin light chains. *J. Cell. Biol.* **1992**, *119*(6), 1541–1557.

[14] (a) Manceva, S.; Lin, T.; Pham, H.; Lewis, J. H.; Goldman, Y. E.; Ostap, E. M. Calcium regulation of calmodulin binding to and dissociation from the myo1c regulatory domain. *Biochemistry* **2007**, *46*(42), 11718–11726. (b) Himmel, D. M.; Mui, S.; O'Neall-Hennessey, E.; Szent-Gyorgyi, A. G.; Cohen, C. The on-off switch in regulated myosins: different triggers but related mechanisms. *J. Mol. Biol.* **2009**, *394*(3), 496–505.

[15] Vicente-Manzanares, M.; Ma, X.; Adelstein, R. S.; Horwitz, A. R. Nonmuscle myosin II takes centre stage in cell adhesion and migration. *Nat. Rev. Mol. Cell Biol.* **2009**, *10*(11), 778–790.

[16] Rey, M.; Valenzuela-Fernandez, A.; Urzainqui, A.; Yanez-Mo, M.; Perez-Martinez, M.; Penela, P.; Mayor, Jr F.; Sanchez-Madrid, F. Myosin IIA is involved in the endocytosis of CXCR4 induced by SDF-1alpha. *J. Cell Sci.* **2007**, *120*(Pt 6), 1126–1133.

[17] Heath, K. E.; Campos-Barros, A.; Toren, A.; Rozenfeld-Granot, G.; Carlsson, L. E.; Savige, J.; Denison, J. C.; Gregory, M. C.; White, J. G.; Barker, D. F.; Greinacher, A.; Epstein, C. J.; Glucksman, M. J.; Martignetti, J. A. Nonmuscle myosin heavy chain IIA mutations define a spectrum of autosomal dominant macrothrombocytopenias: May-Hegglin anomaly and Fechtner, Sebastian, Epstein, and Alport-like syndromes. *Am. J. Hum. Genet.* **2001**, *69*(5), 1033–1045.

[18] Lalwani, A. K.; Goldstein, J. A.; Kelley, M. J.; Luxford, W.; Castelein, C. M.; Mhatre, A. N. Human nonsyndromic hereditary deafness DFNA17 is due to a mutation in nonmuscle myosin MYH9. *Am. J. Hum. Genet.* **2000**, *67*(5), 1121–1128.

[19] Donaudy, F.; Snoeckx, R.; Pfister, M.; Zenner, H. P.; Blin, N.; Di Stazio, M.; Ferrara, A.; Lanzara, C.; Ficarella, R.; Declau, F.; Pusch, C. M.; Nurnberg, P.; Melchionda, S.; Zelante, L.; Ballana, E.; Estivill, X.; Van Camp, G.; Gasparini, P.; Savoia, A. Nonmuscle myosin heavy-chain gene MYH14 is expressed in cochlea and mutated in patients affected by autosomal dominant hearing impairment (DFNA4). *Am. J. Hum. Genet.* **2004**, *74*(4), 770–776.

[20] (a) De Lozanne, A.; Spudich, J. A. Disruption of the *Dictyostelium* myosin heavy chain gene by homologous recombination. *Science* **1987**, *236*(4805), 1086–1091. (b) Edwards, K. A.; Kiehart, D. P. *Drosophila* nonmuscle myosin II has multiple essential roles in imaginal disc and egg chamber morphogenesis. *Development* **1996**, *122*(5), 1499–1511.

[21] Tullio, A. N.; Accili, D.; Ferrans, V. J.; Yu, Z. X.; Takeda, K.; Grinberg, A.; Westphal, H.; Preston, Y. A.; Adelstein, R. S. Nonmuscle myosin II-B is required for normal development of the mouse heart. *Proc. Natl. Acad. Sci. USA* **1997**, *94*(23), 12407–12412.

[22] Betapudi, V.; Licate, L. S.; Egelhoff, T. T. Distinct roles of nonmuscle myosin II isoforms in the regulation of MDA-MB-231 breast cancer cell spreading and migration. *Cancer Res.* **2006**, *66*(9), 4725–4733.

[23] Jana, S. S.; Kawamoto, S.; Adelstein, R. S. A specific isoform of nonmuscle myosin II-C is required for cytokinesis in a tumor cell line. *J. Biol. Chem.* **2006**, *281*(34), 24662–24670.

[24] van Leeuwen, H.; Elliott, G.; O'Hare, P. Evidence of a role for nonmuscle myosin II in herpes simplex virus type 1 egress. *J. Virol.* **2002**, *76*(7), 3471–3481.

[25] De La Cruz, E. M.; Ostap, E. M. Relating biochemistry and function in the myosin superfamily. *Curr. Opin. Cell Biol.* **2004**, *16*(1), 61–67.

[26] Donaudy, F.; Ferrara, A.; Esposito, L.; Hertzano, R.; Ben-David, O.; Bell, R. E.; Melchionda, S.; Zelante, L.; Avraham, K. B.; Gasparini, P. Multiple mutations of MYO1A, a cochlear-expressed gene, in sensorineural hearing loss. *Am. J. Hum. Genet.* **2003**, *72*(6), 1571–1577.

[27] LeMasurier, M.; Gillespie, P. G. Hair-cell mechanotransduction and cochlear amplification. *Neuron* **2005**, *48*(3), 403–415.

[28] (a) Percipalle, P.; Fomproix, N.; Cavellan, E.; Voit, R.; Reimer, G.; Kruger, T.; Thyberg, J.; Scheer, U.; Grummt, I.; Farrants, A. K. The chromatin remodelling complex WSTF-SNF2h interacts with nuclear myosin 1 and has a role in RNA polymerase I transcription. *EMBO Rep.* **2006**, *7*(5), 525–530. (b) Hofmann, W. A.; Arduini, A.; Nicol, S. M.; Camacho, C. J.; Lessard, J. L.; Fuller-Pace, F. V.; de Lanerolle, P. SUMOylation of nuclear actin. *J. Cell. Biol.* **2009**, *186*(2), 193–200.

[29] Pestic-Dragovich, L.; Stojiljkovic, L.; Philimonenko, A. A.; Nowak, G.; Ke, Y.; Settlage, R. E.; Shabanowitz, J.; Hunt, D. F.; Hozak, P.; de Lanerolle, P. A myosin I isoform in the nucleus. *Science* **2000**, *290*(5490), 337–341.

[30] Chuang, C. H.; Carpenter, A. E.; Fuchsova, B.; Johnson, T.; de Lanerolle, P.; Belmont, A. S. Long-range directional movement of an interphase chromosome site. *Curr. Biol.* **2006**, *16*(8), 825–831.

[31] Walsh, T.; Walsh, V.; Vreugde, S.; Hertzano, R.; Shahin, H.; Haika, S.; Lee, M. K.; Kanaan, M.; King, M. C.; Avraham, K. B. From flies' eyes to our ears: mutations in a human class III myosin cause progressive nonsyndromic hearing loss DFNB30. *Proc. Natl. Acad. Sci. USA* **2002**, *99*(11), 7518–7523.

[32] Porter, J. A.; Montell, C. Distinct roles of the *Drosophila* ninaC kinase and myosin domains revealed by systematic mutagenesis. *J. Cell. Biol.* **1993**, *122*(3), 601–612.

[33] Veigel, C.; Wang, F.; Bartoo, M. L.; Sellers, J. R.; Molloy, J. E. The gated gait of the processive molecular motor, myosin V. *Nat. Cell Biol.* **2002**, *4*(1), 59–65.

[34] Smith, D. A. How processive is the myosin-V motor? *J. Muscle Res. Cell Motil.* **2004**, *25*(3), 215–217.

[35] Forgacs, E.; Cartwright, S.; Sakamoto, T.; Sellers, J. R.; Corrie, J. E.; Webb, M. R.; White, H. D. Kinetics of ADP dissociation from the trail and lead heads of actomyosin V following the power stroke. *J. Biol. Chem.* **2008**, *283*(2), 766–773.

[36] Yildiz, A.; Forkey, J. N.; McKinney, S. A.; Ha, T.; Goldman, Y. E.; Selvin, P. R. Myosin V walks hand-over-hand: single fluorophore imaging with 1.5-nm localization. *Science* **2003**, *300*(5628), 2061–2065.

[37] (a) Snyder, G. E.; Sakamoto, T.; Hammer, 3rd J. A.; Sellers, J. R.; Selvin, P. R. Nanometer localization of single green fluorescent proteins: evidence that myosin V walks hand-over-hand via telemark configuration. *Biophys. J.* **2004**, *87*(3), 1776–1783. (b) Sakamoto, T.; Yildez, A.; Selvin, P. R.; Sellers, J. R. Step-size is determined by neck length in myosin V. *Biochemistry* **2005**, *44*(49), 16203–16210.

[38] Pastural, E.; Barrat, F. J.; Dufourcq-Lagelouse, R.; Certain, S.; Sanal, O.; Jabado, N.; Seger, R.; Griscelli, C.; Fischer, A.; de Saint Basile, G. Griscelli disease maps to chromosome 15q21 and is associated with mutations in the myosin-Va gene. *Nat. Genet.* **1997**, *16*(3), 289–292.

[39] Mukherjea, M.; Llinas, P.; Kim, H.; Travaglia, M.; Safer, D.; Menetrey, J.; Franzini-Armstrong, C.; Selvin, P. R.; Houdusse, A.; Sweeney, H. L. Myosin VI dimerization triggers an unfolding of a three-helix bundle in order to extend its reach. *Mol. Cell* **2009**, *35*(3), 305–315.

[40] Yu, C.; Feng, W.; Wei, Z.; Miyanoiri, Y.; Wen, W.; Zhao, Y.; Zhang, M. Myosin VI undergoes cargo-mediated dimerization. *Cell* **2009**, *138*(3), 537–548.

[41] Phichith, D.; Travaglia, M.; Yang, Z.; Liu, X.; Zong, A. B.; Safer, D.; Sweeney, H. L. Cargo binding induces dimerization of myosin VI. *Proc. Natl. Acad. Sci. USA* **2009**, *106*(41), 17320–17324.

[42] (a) Sahlender, D. A.; Roberts, R. C.; Arden, S. D.; Spudich, G.; Taylor, M. J.; Luzio, J. P.; Kendrick-Jones, J.; Buss, F. Optineurin links myosin VI to the Golgi complex and is involved in Golgi organization and exocytosis. *J. Cell. Biol.* **2005**, *169*(2), 285–295. (b) Au, J. S.; Puri, C.; Ihrke, G.; Kendrick-Jones, J.; Buss, F. Myosin VI is required for sorting of AP-1B-dependent cargo to the basolateral domain in polarized MDCK cells. *J. Cell. Biol.* **2007**, *177*(1), 103–114. (c) Spudich, G.; Chibalina, M. V.; Au, J. S.; Arden, S. D.; Buss, F.; Kendrick-Jones, J. Myosin VI targeting to clathrin-coated structures and dimerization is mediated by binding to disabled-2 and PtdIns(4,5)P2. *Nat. Cell Biol.* **2007**, *9*(2), 176–183.

[43] Morriswood, B.; Ryzhakov, G.; Puri, C.; Arden, S. D.; Roberts, R.; Dendrou, C.; Kendrick-Jones, J.; Buss, F. T6BP and NDP52 are myosin VI binding partners with potential roles in cytokine signalling and cell adhesion. *J. Cell Sci.* **2007**, *120*(Pt 15), 2574–2585.

[44] Mohiddin, S. A.; Ahmed, Z. M.; Griffith, A. J.; Tripodi, D.; Friedman, T. B.; Fananapazir, L.; Morell, R. J. Novel association of hypertrophic cardiomyopathy, sensorineural deafness, and a mutation in unconventional myosin VI (MYO6). *J. Med. Genet.* **2004**, *41*(4), 309–314.

[45] (a) Dunn, T. A.; Chen, S.; Faith, D. A.; Hicks, J. L.; Platz, E. A.; Chen, Y.; Ewing, C. M.; Sauvageot, J.; Isaacs, W. B.; De Marzo, A. M.; Luo, J. A novel role of myosin VI in human prostate cancer. *Am. J. Pathol.* **2006**, *169*(5), 1843–1854. (b) Yoshida, H.; Cheng, W.; Hung, J.; Montell, D.; Geisbrecht, E.; Rosen, D.; Liu, J.; Naora, H. Lessons from border cell migration in the *Drosophila* ovary: a role for myosin VI in dissemination of human ovarian cancer. *Proc. Natl. Acad. Sci. USA* **2004**, *101*(21), 8144–8149.

[46] Hicks, J. L.; Deng, W. M.; Rogat, A. D.; Miller, K. G.; Bownes, M. Class VI unconventional myosin is required for spermatogenesis in *Drosophila*. *Mol. Biol. Cell* **1999**, *10*(12), 4341–4353.

[47] Geisbrecht, E. R.; Montell, D. J. Myosin VI is required for E-cadherin-mediated border cell migration. *Nat. Cell Biol.* **2002**, *4*(8), 616–620.

[48] Petritsch, C.; Tavosanis, G.; Turck, C. W.; Jan, L. Y.; Jan, Y. N. The Drosophila myosin VI jaguar is required for basal protein targeting and correct spindle orientation in mitotic neuroblasts. *Dev. Cell* **2003**, *4*(2), 273–281.

[49] Melchionda, S.; Ahituv, N.; Bisceglia, L.; Sobe, T.; Glaser, F.; Rabionet, R.; Arbones, M. L.; Notarangelo, A.; Di Iorio, E.; Carella, M.; Zelante, L.; Estivill, X.; Avraham, K. B.; Gasparini, P. MYO6, the human homologue of the gene responsible for deafness in Snell's Waltzer mice, is mutated in autosomal dominant nonsyndromic hearing loss. *Am. J. Hum. Genet.* **2001**, *69*(3), 635–640.

[50] Yang, Y.; Baboolal, T. G.; Siththanandan, V.; Chen, M.; Walker, M. L.; Knight, P. J.; Peckham, M.; Sellers, J. R. A FERM domain autoregulates *Drosophila* myosin 7a activity. *Proc. Natl. Acad. Sci. USA* **2009**, *106*(11), 4189–4194.

[51] Baboolal, T. G.; Sakamoto, T.; Forgacs, E.; White, H. D.; Jackson, S. M.; Takagi, Y.; Farrow, R. E.; Molloy, J. E.; Knight, P. J.; Sellers, J. R.; Peckham, M. The SAH domain extends the functional length of the myosin lever. *Proc. Natl. Acad. Sci. USA* **2009**, *106*(52), 22193–22198.

[52] Soni, L. E.; Warren, C. M.; Bucci, C.; Orten, D. J.; Hasson, T. The unconventional myosin-VIIa associates with lysosomes. *Cell Motil. Cytoskeleton* **2005**, *62*(1), 13–26.

[53] (a) Tamagawa, Y.; Kitamura, K.; Ishida, T.; Ishikawa, K.; Tanaka, H.; Tsuji, S.; Nishizawa, M. A gene for a dominant form of nonsyndromic sensorineural deafness (DFNA11) maps within the region containing the DFNB2 recessive deafness gene. *Hum. Mol. Genet.* **1996**, *5*(6), 849–852. (b) Weil, D.; Kussel, P.; Blanchard, S.; Levy, G.; Levi-Acobas, F.; Drira, M.; Ayadi, H.; Petit, C. The autosomal recessive isolated deafness, DFNB2, and the Usher 1B syndrome are allelic defects of the myosin-VIIA gene. *Nat. Genet.* **1997**, *16*(2), 191–193.

[54] Petit, C. Usher syndrome: from genetics to pathogenesis. *Annu. Rev. Genom. Hum. Genet.* **2001**, *2*, 271–297.

[55] Liao, W.; Elfrink, K.; Bähler, M. Head of myosin IX binds calmodulin and moves processively toward the plus-end of actin filaments. *J. Biol. Chem.* **2010**, *285*(32), 24933–24942.

[56] (a) Post, P. L.; Tyska, M. J.; O'Connell, C. B.; Johung, K.; Hayward, A.; Mooseker, M. S. Myosin-IXb is a single-headed and processive motor. *J. Biol. Chem.* **2002**, *277*(14), 11679–11683. (b) O'Connell, C. B.; Mooseker, M. S. Native myosin-IXb is a plus-, not a minus-end-directed motor. *Nat. Cell Biol.* **2003**, *5*(2), 171–172.

[57] (a) Reinhard, J.; Scheel, A. A.; Diekmann, D.; Hall, A.; Ruppert, C.; Bahler, M. A novel type of myosin implicated in signalling by Rho family GTPases. *EMBO J.* **1995**, *14*(4), 697–704. (b) van den Boom, F.; Dussmann, H.; Uhlenbrock, K.; Abouhamed, M.; Bahler, M. The myosin IXb motor activity targets the myosin IXb RhoGAP domain as cargo to sites of actin polymerization. *Mol. Biol. Cell* **2007**, *18*(4), 1507–1518.

[58] Zhu, X. J.; Wang, C. Z.; Dai, P. G.; Xie, Y.; Song, N. N.; Liu, Y.; Du, Q. S.; Mei, L.; Ding, Y. Q.; Xiong, W. C. Myosin X regulates netrin receptors and functions in axonal path-finding. *Nat. Cell Biol.* **2007**, *9*(2), 184–192.

[59] Weber, K. L.; Sokac, A. M.; Berg, J. S.; Cheney, R. E.; Bement, W. M. A microtubule-binding myosin required for nuclear anchoring and spindle assembly. *Nature* **2004**, *431*(7006), 325–329.

[60] Woolner, S.; O'Brien, L. L.; Wiese, C.; Bement, W. M. Myosin-10 and actin filaments are essential for mitotic spindle function. *J. Cell. Biol.* **2008**, *182*(1), 77–88.

[61] Boger, E. T.; Sellers, J. R.; Friedman, T. B. Human myosin XVBP is a transcribed pseudogene. *J. Muscle Res. Cell Motil.* **2001**, *22*(5), 477–483.

[62] (a) La Rosa, S.; Capella, C.; Lloyd, R. V. Localization of myosin XVA in endocrine tumors of gut and pancreas. *Endocr. Pathol.* **2002**, *13*(1), 29–37. (b) Lloyd, R. V.; Vidal, S.; Jin, L.; Zhang, S.; Kovacs, K.; Horvath, E.; Scheithauer, B. W.; Boger, E. T.; Fridell, R. A.; Friedman, T. B. Myosin XVA expression in the pituitary and in other neuroendocrine tissues and tumors. *Am. J. Pathol.* **2001**, *159*(4), 1375–1382.

[63] (a) Belyantseva, I. A.; Boger, E. T.; Friedman, T. B. Myosin XVa localizes to the tips of inner ear sensory cell stereocilia and is essential for staircase formation of the hair bundle. *Proc. Natl. Acad. Sci. USA* **2003**, *100*(24), 13958–13963. (b) Belyantseva, I. A.; Boger, E. T.; Naz, S.; Frolenkov, G. I.; Sellers, J. R.; Ahmed, Z. M.; Griffith, A. J.; Friedman, T. B. Myosin-XVa is required for tip localization of whirlin and differential elongation of hair-cell stereocilia. *Nat. Cell Biol.* **2005**, *7*(2), 148–156.

[64] (a) Liang, Y.; Wang, A.; Belyantseva, I. A.; Anderson, D. W.; Probst, F. J.; Barber, T. D.; Miller, W.; Touchman, J. W.; Jin, L.; Sullivan, S. L.; Sellers, J. R.; Camper, S. A.; Lloyd, R. V.; Kachar, B.; Friedman, T. B.; Fridell, R. A. Characterization of the human and mouse unconventional myosin XV genes responsible for hereditary deafness DFNB3 and shaker 2. *Genomics* **1999**, *61*(3), 243–258. (b) Anderson, D. W.; Probst, F. J.; Belyantseva, I. A.; Fridell, R. A.; Beyer, L.; Martin, D. M.; Wu, D.; Kachar, B.; Friedman, T. B.; Raphael, Y.; Camper, S. A. The motor and tail regions of myosin XV are critical for normal structure and function of auditory and vestibular hair cells. *Hum. Mol. Genet.* **2000**, *9*(12), 1729–1738.

[65] (a) Wang, A.; Liang, Y.; Fridell, R. A.; Probst, F. J.; Wilcox, E. R.; Touchman, J. W.; Morton, C. C.; Morell, R. J.; Noben-Trauth, K.; Camper, S. A.; Friedman, T. B. Association of unconventional myosin MYO15 mutations with human nonsyndromic deafness DFNB3. *Science* **1998**, *280*(5368), 1447–14451. (b) Probst, F. J.; Fridell, R. A.; Raphael, Y.; Saunders, T. L.; Wang, A.; Liang, Y.; Morell, R. J.; Touchman, J. W.; Lyons, R. H.; Noben-Trauth, K.; Friedman, T. B.; Camper, S. A. Correction of deafness in shaker-2 mice by an unconventional myosin in a BAC transgene. *Science* **1998**, *280*(5368), 1444–1447.

[66] Friedman, T. B.; Griffith, A. J. Human nonsyndromic sensorineural deafness. *Annu. Rev. Genom. Hum. Genet.* **2003**, *4*, 341–402.

[67] Liburd, N.; Ghosh, M.; Riazuddin, S.; Naz, S.; Khan, S.; Ahmed, Z.; Liang, Y.; Menon, P. S.; Smith, T.; Smith, A. C.; Chen, K. S.; Lupski, J. R.; Wilcox, E. R.; Potocki, L.; Friedman, T. B. Novel mutations of MYO15A associated with profound deafness in consanguineous families and moderately severe hearing loss in a patient with Smith-Magenis syndrome. *Hum. Genet.* **2001**, *109*(5), 535–541.

[68] Patel, K. G.; Liu, C.; Cameron, P. L.; Cameron, R. S. Myr 8, a novel unconventional myosin expressed during brain development associates with the protein phosphatase catalytic subunits 1alpha and 1gamma1. *J. Neurosci.* **2001**, *21*(20), 7954–7968.

[69] Cameron, R. S.; Liu, C.; Mixon, A. S.; Pihkala, J. P.; Rahn, R. J.; Cameron, P. L. Myosin16b: the COOH-tail region directs localization to the nucleus and overexpression delays S-phase progression. *Cell Motil. Cytoskeleton* **2007**, *64*(1), 19–48.

[70] Isogawa, Y.; Kon, T.; Inoue, T.; Ohkura, R.; Yamakawa, H.; Ohara, O.; Sutoh, K. The N-terminal domain of MYO18A has an ATP-insensitive actin-binding site. *Biochemistry* **2005**, *44*(16), 6190–6196.

[71] Mori, K.; Furusawa, T.; Okubo, T.; Inoue, T.; Ikawa, S.; Yanai, N.; Mori, K. J.; Obinata, M. Genome structure and differential expression of two isoforms of a novel PDZ-containing myosin (MysPDZ) (Myo18A). *J. Biochem. (Tokyo)* **2003**, *133*(4), 405–413.

[72] Hsu, R. M.; Tsai, M. H.; Hsieh, Y. J.; Lyu, P. C.; Yu, J. S. Identification of MYO18A as a novel interacting partner of the PAK2/betaPIX/GIT1 complex and its potential function in modulating epithelial cell migration. *Mol. Biol. Cell.* **2010**, *21*(2), 287–301.

[73] Dippold, H. C.; Ng, M. M.; Farber-Katz, S. E.; Lee, S. K.; Kerr, M. L.; Peterman, M. C.; Sim, R.; Wiharto, P. A.; Galbraith, K. A.; Madhavarapu, S.; Fuchs, G. J.; Meerloo, T.; Farquhar, M. G.; Zhou, H.; Field, S. J. GOLPH3 bridges phosphatidylinositol-4- phosphate and actomyosin to stretch and shape the Golgi to promote budding. *Cell* **2009**, *139*(2), 337–351.

[74] Yanaihara, N.; Nishioka, M.; Kohno, T.; Otsuka, A.; Okamoto, A.; Ochiai, K.; Tanaka, T.; Yokota, J. Reduced expression of MYO18B, a candidate tumor-suppressor gene on chromosome arm 22q, in ovarian cancer. *Int. J. Cancer* **2004**, *112*(1), 150–154.

[75] Inoue, T.; Kon, T.; Ajima, R.; Ohkura, R.; Tani, M.; Yokota, J.; Sutoh, K. MYO18B interacts with the proteasomal subunit Sug1 and is degraded by the ubiquitin-proteasome pathway. *Biochem. Biophys. Res. Commun.* **2006**, *342*(3), 829–834.

[76] Salamon, M.; Millino, C.; Raffaello, A.; Mongillo, M.; Sandri, C.; Bean, C.; Negrisolo, E.; Pallavicini, A.; Valle, G.; Zaccolo, M.; Schiaffino, S.; Lanfranchi, G. Human MYO18B, a novel unconventional myosin heavy chain expressed in striated muscles moves into the myonuclei upon differentiation. *J. Mol. Biol.* **2003**, *326*(1), 137–149.

[77] Ajima, R.; Kajiya, K.; Inoue, T.; Tani, M.; Shiraishi-Yamaguchi, Y.; Maeda, M.; Segawa, T.; Furuichi, T.; Sutoh, K.; Yokota, J. HOMER2 binds MYO18B and enhances its activity to suppress anchorage independent growth. *Biochem. Biophys. Res. Commun.* **2007**, *356*(4), 851–856.

[78] Higashi-Fujime, S.; Ishikawa, R.; Iwasawa, H.; Kagami, O.; Kurimoto, E.; Kohama, K.; Hozumi, T. The fastest actin-based motor protein from the green algae, Chara, and its distinct mode of interaction with actin. *FEBS Lett.* **1995**, *375*(1–2), 151–154.

[79] Tominaga, M.; Kojima, H.; Yokota, E.; Orii, H.; Nakamori, R.; Katayama, E.; Anson, M.; Shimmen, T.; Oiwa, K. Higher plant myosin XI moves processively on actin with 35 nm steps at high velocity. *EMBO J.* **2003**, *22*(6), 1263–1272.

[80] Heintzelman, M. B.; Schwartzman, J. D. Myosin diversity in apicomplexa. *J. Parasitol.* **2001**, *87*(2), 429–432.

[81] (a) Dobrowolski, J. M.; Sibley, L. D. Toxoplasma invasion of mammalian cells is powered by the actin cytoskeleton of the parasite. *Cell* **1996**, *84*(6), 933–939. (b) Cowman, A. F.; Crabb, B. S. Invasion of red blood cells by malaria parasites. *Cell* **2006**, *124*(4), 755–766. (c) Kappe, S. H.; Buscaglia, C. A.; Bergman, L. W.; Coppens, I.; Nussenzweig, V. Apicomplexan gliding motility and host cell invasion: overhauling the motor model. *Trends Parasitol.* **2004**, *20*(1), 13–16.

[82] (a) Heintzelman, M. B.; Schwartzman, J. D. A novel class of unconventional myosins from Toxoplasma gondii. *J. Mol. Biol.* **1997**, *271*(1), 139–146. (b) Lew, A. E.; Dluzewski, A. R.; Johnson, A. M.; Pinder, J. C. Myosins of Babesia bovis: molecular characterisation, erythrocyte invasion, and phylogeny. *Cell Motil. Cytoskeleton* **2002**, *52*(4), 202–220.

[83] Delbac, F.; Sänger, A.; Neuhaus, E. M.; Stratmann, R.; Ajioka, J. W.; Toursel, C.; Herm-Götz, A.; Tomavo, S.; Soldati, T.; Soldati, D. Toxoplasma gondii myosins B/C: one gene, two tails, two localizations, and a role in parasite division. *J. Cell. Biol.* **2001**, *155*(4), 613–623.

[84] Reubold, T. F.; Eschenburg, S.; Becker, A.; Kull, F. J.; Manstein, D. J. A structural model for actin-induced nucleotide release in myosin. *Nat. Struct. Biol.* **2003**, *10*(10), 826–830.

[85] (a) Lorenz, M.; Holmes, K. C. The actin-myosin interface. *Proc. Natl. Acad. Sci. USA* **2010**, *107*(28), 12529–12534. (b) Holmes, K. C.; Angert, I.; Kull, F. J.; Jahn, W.; Schroder, R. R. Electron cryo-microscopy shows how strong binding of myosin to actin releases nucleotide. *Nature* **2003**, *425*(6956), 423–427. (c) Tirion, M. M.; ben-Avraham, D.; Lorenz, M.; Holmes, K. C. Normal modes as refinement parameters for the F-actin model. *Biophys. J.* **1995**, *68*(1), 5–12.

[86] Lymn, R. W.; Taylor, E. W. Mechanism of adenosine triphosphate hydrolysis by actomyosin. *Biochemistry* **1971**, *10*(25), 4617–4624.

[87] Holmes, K. C.; Schroder, R. R.; Sweeney, H. L.; Houdusse, A. The structure of the rigor complex and its implications for the power stroke. *Philos. Trans. R. Soc. Lond. B Biol. Sci.* **2004**, *359*(1452), 1819–1828.

[88] (a) Van Dijk, J.; Furch, M.; Lafont, C.; Manstein, D. J.; Chaussepied, P. Functional characterization of the secondary actin binding site of myosin II. *Biochemistry* **1999**, *38*(46), 15078–15085. (b) Van Dijk, J.; Furch, M.; Derancourt, J.; Batra, R.; Knetsch, M. L.; Manstein, D. J.; Chaussepied, P. Differences in the ionic interaction of actin with the motor domains of nonmuscle and muscle myosin II. *Eur. J. Biochem.* **1999**, *260*(3), 672–683. (c) Furch, M.; Remmel, B.; Geeves, M. A.; Manstein, D. J. Stabilization of the actomyosin complex by negative charges on myosin. *Biochemistry* **2000**, *39*(38), 11602–11608. (d) Miller, C. J.; Wong, W. W.; Bobkova, E.; Rubenstein, P. A.; Reisler, E. Mutational analysis of the role of the N terminus of actin in actomyosin interactions: comparison with other mutant actins and implications for the cross-bridge cycle. *Biochemistry* **1996**, *35*(51), 16557–16565. (e) Wong, W. W.; Doyle, T. C.; Reisler, E. Nonspecific weak actomyosin interactions: relocation of charged residues in subdomain 1 of actin does not alter actomyosin function. *Biochemistry* **1999**, *38*(4), 1365–1370.

[89] (a) Johara, M.; Toyoshima, Y. Y.; Ishijima, A.; Kojima, H.; Yanagida, T.; Sutoh, K. Charge-reversion mutagenesis of *Dictyostelium* actin to map the surface recognized by myosin during ATP-driven sliding motion. *Proc. Natl. Acad. Sci. USA* **1993**, *90*(6), 2127–2131. (b) Uyeda, T. Q.; Ruppel, K. M.; Spudich, J. A. Enzymatic activities correlate with chimaeric substitutions at the actin-binding face of myosin. *Nature* **1994**, *368*(6471), 567–569. (c) Knetsch, M. L.; Uyeda, T. Q.; Manstein, D. J. Disturbed communication between actin- and nucleotide-binding sites in a myosin II with truncated 50/20-kDa junction. *J. Biol. Chem.* **1999**, *274*(29), 20133–20138. (d) Ponomarev, M. A.; Furch, M.; Levitsky, D. I.; Manstein, D. J. Charge changes in loop 2 affect the thermal unfolding of the myosin motor domain bound to F-actin. *Biochemistry* **2000**, *39*(15), 4527–4532. (e) Joel, P. B.; Trybus, K. M.; Sweeney, H. L. Two conserved lysines at the 50/20-kDa junction of myosin are necessary for triggering actin activation. *J. Biol. Chem.* **2001**, *276*(5), 2998–3003. (f) Yengo, C. M.; Sweeney, H. L. Functional role of loop 2 in myosin V. *Biochemistry* **2004**, *43*(9), 2605–2612.

[90] Furch, M.; Geeves, M. A.; Manstein, D. J. Modulation of actin affinity and actomyosin adenosine triphosphatase by charge changes in the myosin motor domain. *Biochemistry* **1998**, *37*(18), 6317–6326.

[91] Goodson, H. V.; Warrick, H. M.; Spudich, J. A. Specialized conservation of surface loops of myosin: evidence that loops are involved in determining functional characteristics. *J. Mol. Biol.* **1999**, *287*(1), 173–185.

[92] (a) Nalavadi, V.; Nyitrai, M.; Bertolini, C.; Adamek, N.; Geeves, M. A.; Bahler, M. Kinetic mechanism of myosin IXB and the contributions of two class IX-specific regions. *J. Biol. Chem.* **2005**, *280*(47), 38957–38968. (b) Kambara, T.; Ikebe, M. A unique ATP hydrolysis mechanism of single-headed processive myosin, myosin IX. *J. Biol. Chem.* **2006**, *281*(8), 4949–4957.

[93] (a) Sweeney, H. L.; Straceski, A. J.; Leinwand, L. A.; Tikunov, B. A.; Faust, L. Heterologous expression of a cardiomyopathic myosin that is defective in its actin interaction. *J. Biol. Chem.* **1994**, *269*(3), 1603–1605. (b) Fujita, H.; Sugiura, S.; Momomura, S.; Sugi, H.; Sutoh, K. Functional characterization of *Dictyostelium discoideum* mutant myosins equivalent to human familial hypertrophic cardiomyopathy. *Adv. Exp. Med. Biol.* **1998**, *453*, 131–137.

[94] Bement, W. M.; Mooseker, M. S. TEDS rule: a molecular rationale for differential regulation of myosins by phosphorylation of the heavy chain head. *Cell Motil. Cytoskeleton* **1995**, *31*(2), 87–92.

[95] (a) Ostap, E. M.; Lin, T.; Rosenfeld, S. S.; Tang, N. Mechanism of regulation of Acanthamoeba myosin-IC by heavy-chain phosphorylation. *Biochemistry* **2002**, *41*(41), 12450–12456. (b) Fujita-Becker, S.; Dürrwang, U.; Erent, M.; Clark, R. J.; Geeves, M. A.; Manstein, D. J. Changes in Mg^{2+} ion concentration and heavy chain phosphorylation regulate the motor activity of a class I myosin. *J. Biol. Chem.* **2005**, *280*(7), 6064–6071. (c) Dürrwang, U.; Fujita-Becker, S.; Erent, M.; Kull, F. J.; Tsiavaliaris, G.; Geeves, M. A.; Manstein, D. J. Dictyostelium myosin-IE is a fast molecular motor involved in phagocytosis. *J. Cell Sci.* **2006**, *119*(Pt 3), 550–558. (d) Wang, Z. Y.; Wang, F.; Sellers, J. R.; Korn, E. D.; Hammer, 3rd J. A. Analysis of the regulatory phosphorylation site in Acanthamoeba myosin IC by using site-directed mutagenesis. *Proc. Natl. Acad. Sci. USA* **1998**, *95*(26), 15200–15205. (e) De La Cruz, E. M.; Ostap, E. M.; Sweeney, H. L. Kinetic mechanism and regulation of myosin VI. *J. Biol. Chem.* **2001**, *276*(34), 32373–32381.

[96] Sasaki, N.; Asukagawa, H.; Yasuda, R.; Hiratsuka, T.; Sutoh, K. Deletion of the myopathy loop of Dictyostelium myosin II and its impact on motor functions. *J. Biol. Chem.* **1999**, *274*(53), 37840–37844.

[97] Milligan, R. A. Protein-protein interactions in the rigor actomyosin complex. *Proc. Natl. Acad. Sci. USA* **1996**, *93*(1), 21–22.

[98] Giese, K. C.; Spudich, J. A. Phenotypically selected mutations in myosin's actin binding domain demonstrate intermolecular contacts important for motor function. *Biochemistry* **1997**, *36*(28), 8465–8473.

[99] Tama, F.; Miyashita, O.; Brooks, 3rd C. L. Normal mode based flexible fitting of high-resolution structure into low-resolution experimental data from cryo-EM. *J. Struct. Biol.* **2004**, *147*(3), 315–326.

[100] Rusu, M.; Birmanns, S.; Wriggers, W. Biomolecular pleiomorphism probed by spatial interpolation of coarse models. *Bioinformatics* **2008**, *24*(21), 2460–2466.

[101] Trabuco, L. G.; Villa, E.; Mitra, K.; Frank, J.; Schulten, K. Flexible fitting of atomic structures into electron microscopy maps using molecular dynamics. *Structure* **2008**, *16*(5), 673–683.

[102] (a) Webb, M. R.; Grubmeyer, C.; Penefsky, H. S.; Trentham, D. R. The stereochemical course of phosphoric residue transfer catalyzed by beef heart mitochondrial ATPase. *J. Biol. Chem.* **1980**, *255*(24), 11637–11639. (b) Webb, M. R.; Trentham, D. R. The mechanism of ATP hydrolysis catalyzed by myosin and actomyosin, using rapid reaction techniques to study oxygen exchange. *J. Biol. Chem.* **1981**, *256*(21), 10910–10916.

[103] Sartorelli, L.; Fromm, H. J.; Benson, R. W.; Boyer, P. D. Direct and ^{18}O-exchange measurements relevant to possible activated or phosphorylated states of myosin. *Biochemistry* **1966**, *5*(9), 2877–2884.

[104] Yang, Y.; Cui, Q. The hydrolysis activity of adenosine triphosphate in myosin: a theoretical analysis of anomeric effects and the nature of the transition state. *J. Phys. Chem. A* **2009**, *113*(45), 12439–12446.

[105] Bagshaw, C. R.; Trentham, D. R. The characterization of myosin-product complexes and of product-release steps during the magnesium ion-dependent adenosine triphosphatase reaction. *Biochem. J* **1974**, *141*(2), 331–349.

[106] (a) Fisher, A. J.; Smith, C. A.; Thoden, J. B.; Smith, R.; Sutoh, K.; Holden, H. M.; Rayment, I. X-ray structures of the myosin motor domain of Dictyostelium discoideum complexed with $MgADP \cdot BeF_x$ and $MgADP \cdot AlF_4$. *Biochemistry* **1995**, *34*(28), 8960–8972. (b) Rayment, I. The structural basis of the myosin ATPase activity. *J. Biol. Chem.* **1996**, *271*(27), 15850–15853.

[107] Kagawa, H.; Mori, K. Molecular orbital study of the interaction between MgATP and the myosin motor domain: the highest occupied molecular orbitals indicate the reaction site of ATP hydrolysis. *J. Phys. Chem. B* **1999**, *103*(34), 7346–7352.

[108] Minehardt, T. J.; Marzari, N.; Cooke, R.; Pate, E.; Kollman, P. A.; Car, R. A classical and *ab initio* study of the interaction of the myosin triphosphate binding domain with ATP. *Biophys. J.* **2002**, *82*(2), 660–675.

[109] Onishi, H.; Mochizuki, N.; Morales, M. F. On the myosin catalysis of ATP hydrolysis. *Biochemistry* **2004**, *43*(13), 3757–3763.

[110] (a) Li, G.; Cui, Q. Mechanochemical coupling in myosin: a theoretical analysis with molecular dynamics and combined QM/MM reaction path calculations. *J. Phys. Chem.* **2004**, *108*(10), 3342–3357. (b) Schwarzl, S. M.; Smith, J. C.; Fischer, S. Insights into the chemomechanical coupling of the myosin motor from simulation of its ATP hydrolysis mechanism. *Biochemistry* **2006**, *45*(18), 5830–5847.

[111] (a) Miller, D. L.; Westheimer, F. H. The hydrolysis of γ-phenylpropyl di- and triphosphates. *J. Am. Chem. Soc.* **1966**, *88*(7), 1507–1511. (b) Admiraal, S. J.; Herschlag, D. Mapping the transition state for ATP hydrolysis: implications for enzymatic catalysis. *Chem. Biol.* **1995**, *2*(11), 729–739.

[112] Okimoto, N.; Yamanaka, K.; Ueno, J.; Hata, M.; Hoshino, T.; Tsuda, M. Theoretical studies of the ATP hydrolysis mechanism of myosin. *Biophys. J.* **2001**, *81*(5), 2786–2794.

[113] Grigorenko, B. L.; Rogov, A. V.; Topol, I. A.; Burt, S. K.; Martinez, H. M.; Nemukhin, A. V. Mechanism of the myosin catalyzed hydrolysis of ATP as rationalized by molecular modeling. *Proc. Natl. Acad. Sci. USA* **2007**, *104*(17), 7057–7061.

[114] Coureux, P. D.; Wells, A. L.; Menetrey, J.; Yengo, C. M.; Morris, C. A.; Sweeney, H. L.; Houdusse, A. A structural state of the myosin V motor without bound nucleotide. *Nature* **2003**, *425*(6956), 419–423.

[115] (a) Shimada, T.; Sasaki, N.; Ohkura, R.; Sutoh, K. Alanine scanning mutagenesis of the switch I region in the ATPase site of *Dictyostelium discoideum* myosin II. *Biochemistry* **1997**, *36*(46), 14037–14043. (b) Sasaki, N.; Shimada, T.; Sutoh, K. Mutational analysis of the switch II loop of *Dictyostelium myosin* II. *J. Biol. Chem.* **1998**, *273*(32), 20334–20340. (c) Li, X. D.; Rhodes, T. E.; Ikebe, R.; Kambara, T.; White, H. D.; Ikebe, M. Effects of mutations in the γ-phosphate binding site of myosin on its motor function. *J. Biol. Chem.* **1998**, *273*(42), 27404–27411.

[116] (a) Furch, M.; Fujita-Becker, S.; Geeves, M. A.; Holmes, K. C.; Manstein, D. J. Role of the salt-bridge between switch-1 and switch-2 of *Dictyostelium* myosin. *J. Mol. Biol.* **1999**, *290*(3), 797–809. (b) Kliche, W.; Fujita-Becker, S.; Kollmar, M.; Manstein, D. J.; Kull, F. J. Structure of a genetically engineered molecular motor. *EMBO J.* **2001**, *20*(1–2), 40–46.

[117] Malnasi-Csizmadia, A.; Pearson, D. S.; Kovacs, M.; Woolley, R. J.; Geeves, M. A.; Bagshaw, C. R. Kinetic resolution of a conformational transition and the ATP hydrolysis step using relaxation methods with a *Dictyostelium* myosin II mutant containing a single tryptophan residue. *Biochemistry* **2001**, *40*(42), 12727–12737.

[118] Kollmar, M.; Dürrwang, U.; Kliche, W.; Manstein, D. J.; Kull, F. J. Crystal structure of the motor domain of a class-I myosin. *EMBO J.* **2002**, *21*(11), 2517–2525.

[119] (a) Fischer, S.; Windshugel, B.; Horak, D.; Holmes, K. C.; Smith, J. C. Structural mechanism of the recovery stroke in the myosin molecular motor. *Proc. Natl. Acad. Sci. USA* **2005**, *102*(19), 6873–6878. (b) Koppole, S.; Smith, J. C.; Fischer, S. The structural coupling between ATPase activation and recovery stroke in the myosin II motor. *Structure* **2007**, *15*(7), 825–837. (c) Yu, H.; Ma, L.; Yang, Y.; Cui, Q. Mechanochemical coupling in the myosin motor domain. II. Analysis of critical residues. *PLoS Comput. Biol.* **2007**, *3*(2), e23. (d) Yu, H.; Ma, L.; Yang, Y.; Cui, Q. Mechanochemical coupling in the myosin motor domain. I. Insights from equilibrium active-site simulations. *PLoS Comput. Biol.* **2007**, *3*(2), e21.

[120] (a) Patterson, B.; Ruppel, K. M.; Wu, Y.; Spudich, J. A. Cold-sensitive mutants G680V and G691C of Dictyostelium myosin II confer dramatically different biochemical defects. *J. Biol. Chem.* **1997**, *272*(44), 27612–27617. (b) Batra, R.; Geeves, M. A.; Manstein, D. J. Kinetic analysis of *Dictyostelium discoideum* myosin motor domains with glycine-to-alanine mutations in the reactive thiol region. *Biochemistry* **1999**, *38*(19), 6126–6134. (c) Murphy, C. T.; Rock, R. S.; Spudich, J. A. A myosin II mutation uncouples ATPase activity from motility and shortens step size. *Nat. Cell Biol.* **2001**, *3*(3), 311–315. (d) Tsiavaliaris, G.; Fujita-Becker, S.; Batra, R.; Levitsky, D. I.; Kull, F. J.; Geeves, M. A.; Manstein, D. J. Mutations in the relay loop region result in dominant-negative inhibition of myosin II function in *Dictyostelium*. *EMBO Rep.* **2002**, *3*(11), 1099–1105. (e) Sasaki, N.; Ohkura, R.; Sutoh, K. *Dictyostelium* myosin II mutations that uncouple the converter swing and ATP hydrolysis cycle. *Biochemistry* **2003**, *42*(1), 90–95.

[121] Tsiavaliaris, G.; Fujita-Becker, S.; Manstein, D. J. Molecular engineering of a backwards-moving myosin motor. *Nature* **2004**, *427*(6974), 558–561.

[122] (a) Uyeda, T. Q.; Abramson, P. D.; Spudich, J. A. The neck region of the myosin motor domain acts as a lever arm to generate movement. *Proc. Natl. Acad. Sci. USA* **1996**, *93*(9), 4459–4464. (b) Ruff, C.; Furch, M.; Brenner, B.; Manstein, D. J.; Meyhofer, E. Single-molecule tracking of myosins with genetically engineered amplifier domains. *Nat. Struct. Biol.* **2001**, *8*(3), 226–229.

[123] Menetrey, J.; Bahloul, A.; Wells, A. L.; Yengo, C. M.; Morris, C. A.; Sweeney, H. L.; Houdusse, A. The structure of the myosin VI motor reveals the mechanism of directionality reversal. *Nature* **2005**, *435*(7043), 779–785.

[124] Park, H.; Li, A.; Chen, L. Q.; Houdusse, A.; Selvin, P. R.; Sweeney, H. L. The unique insert at the end of the myosin VI motor is the sole determinant of directionality. *Proc. Natl. Acad. Sci. USA* **2007**, *104*(3), 778–783.

[125] (a) Rock, R. S.; Rice, S. E.; Wells, A. L.; Purcell, T. J.; Spudich, J. A.; Sweeney, H. L. Myosin VI is a processive motor with a large step size. *Proc. Natl. Acad. Sci. USA* **2001**, *98*(24), 13655–13659. (b) Nishikawa, S.; Homma, K.; Komori, Y.; Iwaki, M.; Wazawa, T.; Hikikoshi Iwane, A.; Saito, J.; Ikebe, R.; Katayama, E.; Yanagida, T.; Ikebe, M. Class VI myosin moves processively along actin filaments backward with large steps. *Biochem. Biophys. Res. Commun.* **2002**, *290*(1), 311–317.

[126] Menetrey, J.; Llinas, P.; Mukherjea, M.; Sweeney, H. L.; Houdusse, A. The structural basis for the large power stroke of myosin VI. *Cell* **2007**, *131*(2), 300–308.

[127] Bryant, Z.; Altman, D.; Spudich, J. A. The power stroke of myosin VI and the basis of reverse directionality. *Proc. Natl. Acad. Sci. USA* **2007**, *104*(3), 772–777.

[128] Reifenberger, J. G.; Toprak, E.; Kim, H.; Safer, D.; Sweeney, H. L.; Selvin, P. R. Myosin VI undergoes a 180 degrees power stroke implying an uncoupling of the front lever arm. *Proc. Natl. Acad. Sci. USA* **2009**, *106*(43), 18255–18260.

[129] Knight, P. J.; Thirumurugan, K.; Xu, Y.; Wang, F.; Kalverda, A. P.; Stafford, 3rd W. F.; Sellers, J. R.; Peckham, M. The predicted coiled-coil domain of myosin 10 forms a novel elongated domain that lengthens the head. *J. Biol. Chem.* **2005**, *280*(41), 34702–34708.

[130] Peckham, M.; Knight, P. J. When a predicted coiled coil is really a single α-helix, in myosins and other proteins. *Soft Matter* **2009**, *5*, 2493–2503.

[131] Spink, B. J.; Sivaramakrishnan, S.; Lipfert, J.; Doniach, S.; Spudich, J. A. Long single alpha-helical tail domains bridge the gap between structure and function of myosin VI. *Nat. Struct. Mol. Biol.* **2008**, *15*(6), 591–597.

[132] Goodey, N. M.; Benkovic, S. J. Allosteric regulation and catalysis emerge via a common route. *Nat. Chem. Biol.* **2008**, *4*(8), 474–482.

[133] (a) Tsai, C. J.; del Sol, A.; Nussinov, R. Allostery: absence of a change in shape does not imply that allostery is not at play. *J. Mol. Biol.* **2008**, *378*(1), 1–11. (b) Cui, Q.; Karplus, M. Allostery and cooperativity revisited. *Protein Sci.* **2008**, *17*(8), 1295–1307. (c) Laskowski, R. A.; Gerick, F.; Thornton, J. M. The structural basis of allosteric regulation in proteins. *FEBS Lett.* **2009**, *583*(11), 1692–1698.

[134] Conibear, P. B.; Bagshaw, C. R.; Fajer, P. G.; Kovacs, M.; Malnasi-Csizmadia, A. Myosin cleft movement and its coupling to actomyosin dissociation. *Nat. Struct. Biol.* **2003**, *10*(10), 831–835.

[135] Zheng, W.; Thirumalai, D. Coupling between normal modes drives protein conformational dynamics: illustrations using allosteric transitions in myosin II. *Biophys. J.* **2009**, *96*(6), 2128–2137.

[136] Kuczmarski, E. R.; Spudich, J. A. Regulation of myosin self-assembly: phosphorylation of Dictyostelium heavy chain inhibits formation of thick filaments. *Proc. Natl. Acad. Sci. USA* **1980**, *77*(12), 7292–7296.

[137] (a) Vaillancourt, J. P.; Lyons, C.; Cote, G. P. Identification of two phosphorylated threonines in the tail region of *Dictyostelium* myosin II. *J. Biol. Chem.* **1988**, *263*(21), 10082–10087. (b) Luck-Vielmetter, D.; Schleicher, M.; Grabatin, B.; Wippler, J.; Gerisch, G. Replacement of threonine residues by serine and alanine in a phosphorylatable heavy chain fragment of *Dictyostelium* myosin II. *FEBS Lett.* **1990**, *269*(1), 239–243.

[138] (a) Egelhoff, T. T.; Lee, R. J.; Spudich, J. A. *Dictyostelium* myosin heavy chain phosphorylation sites regulate myosin filament assembly and localization *in vivo*. *Cell* **1993**, *75*(2), 363–371. (b) Sabry, J. H.; Moores, S. L.; Ryan, S.; Zang, J. H.; Spudich, J. A. Myosin heavy chain phosphorylation sites regulate myosin localization during cytokinesis in live cells. *Mol. Biol. Cell* **1997**, *8*(12), 2605–2615. (c) Stites, J.; Wessels, D.; Uhl, A.; Egelhoff, T.; Shutt, D.; Soll, D. R. Phosphorylation of the *Dictyostelium* myosin II heavy chain is necessary for maintaining cellular polarity and suppressing turning during chemotaxis. *Cell Motil. Cytoskeleton* **1998**, *39*(1), 31–51.

[139] Bosgraaf, L.; van Haastert, P. J. The regulation of myosin II in *Dictyostelium*. *Eur. J. Cell. Biol.* **2006**, *85*(9–10), 969–979.

[140] (a) Griffith, L. M.; Downs, S. M.; Spudich, J. A. Myosin light chain kinase and myosin light chain phosphatase from *Dictyostelium*: effects of reversible phosphorylation on myosin structure and function. *J. Cell. Biol.* **1987**, *104*(5), 1309–1323. (b) Liu, X.; Ito, K.; Morimoto, S.; Hikkoshi-Iwane, A.; Yanagida, T.; Uyeda, T. Q. Filament structure as an essential factor for regulation of *Dictyostelium* myosin by regulatory light chain phosphorylation. *Proc. Natl. Acad. Sci. USA* **1998**, *95*(24), 14124–14129.

[141] Ostrow, B. D.; Chen, P.; Chisholm, R. L. Expression of a myosin regulatory light chain phosphorylation site mutant complements the cytokinesis and developmental defects of *Dictyostelium* RMLC null cells. *J. Cell. Biol.* **1994**, *127*(6 Pt 2), 1945–1955.

[142] Lowey, S.; Trybus, K. M. Common structural motifs for the regulation of divergent class II myosins. *J. Biol. Chem.* **2010**, *285*(22), 16403–16407.

[143] (a) Wendt, T.; Taylor, D.; Messier, T.; Trybus, K. M.; Taylor, K. A. Visualization of head-head interactions in the inhibited state of smooth muscle myosin. *J. Cell. Biol.* **1999**, *147*(7), 1385–1390. (b) Wendt, T.; Taylor, D.; Trybus, K. M.; Taylor, K. Three-dimensional image reconstruction of dephosphorylated smooth muscle heavy meromyosin reveals asymmetry in the interaction between myosin heads and placement of subfragment 2. *Proc. Natl. Acad. Sci. USA* **2001**, *98*(8), 4361–4366.

[144] Dominguez, R.; Freyzon, Y.; Trybus, K. M.; Cohen, C. Crystal structure of a vertebrate smooth muscle myosin motor domain and its complex with the

essential light chain: visualization of the pre-power stroke state. *Cell* **1998**, *94*(5), 559–571.

[145] (a) Trybus, K. M.; Huiatt, T. W.; Lowey, S. A bent monomeric conformation of myosin from smooth muscle. *Proc. Natl. Acad. Sci. USA* **1982**, *79*(20), 6151–6155. (b) Trybus, K. M.; Lowey, S. Conformational states of smooth muscle myosin: effects of light chain phosphorylation and ionic strength. *J. Biol. Chem.* **1984**, *259*(13), 8564–8571. (c) Onishi, H.; Wakabayashi, T. Electron microscopic studies of myosin molecules from chicken gizzard muscle I: the formation of the intramolecular loop in the myosin tail. *J. Biochem.* **1982**, *92*(3), 871–879. (d) Craig, R.; Smith, R.; Kendrick-Jones, J. Light-chain phosphorylation controls the conformation of vertebrate nonmuscle and smooth muscle myosin molecules. *Nature* **1983**, *302*(5907), 436–439.

[146] (a) Cross, R. A.; Cross, K. E.; Sobieszek, A. ATP-linked monomer-polymer equilibrium of smooth muscle myosin: the free folded monomer traps ADP · Pi. *EMBO J.* **1986**, *5*(10), 2637–2641. (b) Cross, R. A.; Jackson, A. P.; Citi, S.; Kendrick-Jones, J.; Bagshaw, C. R. Active site trapping of nucleotide by smooth and nonmuscle myosins. *J. Mol. Biol.* **1988**, *203*(1), 173–181.

[147] Woodhead, J. L.; Zhao, F. Q.; Craig, R.; Egelman, E. H.; Alamo, L.; Padron, R. Atomic model of a myosin filament in the relaxed state. *Nature* **2005**, *436*(7054), 1195–1199.

[148] Al-Khayat, H. A.; Morris, E. P.; Squire, J. M. The 7-stranded structure of relaxed scallop muscle myosin filaments: support for a common head configuration in myosin-regulated muscles. *J. Struct. Biol.* **2009**, *166*(2), 183–194.

[149] Zhao, F. Q.; Craig, R.; Woodhead, J. L. Head-head interaction characterizes the relaxed state of *Limulus* muscle myosin filaments. *J. Mol. Biol.* **2009**, *385*(2), 423–431.

[150] Zoghbi, M. E.; Woodhead, J. L.; Moss, R. L.; Craig, R. Three-dimensional structure of vertebrate cardiac muscle myosin filaments. *Proc. Natl. Acad. Sci. USA* **2008**, *105*(7), 2386–2390.

[151] Al-Khayat, H. A.; Morris, E. P.; Kensler, R. W.; Squire, J. M. Myosin filament 3D structure in mammalian cardiac muscle. *J. Struct. Biol.* **2008**, *163*(2), 117–126.

[152] (a) Krementsov, D. N.; Krementsova, E. B.; Trybus, K. M. Myosin V: regulation by calcium, calmodulin, and the tail domain. *J. Cell. Biol.* **2004**, *164*(6), 877–886. (b) Wang, F.; Thirumurugan, K.; Stafford, W. F.; Hammer, 3rd J. A.; Knight, P. J.; Sellers, J. R. Regulated conformation of myosin V. *J. Biol. Chem.* **2004**, *279*(4), 2333–2336.

[153] (a) Wu, X.; Sakamoto, T.; Zhang, F.; Sellers, J. R.; Hammer, 3rd J. A. *In vitro* reconstitution of a transport complex containing Rab27a, melanophilin and myosin Va. *FEBS Lett.* **2006**, *580*(25), 5863–5868. (b) Li, X. D.; Ikebe, R.; Ikebe, M. Activation of myosin Va function by melanophilin, a specific docking partner of myosin Va. *J. Biol. Chem.* **2005**, *280*(18), 17815–17822.

[154] (a) Higuchi, H.; Takemori, S. Butanedione monoxime suppresses contraction and ATPase activity of rabbit skeletal muscle. *J. Biochem.* **1989**, *105*(4), 638–643. (b) McKillop, D. F.; Fortune, N. S.; Ranatunga, K. W.; Geeves, M. A. The influence of 2,3-butanedione 2-monoxime (BDM) on the interaction between actin and myosin in solution and in skinned muscle fibres. *J. Muscle Res. Cell Motil.* **1994**, *15*(3), 309–318.

[155] Herrmann, C.; Wray, J.; Travers, F.; Barman, T. Effect of 2,3-butanedione monoxime on myosin and myofibrillar ATPases: an example of an uncompetitive inhibitor. *Biochemistry* **1992**, *31*(48), 12227–12232.

[156] Wilson, I. B.; Ginsburg, B. A powerful reactivator of alkylphosphate-inhibited acetylcholinesterase. *Biochim. Biophys. Acta* **1955**, *18*(1), 168–170.

[157] Stapleton, M. T.; Fuchsbauer, C. M.; Allshire, A. P. BDM drives protein dephosphorylation and inhibits adenine nucleotide exchange in cardiomyocytes. *Am. J. Physiol.* **1998**, *275*(4 Pt 2), H1260–H1266.

[158] (a) Schlichter, L. C.; Pahapill, P. A.; Chung, I. Dual action of 2,3-butanedione monoxime (BDM) on K^+ current in human T lymphocytes. *J. Pharmacol. Exp. Ther.* **1992**, *261*(2), 438–446. (b) Lopatin, A. N.; Nichols, C. G. Block of delayed rectifier (DRK1) K^+ channels by internal 2,3-butanedione monoxime in *Xenopus* oocytes. *Receptors Channels* **1993**, *1*(4), 279–286.

[159] Ferreira, G.; Artigas, P.; Pizarro, G.; Brum, G. Butanedione monoxime promotes voltage-dependent inactivation of L-type calcium channels in heart: effects on gating currents. *J. Mol. Cell. Cardiol.* **1997**, *29*(2), 777–787.

[160] Siegman, M. J.; Mooers, S. U.; Warren, T. B.; Warshaw, D. M.; Ikebe, M.; Butler, T. M. Comparison of the effects of 2,3-butanedione monoxime on force production, myosin light chain phosphorylation and chemical energy usage in intact and permeabilized smooth and skeletal muscles. *J. Muscle Res. Cell Motil.* **1994**, *15*(4), 457–472.

[161] Cheung, A.; Dantzig, J. A.; Hollingworth, S.; Baylor, S. M.; Goldman, Y. E.; Mitchison, T. J.; Straight, A. F. A small-molecule inhibitor of skeletal muscle myosin II. *Nat. Cell Biol.* **2002**, *4*(1), 83–88.

[162] Hiratsuka, T. Nucleotide-induced closure of the ATP-binding pocket in myosin subfragment-1. *J. Biol. Chem.* **1994**, *269*(44), 27251–27257.

[163] (a) Hiratsuka, T. The interaction of Phe472 with a fluorescent inhibitor bound to the complex of myosin subfragment-1 with nucleotide. *Biochemistry* **2006**, *45*(4), 1234–1241. (b) Bobkov, A. A.; Sutoh, K.; Reisler, E. Nucleotide and actin binding properties of the isolated motor domain from *Dictyostelium discoideum* myosin. *J. Muscle Res. Cell Motil.* **1997**, *18*(5), 563–571.

[164] (a) Trybus, K. M.; Waller, G. S.; Chatman, T. A. Coupling of ATPase activity and motility in smooth muscle myosin is mediated by the regulatory light chain. *J. Cell. Biol.* **1994**, *124*(6), 963–969. (b) Yang, Z.; Sweeney, H. L. Restoration of phosphorylation-dependent regulation to the skeletal muscle myosin regulatory light chain. *J. Biol. Chem.* **1995**, *270*(42), 24646–24649.

[165] Patel, H.; Margossian, S. S.; Chantler, P. D. Locking regulatory myosin in the off-state with trifluoperazine. *J. Biol. Chem.* **2000**, *275*(7), 4880–4888.

[166] Sellers, J. R.; Wang, F.; Chantler, P. D. Trifluoperazine inhibits the MgATPase activity and in vitro motility of conventional and unconventional myosins. *J. Muscle Res. Cell Motil.* **2003**, *24*(8), 579–585.

[167] Straight, A. F.; Cheung, A.; Limouze, J.; Chen, I.; Westwood, N. J.; Sellers, J. R.; Mitchison, T. J. Dissecting temporal and spatial control of cytokinesis with a myosin II inhibitor. *Science* **2003**, *299*(5613), 1743–1747.

[168] Limouze, J.; Straight, A. F.; Mitchison, T.; Sellers, J. R. Specificity of blebbistatin, an inhibitor of myosin II. *J. Muscle Res. Cell Motil.* **2004**, *25*(4–5), 337–341.

[169] Allingham, J. S.; Smith, R.; Rayment, I. The structural basis of blebbistatin inhibition and specificity for myosin II. *Nat. Struct. Mol. Biol.* **2005**, *12*(4), 378–379.

[170] (a) Kovács, M.; Toth, J.; Hetenyi, C.; Málnási-Csizmadia, A.; Sellers, J. R. Mechanism of blebbistatin inhibition of myosin II. *J. Biol. Chem.* **2004**, *279*(34), 35557–35563. (b) Ramamurthy, B.; Yengo, C. M.; Straight, A. F.; Mitchison, T. J.; Sweeney, H. L. Kinetic mechanism of blebbistatin inhibition of nonmuscle myosin IIb. *Biochemistry* **2004**, *43*(46), 14832–14839.

[171] Takács, B.; Billington, N.; Gyimesi, M.; Kintses, B.; Málnási-Csizmadia, A.; Knight, P. J.; Kovács, M. Myosin complexed with ADP and blebbistatin reversibly adopts a conformation resembling the start point of the working stroke. *Proc. Natl. Acad. Sci. USA* **2010**, *107*(15), 6799–6804.

[172] (a) Ohri, R. V.; Radosevich, A. T.; Hrovat, K. J.; Musich, C.; Huang, D.; Holman, T. R.; Toste, F. D. A Re(V)-catalyzed C-N bond-forming route to human lipoxygenase inhibitors. *Org. Lett.* **2005**, *7*(12), 2501–2504. (b) Burkholder, P. R.; Pfister, R. M.; Leitz, F. H. Production of a pyrrole antibiotic by a marine bacterium. *Appl. Microbiol.* **1966**, *14*(4), 649–653.

[173] Fedorov, R.; Böhl, M.; Tsiavaliaris, G.; Hartmann, F. K.; Taft, M. H.; Baruch, P.; Brenner, B.; Martin, R.; Knölker, H. J.; Gutzeit, H. O.; Manstein, D. J. The mechanism of pentabromopseudilin inhibition of myosin motor activity. *Nat. Struct. Mol. Biol.* **2009**, *16*(1), 80–88.

[174] (a) Hanson, J.; Huxley, H. E. Structural basis of the cross-striations in muscle. *Nature* **1953**, *172*(4377), 530–532. (b) Funatsu, T.; Harada, Y.; Tokunaga, M.; Saito, K.; Yanagida, T. Imaging of single fluorescent molecules and individual ATP turnovers by single myosin molecules in aqueous solution. *Nature* **1995**, *374*(6522), 555–559. (c) Finer, J. T.; Simmons, R. M.; Spudich, J. A. Single myosin molecule mechanics: piconewton forces and nanometre steps. *Nature* **1994**, *368*(6467), 113–119. (d) Ishijima, A.; Kojima, H.; Funatsu, T.; Tokunaga, M.; Higuchi, H.; Tanaka, H.; Yanagida, T. Simultaneous observation of individual ATPase and mechanical events by a single myosin molecule during interaction with actin. *Cell* **1998**, *92*(2), 161–171.

[175] Kodera, N.; Yamamoto, D.; Ishikawa, R.; Ando, T. Video imaging of walking myosin V by high-speed atomic force microscopy. *Nature* **2010**, *468*(7320), 72–76.

[176] (a) Holmes, K. C.; Popp, D.; Gebhard, W.; Kabsch, W. Atomic model of the actin filament. *Nature* **1990**, *347*(6288), 44–49. (b) Popp, D.; Holmes, K. C. X-ray diffraction studies on oriented gels of vertebrate smooth muscle thin filaments. *J. Mol. Biol.* **1992**, *224*(1), 65–76.

[177] Gyimesi, M.; Kintses, B.; Bodor, A.; Perczel, A.; Fischer, S.; Bagshaw, C. R.; Malnasi-Csizmadia, A. The mechanism of the reverse recovery step, phosphate release, and actin activation of *Dictyostelium* myosin II. *J. Biol. Chem.* **2008**, *283*(13), 8153–8163.

[178] (a) Toyoshima, Y. Y.; Kron, S. J.; McNally, E. M.; Niebling, K. R.; Toyoshima, C.; Spudich, J. A. Myosin subfragment-1 is sufficient to move actin filaments in vitro. *Nature* **1987**, *328*(6130), 536–539. (b) Hynes, T. R.; Block, S. M.;

White, C.; Spudich, J. A. Movement of myosin fragments in vitro: domains involved in force production. *Cell* **1987**, *48*(6), 953–963.
[179] Niemann, H. H.; Knetsch, M. L.; Scherer, A.; Manstein, D. J.; Kull, F. J. Crystal structure of a dynamin GTPase domain in both nucleotide-free and GDP-bound forms. *EMBO J.* **2001**, *20*(21), 5813–5821.
[180] Bauer, C. B.; Holden, H. M.; Thoden, J. B.; Smith, R.; Rayment, I. X-ray structures of the apo and MgATP-bound states of *Dictyostelium discoideum* myosin motor domain. *J. Biol. Chem.* **2000**, *275*(49), 38494–38499.
[181] Gulick, A. M.; Bauer, C. B.; Thoden, J. B.; Pate, E.; Yount, R. G.; Rayment, I. X-ray structures of the *Dictyostelium discoideum* myosin motor domain with six non-nucleotide analogs. *J. Biol. Chem.* **2000**, *275*(1), 398–408.
[182] Bauer, C. B.; Kuhlman, P. A.; Bagshaw, C. R.; Rayment, I. X-ray crystal structure and solution fluorescence characterization of Mg.2′(3′)-O-(N-methylanthraniloyl) nucleotides bound to the *Dictyostelium discoideum* myosin motor domain. *J. Mol. Biol.* **1997**, *274*(3), 394–407.
[183] Gulick, A. M.; Bauer, C. B.; Thoden, J. B.; Rayment, I. X-ray structures of the MgADP, MgATPγS, and MgAMPPNP complexes of the *Dictyostelium discoideum* myosin motor domain. *Biochemistry* **1997**, *36*(39), 11619–11628.
[184] Smith, C. A.; Rayment, I. X-ray structure of the magnesium(II)-pyrophosphate complex of the truncated head of *Dictyostelium discoideum* myosin to 2.7 Å resolution. *Biochemistry* **1995**, *34*(28), 8973–8981.
[185] Morris, C. A.; Coureux, P. D.; Wells, A. L.; Houdusse, A.; Sweeney, H. L. To be published.
[186] Smith, C. A.; Rayment, I. X-ray structure of the magnesium(II) · ADP · vanadate complex of the *Dictyostelium discoideum* myosin motor domain to 1.9 A resolution. *Biochemistry* **1996**, *35*(17), 5404–5417.
[187] Lucas-Lopez, C.; Allingham, J. S.; Lebl, T.; Lawson, C. P.; Brenk, R.; Sellers, J. R.; Rayment, I.; Westwood, N. J. The small molecule tool (S)-(−)-blebbistatin: novel insights of relevance to myosin inhibitor design. *Org. Biomol. Chem.* **2008**, *6*(12), 2076–2084.
[188] Reubold, T. F.; Eschenburg, S.; Becker, A.; Leonard, M.; Schmid, S. L.; Vallee, R. B.; Kull, F. J.; Manstein, D. J. Crystal structure of the GTPase domain of rat dynamin 1. *Proc. Natl. Acad. Sci. USA* **2005**, *102*(37), 13093–13098.
[189] Coureux, P. D.; Sweeney, H. L.; Houdusse, A. Three myosin V structures delineate essential features of chemo-mechanical transduction. *EMBO J.* **2004**, *23*(23), 4527–4537.
[190] Ménétrey, J.; Llinas, P.; Cicolari, J.; Squires, G.; Liu, X.; Li, A.; Sweeney, H. L.; Houdusse, A. The postrigor structure of myosin VI and implications for the recovery stroke. *EMBO J.* **2008**, *27*(1), 244–252.
[191] Yang, Y.; Gourinath, S.; Kovacs, M.; Nyitray, L.; Reutzel, R.; Himmel, D. M.; O'Neall-Hennessey, E.; Reshetnikova, L.; Szent-Gyorgyi, A. G.; Brown, J. H.; Cohen, C. Rigor-like structures from muscle myosins reveal key mechanical elements in the transduction pathways of this allosteric motor. *Structure* **2007**, *15*(5), 553–564.
[192] Rayment, I.; Rypniewski, W. R.; Schmidt-Base, K.; Smith, R.; Tomchick, D. R.; Benning, M. M.; Winkelmann, D. A.; Wesenberg, G.; Holden, H. M. Three-dimensional structure of myosin subfragment-1: a molecular motor. *Science* **1993**, *261*(5117), 50–58.
[193] Risal, D.; Gourinath, S.; Himmel, D. M.; Szent-Gyorgyi, A. G.; Cohen, C. Myosin subfragment 1 structures reveal a partially bound nucleotide and a complex salt bridge that helps couple nucleotide and actin binding. *Proc. Natl. Acad. Sci. USA* **2004**, *101*(24), 8930–8935.
[194] Himmel, D. M.; Gourinath, S.; Reshetnikova, L.; Shen, Y.; Szent-Györgyi, A. G.; Cohen, C. Crystallographic findings on the Internally uncoupled and near-rigor states of myosin: further insights into the mechanics of the motor. *Proc. Natl. Acad. Sci. USA* **2002**, *99*(20), 12645–12650.
[195] Houdusse, A.; Szent-Györgyi, A. G.; Cohen, C. Three conformational states of scallop myosin S1. *Proc. Natl. Acad. Sci. USA* **2000**, *97*(21), 11238–11243.
[196] Gourinath, S.; Himmel, D. M.; Brown, J. H.; Reshetnikova, L.; Szent-Györgyi, A. G.; Cohen, C. Crystal structure of scallop myosin S1 in the pre-power stroke state to 2.6 A resolution: flexibility and function in the head. *Structure* **2003**, *11*(12), 1621–1627.
[197] Houdusse, A.; Kalabokis, V. N.; Himmel, D.; Szent-Györgyi, A. G.; Cohen, C. Atomic structure of scallop myosin subfragment S1 complexed with MgADP: a novel conformation of the myosin head. *Cell* **1999**, *97*(4), 459–470.